Electronic Processes in Zinc Oxide

G. HEILAND AND E. MOLLWO
Universität Erlangen, Germany

AND

F. STÖCKMANN
Technische Hochschule Darmstadt, Germany

I. Introduction

1. Applications

Zinc oxide, ZnO, occurs in nature as the mineral zincite. It is produced in large quantities in the smelting of zinc ores and can be prepared in pure form by burning of zinc in air or by calcining zinc hydroxide, zinc carbonate, or zinc nitrate. It has been used for a long time as a pigment for paints and in enamel coatings, as an activator for the acceleration of vulcanization of rubber and as a pharmaceutical in zinc salves. Of the applications which depend in a direct way on the electronic processes in zinc oxide, we should mention first of all its use as a catalyst and as a photocatalyst for a series of chemical reactions. Its use in the vulcanization of rubber mentioned above is a good example ("active zinc oxide").

The material has played only a subordinate role as a semiconductor, photoconductor, and phosphor. Occasionally it has been used as a phosphor because of its rapid decay time; for example, in flying spot cathode tubes. It may play an important role in the future in "Electrofax" processes of photographic duplication, in which the photoconductivity of zinc oxide is used.

2. Lattice Structure

Zinc oxide crystallizes in the hexagonal wurtzite lattice in which the oxygen ions are arranged in closest hexagonal packing and the zinc ions occupy half of the tetrahedral interstitial positions and have the same relative arrangement as the oxygen ions (Fig. 1). Actually the environment of each ion does not have exact tetrahedral symmetry. Instead, the spacing between nearest neighbors in the direction of the hexagonal, or c axis, is somewhat smaller than for the other three neighbors. The binding is essentially polar; however, there is a homopolar component[1] of binding between next nearest zinc and oxygen ions in the direction of the c axis. The crystals are usually obtained in the form of hexagonal prisms. In the case of zinc oxide formed by the burning of zinc vapor in air one frequently finds four such prisms originating from the same point in such a manner as to form a tetrahedral array. Chemically deposited zinc oxide usually is a fine-grained powder possessing a particle size less than one micron and a correspondingly large specific surface area which is very important in its efficiency as a catalyst.

3. Physical Data

The most important mechanical and thermal properties of zinc oxide are assembled in Table I. The electrical properties are included only to

[1] K. Lark-Horovitz and C. H. Ehrhardt, *Phys. Rev.* **57**, 603 (1940).

the extent that they are not discussed in later sections of this article. Most of the values differ for specimens of different origin. The differences in the lattice constant are the order of one per cent, whereas the differences in the density are the order of ten per cent. In the case of exceedingly structure-sensitive properties, such as the magnetic susceptibility and the dielectric constant, only the order of magnitude of the values is

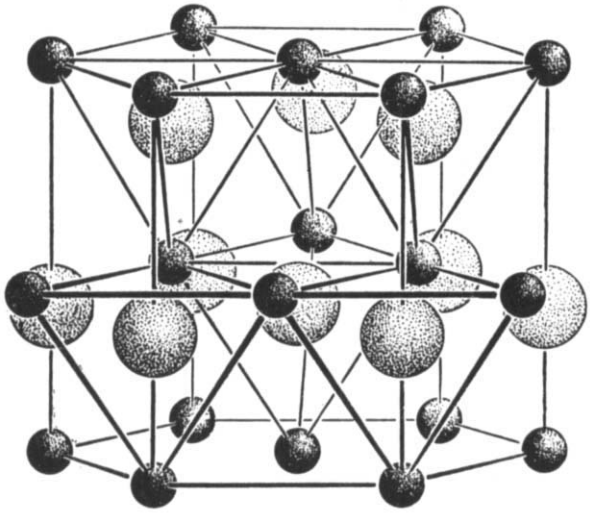

FIG. 1. The wurtzite lattice of zinc oxide.

sure. The values for single crystals are more reliable. The quantities in Table I have been taken from "Gmelins Handbuch der anorganischen Chemie"[2] in which one will find a multitude of other details concerning the preparation and the physical and chemical properties of zinc oxide with an abundant reference to the literature.

A representation of the zinc-oxygen equilibrium at different temperatures and pressures will be found in the work of Pourbaix and Rorive-Bouté.[3]

The electrical and optical properties of zinc oxide have been the subject of a number of investigations in the last 20 years. In many of its

[2] "Gmelins Handbuch der anorganischen Chemie," 8th ed., "Zink, Ergänzungsband." Verlag Chemie, Weinheim/Bergstrasse, Germany, 1956.

[3] M. J. N. Pourbaix and C. M. Rorive-Bouté, *Discussions Faraday Soc.* **4**, 139 (1948); *ibid.* **4**, 223 (1948).

TABLE I. PROPERTIES OF ZINC OXIDE

Lattice	Hexagonal, wurtzite ($B4$-type) (Fig. 1)
Lattice constant	$a = 3.24$ A, $c = 5.19$ A, $c/a = 1.60$
Distance of neighboring Zn^{++}-and O ions	In direction of the c axis $d = uc = 1.96$ A, of the three remaining neighbors $d = \sqrt{a^2/3 + c^2(u - \frac{1}{2})^2} = 1.98$ A ($u = 0.378$ instead of 0.375 for ideal tetrahedral arrangement)
Molecular weight	Zn: 65.38, O: 16.00, ZnO: 81.38
Ionic radius for tetrahedral coordination	$Zn_{neutral}$: 1.31 A, $O_{neutral}$: 0.66 A, for covalent binding (Pauling). Zn^{++}: 0.70 A, O^{--}: 1.32 A for ionic binding (Pauling). Zn^{++}: 0.78 A, O^{--}: 1.24 A for ionic binding (Goldschmidt)
Density	X-ray density 5.62–5.78 g/cm³, corresponding to 4.21 × 10^{22} ZnO-molecule/cm³, pycnometric: maxim 5.84 g/cm³, active ZnO: <5 g/cm³
Specific surface	Maximal larger than 80 m²/g for active ZnO
Enthalpy of formation	Zn (solid) + $\frac{1}{2}O_2$ (gas) → ZnO (solid): −83.17 kcal/mole corresponding to −3.61 ev/ZnO-molecules in lattice
Lattice energy	965 kcal/mole (from the Born-Haber cycle)
Specific heat	20 30 50 100 150 200 300 500 900 °K 0.17 0.60 1.98 4.24 6.22 7.20 9.66 11.2 12.3 cal/mole deg
Vapor pressure	12 torr at 1500°C, 1 torr at 1400°C, sublimation in high vacuum is appreciable at 1000°C
Melting point	≈ 2000°C only at high pressures
Dielectric constant	Values in literature for powder and sintered specimens between 10 and 36. Single crystals (2.4 × 10^{10} cps): $\epsilon = 8.5$[4]
Magnetic susceptibility	Temperature 273 196 83 °K ZnO(active) −0.31 −0.20 +0.62 ZnO(tempered) −0.26 −0.25 −0.25 } × 10^{-6}

properties zinc oxide stands somewhat between the heteropolar alkali halides and the homopolar semiconductors of group IV. This is exactly what one would expect from a II–VI compound such as zinc oxide and is an implicit reason for the many investigations of the material. In this

[4] A. R. Hutson and T. S. Benedict, Bell Telephone Laboratories, Murray Hill, N.J., Private communication.

sense the present article is a sequel to earlier articles in this series on the valence semiconductors and the III–V compounds.

II. Preparation of Samples

The optical and electrical properties of solids can vary greatly from one specimen to another when the structure and purity of the specimens vary. The most reproducible and reasonable conditions may be expected from chemically well-defined single crystals. Such crystals of zinc oxide are not easily made. As a result, many investigations are based on the use of polycrystalline materials in the form of sintered specimens or thin layers. The results obtained in this way are difficult to interpret, although they are highly characteristic of the preparations. They will be treated in this article in the same way as the results obtained from single crystals. We shall now review the methods of obtaining the different types of specimens.

4. Thin Layers

The thin layers are usually prepared by evaporation in a high vacuum. Zinc oxide decomposes in this process, and one obtains a zinc deposit. As a result, it is appropriate to evaporate metallic zinc on to a plate of quartz glass or plain glass and oxidize the coating after formation. The condensation starts only if the plate has been cooled below 190°K. If the condensing plate has been covered with a thin, perhaps a monatomic, layer of a material which condenses at room temperature, for example, with copper, the zinc will condense well to temperatures as high as 420°K.[5,6] Both condensation procedures have been used. The oxidation is usually carried out by heating the thin metallic layer in an electric oven in air to the range between 600° and 900°K. By varying the temperature and the duration of the oxidation process, one can make the conductivity vary over a wide range (see Section 17). The attainable thicknesses extend to about 0.3 μ, the values employed most being of the order of 0.1 μ. Apart from a light turbidness arising from Rayleigh scattering, the layers are glass-clear and are colored solely by interference. A study of the structure of layers prepared in this way with the help of electron diffraction at grazing incidence[7] (reflection) yields the following results. Layers having a thickness of about 10^{-5} cm possess crystallites of the order of 3×10^{-6} cm in size on the surface, oriented in a statistical manner. The crystal size decreases with decreasing thickness

[5] E. Scharowsky, Diplomarbeit, University of Erlangen, 1950.
[6] E. Mollwo, *Reichsber. Physik* **1**, 1 (1943).
[7] G. Seitz, Diplomarbeit, University of Erlangen, 1955.

of the layers. At the same time, one finds a preferred orientation of the crystallites (oriented texture) of such a type that the *c* axis is perpendicular to the support. This orientation is promoted by long heating and occurs for both amorphous and single crystal supports (Fig. 2).

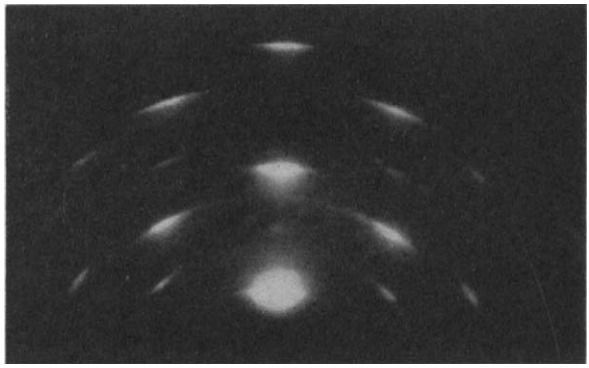

FIG. 2. Thin layer (20 mμ) evaporated on quartz glass. Electron diffraction at grazing incidence. The layer was oxidized at 400°C for 20 minutes and tempered in air at 500°C. After Seitz.[7]

Fritzsche[8] has worked with thin layers obtained by cathode sputtering of zinc in pure dry oxygen. The layers formed in this way were about 0.1 μ thick.

5. SINTERED SPECIMENS

a. Sintered Layers

Polycrystalline specimens in the form of layers having appreciably larger thicknesses (30 μ) and crystallite dimensions of the order of 1 μ can be obtained by the following procedure.[9] Metallic zinc in an appropriate crucible is vaporized in air by heating with a torch. The zinc vapor is oxidized and is deposited on a glass or quartz plate at a high temperature. In this process it is important to control the rate of oxidation by regulating the amount of oxygen in the flame. The layers are colored more or less intensively yellow for weak oxidation and are white for stronger oxidation. The layers can adhere fast to the underlying support, or they can be produced in such a way as to be free (Fig. 3). A representation of the surface of such layers is shown in Fig. 4.

[8] H. Fritzsche, *Z. Physik* **133**, 422 (1952).
[9] E. Mollwo and F. Stöckmann, *Ann. Physik* [6] **3**, 223 (1948).

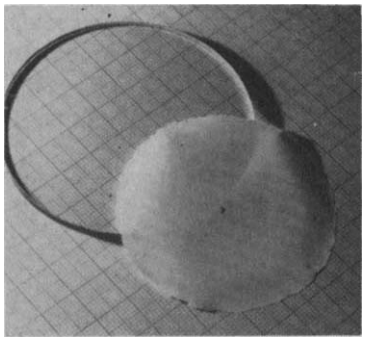

FIG. 3. Free transparent layer formed by sintering. Thickness about 20 μ. After Mollwo and Stöckmann.[9]

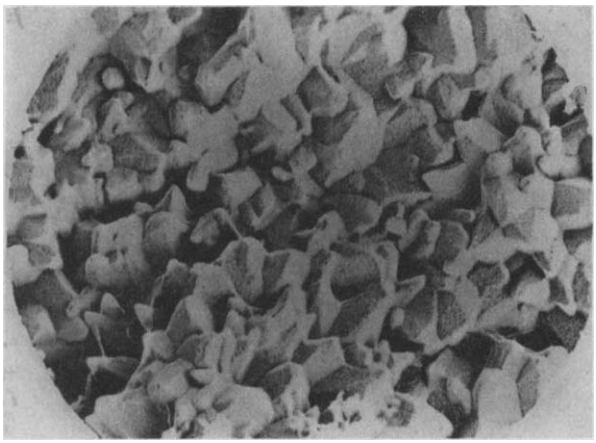

FIG. 4. Sintered layer. Electron-microscopic replica photograph of the surface made with an obliquely evaporated gold layer. Magnification about 7000 times. From H. König.

b. Compact Sintered Specimens

Compact sintered specimens are used in many investigations. They can be produced in the following way.[10–12] The most chemically pure zinc oxide powder is compacted with pressures of the order of 10^4 newton/cm^2 into cylinders or other forms having linear dimensions of the order of centimeters. The specimens are surrounded by zinc oxide powder in order to avoid contamination and heated in a crucible in air to high temperatures (700–1300°C). They are then tempered for times extending to

[10] T. T. Reboul, University of Pennsylvania Report No. 7, June 1953.
[11] E. E. Hahn, *J. Appl. Phys.* **22,** 855 (1951).
[12] S. E. Harrison, *Phys. Rev.* **93,** 52 (1954).

18 hours. It is essential to cool the specimens slowly to a temperature below 600°C and then quench them. Fissures and cracks develop if the specimens are cooled too rapidly. The samples have the appearance of porcelain. Their density is of the order of 5.5 g/cm^3 relative to a density of 5.6 g/cm^3 for single crystals. The size of the grains grows with increasing time of sintering and attains values in the range from 5 to 20 μ. The crystal size in the original zinc oxide powder is usually smaller than 1 μ. Recent investigations[13] show that the speed of sintering depends upon the atomsphere of gas.

The zinc oxide powder used in adsorption and in catalysis is usually prepared freshly,[14] for example, by heating zinc oxalate in air to 400°C. The zinc oxalate can be prepared by precipitation from solutions of ammonium oxalate and zinc nitrate. In order to obtain large surface areas the zinc oxide powder is heated either slightly or not at all, or the sintered material may again be crushed. Sintered specimens of zinc oxide containing specific admixtures[15–17] can be prepared in a similar way. It is only necessary to add an appropriate amount of the substance to the zinc oxide in solid form and to grind them together. It is also possible to dope by impregnating the zinc oxide powder with solutions of a corresponding nitrate and drying and sintering the product.[18] Additions which have been used are Cr_2O_3, Al_2O_3, Ga_2O_3, MgO, Li_2O, Na_2O. The admixed substances may be distributed uniformly by sintering at high temperatures. There is, however, the danger that the admixtures will accumulate on surface layers and grain boundaries. There has been no satisfactory way of controlling the atomically dispersed distribution of the additions in specimens used for the measurement of conductivity, adsorption, or catalysis.

Sintering can be accelerated by the admixture of Li_2O. This is indicated by an increased shrinking of zinc oxide pastilles on sintering[19] and by a decrease in the specific area[18] as determined by nitrogen adsorption.[20]

6. Single Crystals

Zinc oxide occurs in nature in the form of large single crystals of the so-called red zinc ore or as zincite. The intensive red color of the crystals

[13] J. Hutchings and J. P. Roberts, Royal Aircraft Establishment, Farnborough, Hants, England, Report MET 91, 1956.
[14] H. S. Taylor and D. V. Sickman, *J. Am. Chem. Soc.* **54,** 602 (1932).
[15] C. Wagner, *J. Chem. Phys.* **18,** 69 (1950).
[16] K. Hauffe, R. Glang, and H. J. Engell, *Z. physik. Chem. (Frankfurt)* **201,** 223 (1952).
[17] K. Hauffe and A. L. Vierk, *Z. physik. Chem. (Frankfurt)* **196,** 160 (1950).
[18] E. Molinari and G. Parravano, *J. Am. Chem. Soc.* **75,** 5233 (1953).
[19] G. M. Schwab and J. Block, *Z. physik. Chem. (Frankfurt)* [N.S.] **1,** 42 (1954).
[20] S. Brunauer, P. H. Emmet, and E. Teller, *J. Am. Chem. Soc.* **60,** 309 (1938).

is a consequence of the presence of appreciable fractions of impurities, usually of manganese and iron in the amount of a few per cent. As a result, such natural crystals are not useful for quantitative investigations. So-called seminatural crystals actually have been used for detailed investigations; however, they have proved relatively useless for precise measurements. The specimens are gray-green crystals of irregular form a few millimeters in thickness, several centimeters long. They occur occasionally and often unnoted in large-scale production of zinc or its compounds.

An essential difficulty of preparing the crystals synthetically lies in the fact that zinc oxide cannot be melted at atmospheric pressure. Instead, it dissociates and sublimes (see, for example, Pourbaix[3]). As long ago as 1935 Fritsch[21] attempted to prepare synthetic crystals. His method rested, in essence, upon the sublimation of highly heated specimens of pressed zinc oxide. He obtained clear prismatic needles about 5 mm long and a few tenths of a millimeter thick.

A number of investigators[22–24] developed the following procedure[25] in parallel to the preparation of sintered zinc oxide layers. Two electric ovens are mounted with vertical axis on vertically displaceable racks (Fig. 5). Metallic zinc is vaporized in the lower oven I, and the vapor is transported by a gas into the upper oven II. The vaporization is carried out in a quartz tube. The lower end of this tube is held by a water-cooled ring and can be made vacuum tight by means of a water-cooled closing plate. The carrier gas ($H_2 + N_2$) can be introduced into the vaporization chamber through an opening in the closing plate. Metallic zinc is placed in a quartz boat. The vaporization temperature is about 720–760°C.

The quartz tube in which the vaporization of metallic zinc occurs projects considerable beyond oven I. A section of the tube is made narrow in order to prevent the migration of oxygen against the stream of the carrying gas. The tube widens again shortly before its end. Oxygen is introduced through a second quartz tube which runs coaxially. By manipulation, the two ovens are brought to a distance of about 8 cm so that the upper edge of the arrangement projects into oven II in which the temperature is maintained in the range of 1330–1380°C. A third oven III is introduced in order to avoid condensation of the zinc vapor in the transition region between ovens I and II. The zinc vapor is oxidized as it emerges from the upper end of the arrangement. By varying the various

[21] O. Fritsch, *Ann. Physik* [5] **22**, 375 (1935).
[22] G. Tischer, Diplomarbeit, University of Erlangen, 1951.
[23] E. Scharowsky, *Z. Physik* **135**, 318 (1953).
[24] H. Rupprecht, Diplomarbeit, University of Erlangen, 1955.
[25] G. Bogner and E. Mollwo, *J. Phys. Chem. Solids* **6**, 136 (1958).

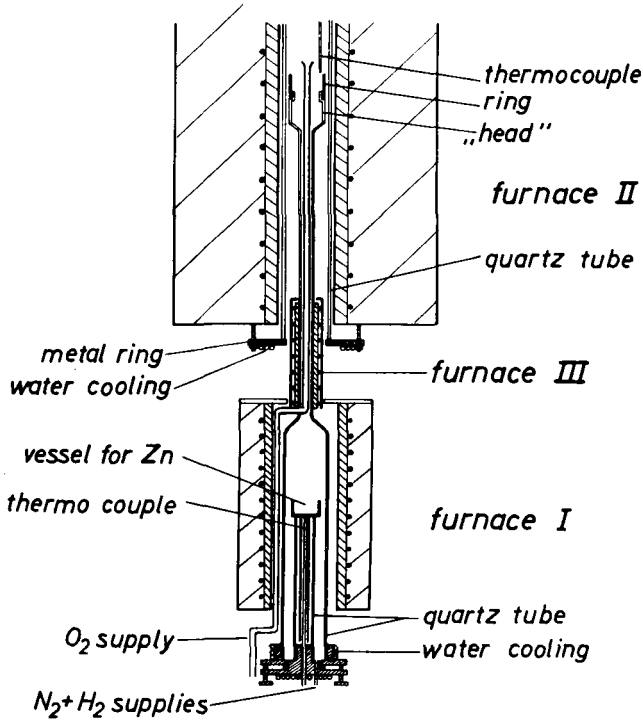

FIG. 5. Arrangement to grow single crystals of zinc oxide from the vapor phase. After Bogner and Mollwo.[25]

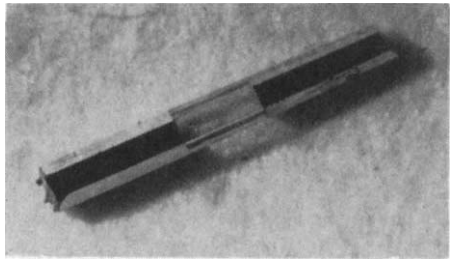

FIG. 6. Zinc oxide crystal (hexagonal prism) with evaporated platinum electrodes. Spacing 0.5 mm. After Heiland.[25a]

parameters of the assembly, in particularly the stream of carrier gas, the position of the reaction zone can be made to lie on the upper edge of the closing ring. The crystals grow there under appropriate conditions.

Zinc oxide crystals grow in the form of needles having a cross section in the range of 0.3–1 mm and a length of the order 1–2 cm. They are colorless and have the form of very regular hexagonal prisms (Fig. 6).

[25a] G. Heiland, *Z. Physik* **142**, 415 (1955).

Under special circumstances one obtains tiny plates or leaflets with a thickness in the range 0.05–0.15 mm, a width of 0.3–0.5 mm, and a length in the range of 1–2 cm. With the use of polarized light and x-ray diffraction it is possible to show that one always obtains single crystals. The axes of the hexagonal prisms are always along the c axis of the crystals. In the case of the leaflets the c axis lies in the plane of the plate and makes an angle below 11° with the long axis of the leaf.

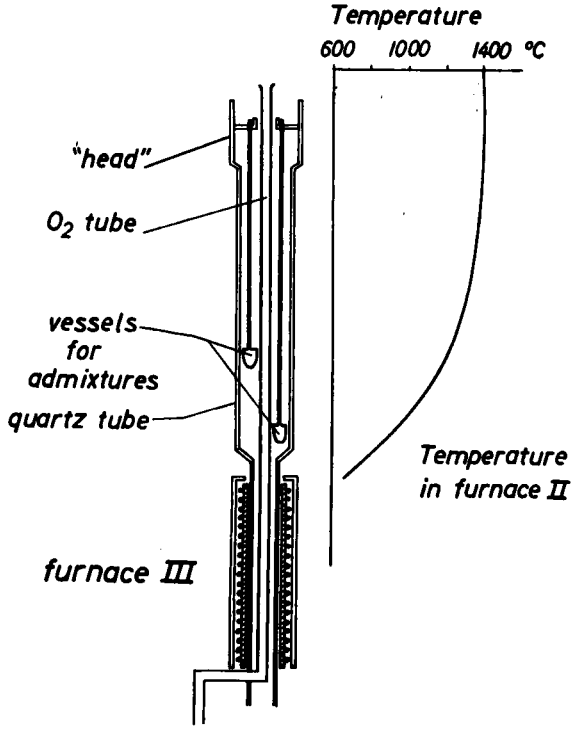

FIG. 7. Part of the arrangement to grow zinc oxide crystals containing additions from the vapor phase. After Bogner and Mollwo.[25]

Spectral analysis has demonstrated the presence of the following impurities:

$$\text{Cu} = 5 \times 10^{-4}\% \qquad \text{Si} \ll 1.5 \times 10^{-3}\%$$
$$\text{Mg} = 3 \times 10^{-4}\% \qquad \text{Al} \ll 2.2 \times 10^{-3}\%.$$

The same method may be used to obtain zinc oxide crystals with specific foreign admixtures (Fig. 7). The system is modified to the extent that a small quartz container is hung in the perpendicular quartz tube. The additions are placed in this container in the form of metals and are

vaporized at an appropriate temperature. In this way it has been possible to obtain zinc oxide crystals with additions of copper and indium. The concentrations of admixtures can be varied over several factors of ten.

Although copper and indium have been introduced into the growing crystals in this way, it is also possible to add a stoichiometric excess of zinc as well as hydrogen by diffusion into the completed crystal. To do this, the crystals are heated in zinc vapor or in hydrogen to temperatures between 500 and 1300°C. Further details will be discussed in Part III "Diffusion of Defects" and in Section 19 "Conductivity of Crystals."

III. Diffusion of Defects

As was pointed out in Section 6, it is possible to introduce foreign atoms or imperfections into the completed crystal by the use of diffusion as well as by additions to the growing crystals. Quantitative investigations are available concerning the diffusion of defects, which yield electrons, as a result of heating in hydrogen or zinc. The results will be discussed in the following in connection with observations of the so-called tarnishing reactions of metallic zinc and oxygen. The latter processes involve diffusion in thin layers. As in the other sections, we shall discuss the investigations on thin layers first.

7. Zinc

a. Thin Layers (Tarnishing Processes with Metallic Zinc)

If one exposes an even and reflecting surface of metallic zinc to oxygen at high temperatures (about 400°C), the surface becomes covered with a thin transparent layer of zinc oxide of the order of 0.1 μ thick which is colored by interference. It is said that the metal displays tarnishing colors and the tarnishing process. One can follow the growth of the tarnishing layer produced by long exposure to oxygen either by quantitative measurement of the interference colors or by weighing the specimen. The first method suffers from the difficulty that one must know the refractive index of the oxide layer; thus, the second method is the most reliable. It is always found that the thickness Δx or the mass Δm of the layer varies quadratically with the time:

$$(\Delta x)^2 = 2k't \tag{7.1}$$

or

$$\left(\frac{\Delta m}{q}\right)^2 = k''t \qquad q = \text{surface area.} \tag{7.2}$$

The two tarnishing constants k' and k'' can be interrelated by the equation $k'' = fk'$. In the case of ZnO we have the relation $f = 2.5\ \text{g}^2\ \text{cm}^{-6}$.

Investigations show that k' and k'' are independent of the pressure of oxygen for thick, coherent, compact layers ($\Delta x > 10^{-5}$ cm). Results of investigations by various authors are expressed in Table II in terms of

TABLE II. TARNISHING CONSTANTS k' FOR PURE AND ALLOYED ZINC IN OXYGEN

Material	O_2-pressure (atmos)	Temperature (°C)	k' ($cm^2\ sec^{-1}$)	Author
Zn	1	390	8×10^{-15}	Wagner and Grünewald[a]
Zn	0.022	390	8.4×10^{-15}	Wagner and Grünewald[a]
Zn	0.21 (air)	390	8.4×10^{-14}	Hauffe and Gensch[b]
Zn	...	450	1×10^{-14}	Gebhard[c]
Zn	0.21 (air)	650	5.5×10^{-14}	Krupkowski and Balicki[d]
Zn + 0.1 atom % Al	0.21 (air)	390	5.6×10^{-15}	Hauffe and Gensch[b]
Zn + 1 atom % Al	0.21 (air)	390	5.6×10^{-16}	Hauffe and Gensch[b]
Zn + 0.4 atom % Li	0.21 (air)	390	2.2×10^{-11}	Hauffe and Gensch[b]

[a] C. Wagner and K. Grünewald, *Z. physik. Chem. (Leip ig)* **B40,** 455 (1938).
[b] K. Hauffe and C. Gensch, *Z. physik. Chem. (Leip.ig)* **195,** 116 (1950).
[c] E. Gebhard, *Z. Metallk.* **37,** 87 (1940).
[d] A. Krupkowski and S. Balicki, *Métaux et corrosion* **12,** 89 (1937).

the constant k'. The results of tarnishing investigations involving alloys of zinc with aluminum and lithium are expressed in terms of k' in the same table. The tarnishing velocity is somewhat smaller for aluminum

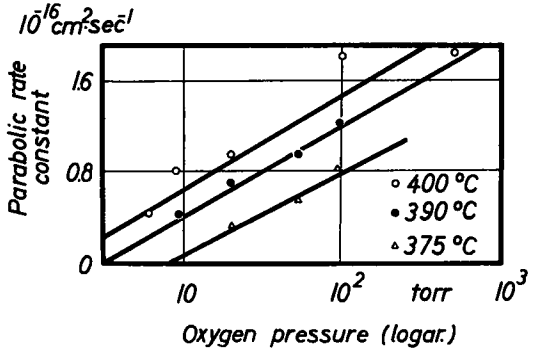

FIG. 8. Thin layer (thickness less than 10^{-5} cm). Parabolic rate constant k' for oxidation of zinc as a function of oxygen pressure. After Moore and Lee.[26]

alloys than for pure zinc under the same conditions; the velocities for lithium alloys are somewhat greater.

The constants k' obtained are somewhat smaller and depend upon oxygen pressure (Fig. 8)[26] in the case of thin films ($\Delta x < 10^{-5}$ cm) and for small values of the oxygen pressure. Such values are not included in

[26] W. J. Moore and J. K. Lee, *Trans. Faraday Soc.* **47,** 501 (1951).

the table. One cannot convert the measurements of the diffusion coefficients on single crystals into constants k' and k'' without making special assumptions. Therefore, this conversion will be treated in the general discussion of diffusion processes.

b. Crystals and Sintered Specimens

Direct measurements of the diffusion coefficients of imperfections in crystals and sintered specimens have been made by heating in zinc vapor

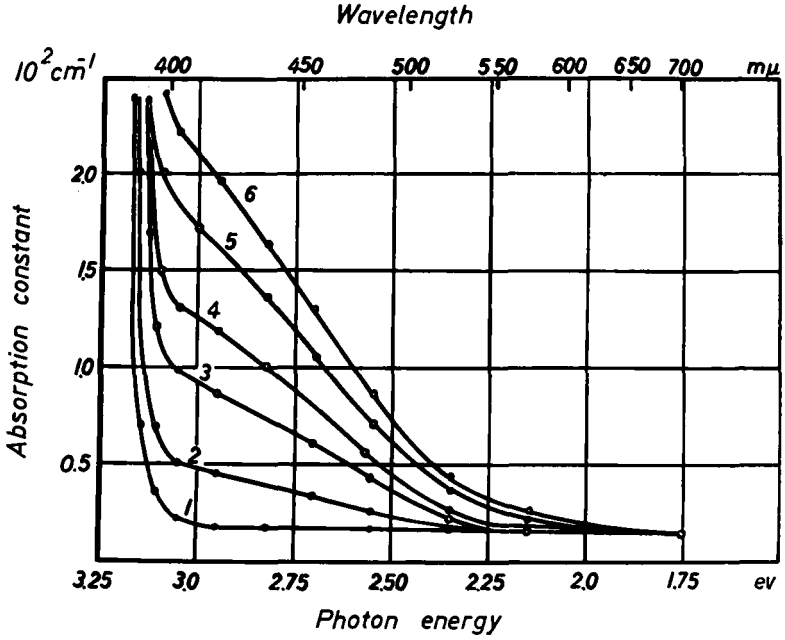

FIG. 9. Crystals. Absorption spectrum on the edge of the ultraviolet, fundamental absorption band after various times of heating in saturated zinc vapor at 940°C (*b* absorption). 1:0 min, 2:10 min, 3:30 min, 4:1 hr, 5:2 hr, 6:4 hr. Compare Figs. 19 and 20. After Arneth.[27]

(*1*) *Observation of diffusion by the increase of conductivity of crystals.* The conductivity of a crystal is increased by heating in zinc vapor. Simultaneously, there is an increase in the optical absorption in the infrared region of the spectrum, and an absorption which is close to the fundamental absorption edge appears (*b* absorption, Section 11b and Figs. 19 and 20). If one allows the zinc vapor to act upon the crystals for different lengths of time and follows both the *b* absorption and the electrical conductivity after quenching the specimens, one finds that these quantities grow and attain a saturation value (Fig. 9).[27] The time

[27] R. Arneth, Diplomarbeit, University of Erlangen, 1955.

required is the same for the absorption and the conductivity. The diameters of the crystals range from 1.7 to 6.4 $\times$ 10^{-2} cm. If one heats a saturated crystal in vacuum or in air to a definite temperature T and measures the conductivity simultaneously, one finds a decrease with time which can be described in terms of the equations for diffusion. Thus, one can derive a diffusion coefficient for the process. This coefficient is always the same if the heating temperature is the same and if the crystals have been given prior treatment in zinc vapor at the same temperature θ.

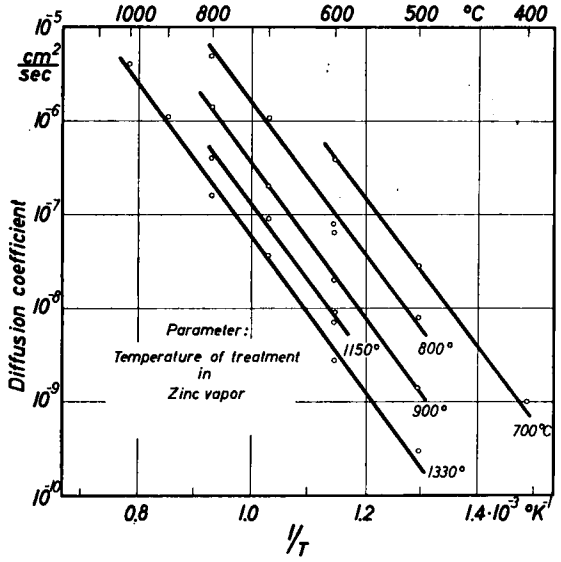

FIG. 10. Crystals. Diffusion coefficient of "zinc" determined from the decrease of the conductivity by diffusion, as a function of temperature. Activation energy 1.7 ev. After Pohl.[28]

If the temperature T is kept fixed and the temperature θ of prior treatment is varied, the diffusion coefficient changes in a wide range. In fact, the diffusion coefficient is small when the temperature θ is large and conversely.

Figure 10 shows values of the diffusion coefficient as a function of temperature as determined from the decay of conductivity during annealing.[28] The parameter given with each curve is the temperature at which the specimen was heated in zinc vapor before the annealing. Quantitively one can represent the diffusion coefficient in the following way:

$$D = D_0 \exp\left(\frac{1 \text{ ev}}{k\theta} - \frac{1.7 \text{ ev}}{kT}\right), \qquad D_0 = 1.6 \times 10^{-2} \frac{\text{cm}^2}{\text{sec}} \tag{7.3}$$

[28] R. Pohl, Dissertation, University of Erlangen, 1957.

θ = temperature of treatment in Zn vapor

T = temperature of removal of extra conductivity by diffusion.

The time required to anneal a specimen at a given temperature is many times (about 10^3) smaller than the time required to reach the saturation value of the conductivity of a virgin specimen when exposed to zinc vapor for the first time at the same temperature. Similarly, the optical absorption grows much more slowly in a virgin specimen than it vanishes when the specimen is exposed to air or a vacuum. Nevertheless, the optical bleaching takes place more slowly than the decrease in conductivity. In contrast, one can reproduce the absorption and the conductivity by heating in zinc vapor after bleaching in about the same time as that required for bleaching, that is, many times faster than when treating a virgin specimen in zinc vapor for the first time. The time for subsequent bleaching remains unchanged. The diffusion constant is determined by the highest temperature θ of treatment in zinc vapor.

(*2*) *Observation of diffusion with the use of radioactive zinc in sintered specimens and in single crystals.* The diffusion of zinc has been examined with the use of radioactive zinc in a number of investigations. The methods employed by different authors are not the same. As a result, it is not known whether the results differ because of differences in the method of measurement or as a result of variations in the properties of the samples. The zinc isotope Zn^{65} is used in this work. It is transformed into Cu^{65} as a result of K capture. Gamma radiation having an energy of 1.14 Mev is emitted, in addition to positrons. The half-life is 250 days.

Lindner[29] employed sintered tablets having a density in the range from 4.6 to 5.5 g/cm^3. Compact material has a density of 5.6 g/cm^3. Radioactive zinc was either evaporated in a thin sheet and oxidized, or it was incorporated in a second sintered tablet which was pressed against the inactive one. In the case of the thin deposits, the decrease of the positron activity was observed as the specimen was heated. As diffusion proceeded, the thickness of the absorbing layer through which the positrons had to penetrate, increased. Thus, a value of the diffusion coefficient D could be obtained. The value found at 1000°C was

$$D_{1000°C} = 2.10^{-13} \frac{\text{cm}^2}{\text{sec}}.$$

The diffusion coefficient could be expressed in the manner:

$$D = 1.3 \exp\left(-\frac{73.7 \text{ kcal/mol}}{RT}\right) \frac{\text{cm}^2}{\text{sec}} = 1.3 \exp\left(-\frac{3.2 \text{ ev}}{kT}\right) \frac{\text{cm}^2}{\text{sec}} \quad (7.4)$$

in the range of temperature between 900 and 1400°C. In the case of the

[29] R. Lindner, *Acta Chem. Scand.* **6**, 457 (1952).

two pressed tablets, observations centered about the increase of gamma activity in the initially inactive tablet as a function of time. The value of the diffusion coefficient obtained for 1000°C was

$$D_{1000°C} = 3.10^{-12} \frac{\text{cm}^2}{\text{sec}}.$$

The following relation was valid:

$$D = 3.5 \exp\left(-\frac{70.4 \text{ kcal/mole}}{RT}\right) \frac{\text{cm}^2}{\text{sec}} = 3.5 \exp\left(-\frac{3.0 \text{ ev}}{kT}\right) \frac{\text{cm}^2}{\text{sec}} \quad (7.5)$$

between 800 and 1400°C. Moore and Secco[30] employed very thin crystals (cross section about 0.01 mm) in their investigations. Zn^{65} was incorporated in the crystals during growth. A decrease in activity was observed when the crystals were heated in inactive zinc vapor. The diffusion coefficient calculated in this way was found to be dependent upon the pressure of the zinc atmosphere. It was larger at high vapor pressures than at small. The diffusion coefficient found at 1000°C in a saturated atmosphere was $D_{1000°C} = 2.3 \times 10^{-12}$ cm²/sec. The diffusion coefficient could be expressed in the form:

$$D = 4.8 \exp\left(-\frac{73 \text{ kcal/mole}}{RT}\right) \frac{\text{cm}^2}{\text{sec}} = 4.8 \exp\left(-\frac{3.2 \text{ ev}}{kT}\right) \frac{\text{cm}^2}{\text{sec}} \quad (7.6)$$

in the temperature range between 900 and 1000°C. The vapor pressure of zinc was held constant at one atmosphere in this work.

Münnich[31] also used single crystals. The crystals were made of inactive material and had a relatively large diameter (about 0.4 mm). They were placed in an atmosphere of radioactive zinc, and the activity was then investigated. Moreover, the distribution of concentration was measured by repetitive etching. It was found that there is a complete exchange of the atoms between the vapor and the crystal near the surface. The diffusion coefficient was determined from the continuous decrease of activity in going from the surface into the interior of the crystal. The values found at 1000°C and 1100°C are as follows:

$$D_{1000°C} \approx 4.10^{-11} \frac{\text{cm}^2}{\text{sec}}$$

$$D_{1100°C} \approx 5.10^{-10} \frac{\text{cm}^2}{\text{sec}}.$$

The dependence on concentration found in this work does not appear to be reliable.

[30] W. J. Moore and E. A. Secco, Indiana University Report, 1955.
[31] F. Münnich, *Naturwiss.* **42**, 340 (1955).

8. Hydrogen

The studies of the diffusion of the imperfections produced by hydrogen exhibit a relatively clear behavior. All the available investigations deal with single crystals.

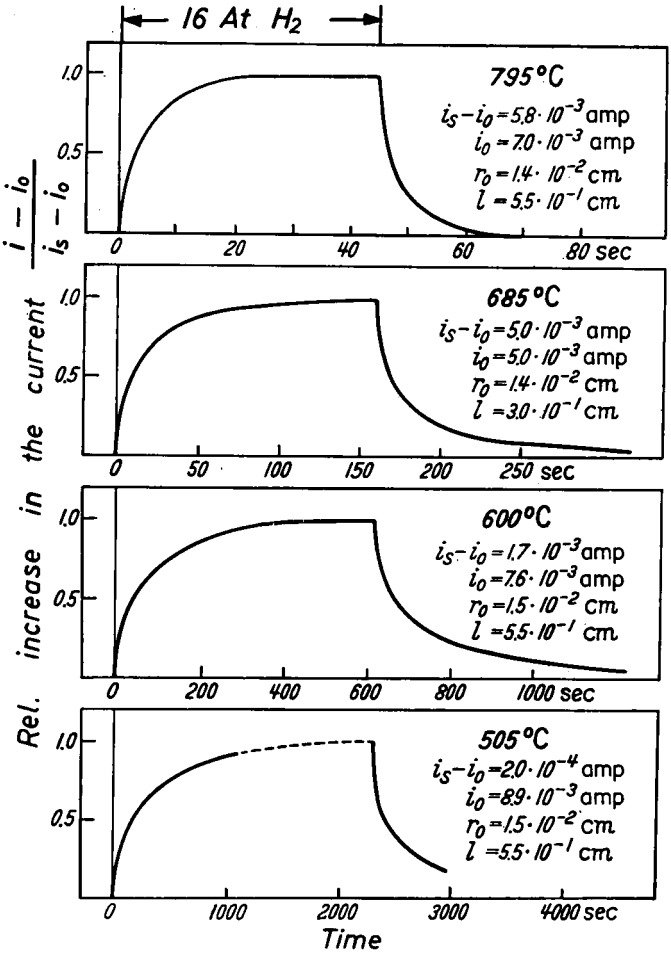

FIG. 11. Crystals. Variation of the current with time during the action of hydrogen (16 atmos) at constant voltage. i_0 = current before introduction of hydrogen. i_s = saturation current. After Mollwo.[32]

Specimens as grown were placed in a closed container, such as a quartz tube. They were provided with electrodes for conductivity measurements. A constant voltage was applied. If one admits hydro-

[32] E. Mollwo, *Z. Physik* **138**, 478 (1954).

gen at a definite pressure into the container at an elevated temperature ($T > 200°C$), one finds an increase in the current until the saturation value is obtained. If the hydrogen is removed, the current sinks to the original value i_0 (Fig. 11).[32] One can describe the variation of the current or the conductivity with time in terms of well-known equations for the penetration of material in an infinitely long cylindrical body by diffusion.

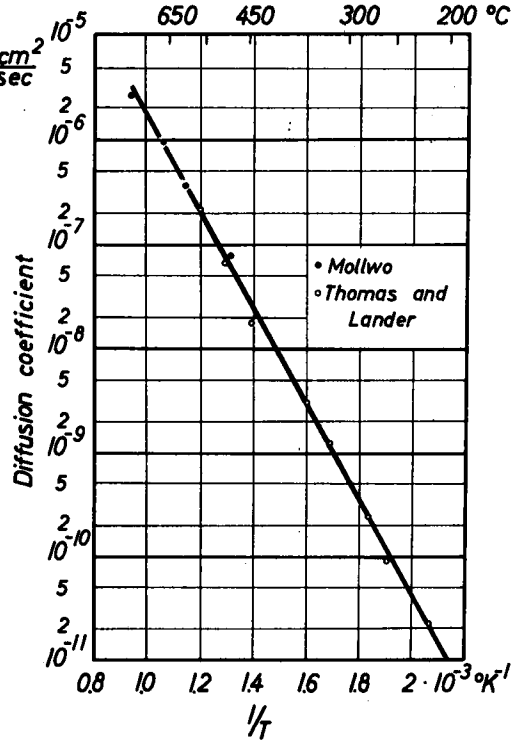

FIG. 12. Crystals. Diffusion coefficient of "hydrogen" obtained from measurements of conductivity as a function of temperature. Activation energy 0.91 ev. After Mollwo,[32] Thomas and Lander.[33]

Conversely, one can determine a diffusion coefficient from the measurements. The values obtained are the same for diffusion in and out of the specimen and are independent of the size of the crystal. The values of the diffusion coefficients found in this way for different temperatures are given in Fig. 12.[32,33] The slope of the line obtained from a Boltzmann plot yields an activation energy of 0.91 ev. The fact that the increase in conductivity actually is associated with a diffusion process in the interior

[33] D. G. Thomas and J. J. Lander, *J. Chem. Phys.* **25**, 1136 (1956).

of the crystal can be demonstrated in the following manner. One interrupts the process of heating the crystal in hydrogen before saturation is obtained and quenches the specimen. The crystal can then be split along a plane perpendicular to the c axis and provided with electrodes. The distribution of conductivity in the cross section may then be examined with a sharp probe. One finds that crystals which are homogeneous

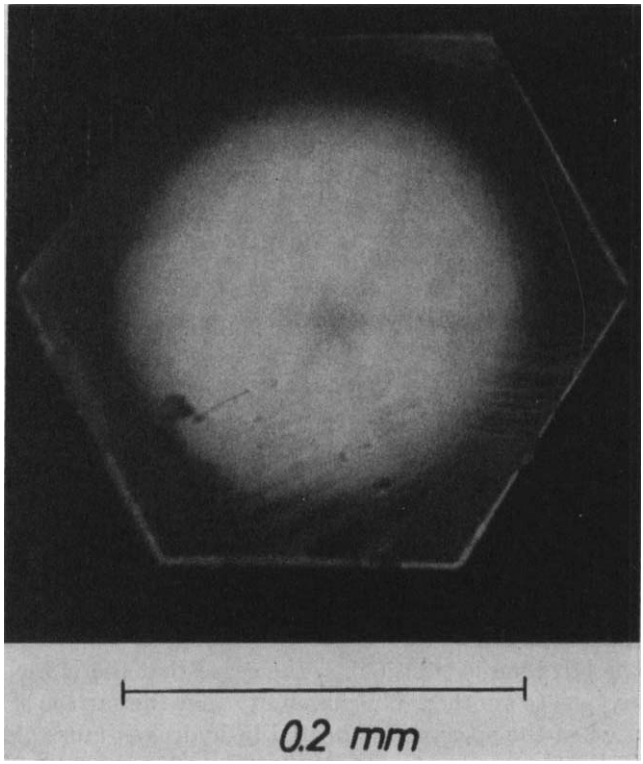

FIG. 13. Crystal. Green luminescence obtained after heating in hydrogen (30 atmos, 40 sec, 600°C) and quenching. Excitation with ultraviolet light (λ = 366 mμ). After Mollwo.[32]

prior to the treatment, now have a high conductivity at the edge and that this decreases continuously toward the center.[34] Such electrical investigations have been accompanied by optical studies. The green luminescence which can be stimulated with ultraviolet light is completely quenched in the most conducting parts near the surface of the crystal. The brightness of luminescence decreases continuously toward the interior of the crystal (Fig. 13). (Compare Section 12c.) The original

[34] E. Mollwo, private communication.

homogeneous distribution of conductivity and luminescence can be re-established by heating.[32]

9. Other Substances

It has also been demonstrated qualitatively that the process of heating in an atmosphere of cadmium[28] produces an increase in the conductivity of a crystal. Similarly, heating in the presence of platinum and nickel at temperatures above 1000°C leads to an increase in conductivity. In contrast to the other cases, however, this behavior has been substantiated only at higher temperatures. One finds the same conductivity as in the untreated crystal at lower temperatures, such as room temperature. More exact investigations of the effect are not available.

10. Discussion of the Diffusion of Imperfections

The question of the manner in which the imperfections are incorporated in the crystals is basic for a discussion of the diffusion of imperfections. Both substitutional and interstitial positions in the lattice are of interest. The relationships presumably would be clearest in those cases in which only one method of incorporation is possible, for example, when one has neutral foreign atoms in interstitial positions. In general, however, the relations are much more complicated. The neutral atom loses an electron, and the electron and ion diffuse separately.

The available evidence indicates that hydrogen diffuses in accordance with a mechanism in which the neutral atom becomes ionized. One must assume, however, that the H^+ does not diffuse freely in the interstitial lattice. Instead, it forms an OH^- ion by joining an O^{--} ion at a normal site.[33,35] The OH^- ion is transient in the sense that the H^+ ion can jump from one oxygen to another. The possibility that the surface of the crystal is reduced when the specimen is heated in hydrogen must also be taken into account. The increase in conductivity in the interior of the crystal could also be a result of the diffusion of an excess of zinc which is produced by reduction at the surface. A similar reduction could be produced by exposing the crystal to cadmium. This alternative mechanism does not receive support from observations of the change in color. The specimens heated in zinc vapor darken, whereas those treated in hydrogen and cadmium do not. The same point of view is supported by the fact that the diffusion coefficient is not sensitive to prior treatment of the specimens (see Section 7b).

Another mechanism for the migration of a foreign substance is one in which an atom or ion in an interstitial position interchanges with one in

[35] G. Parravano and M. Boudart, *Advances in Catalysis* **7**, 50 (1955).

a substitutional position (interstitialcy mechanism).[36] This mechanism does not seem likely in specimens treated with hydrogen, for hydrogen acts as a donor. If hydrogen or alkali metals enter the crystal substitutionally, one would expect them to act as acceptors and, hence, to decrease the conductivity, which is always n type.

The diffusion of excess zinc also appears to take place by a simple process. It has not been demonstrated as yet, however, that the excess zinc is situated in interstitial positions and diffuses by motion of Zn^+ ($Zn_0^{\cdot}$) or Zn^{++} ($Zn_0^{\cdot\cdot}$) ions and electrons. It is also possible that the excess zinc is present in the form of vacancies in the oxygen lattice which are occupied by two electrons. In this case the diffusion would occur by migration of the O^{--} ions of the lattice and electrons. Perhaps both processes occur simultaneously. It is generally assumed, however, that diffusion through interstitial positions is essentially more rapid and dominates in normal investigations. The processes which occur during the *first* heating of crystals in zinc vapor are still very uncertain. The only matter which is certain in this case is that the diffusion of excess zinc is not the limiting factor which determines the rate of increase of the conductivity and absorption. Another relatively slow reaction in the interior of the crystal seems to be responsible for the rate (compare Section 19b).

The relationships which occur when the diffusing substance possesses many states that can be in equilibrium with one another are much more complicated. One case which is easy to comprehend is that in which one of the states (I) does not diffuse and is in equilibrium with another state (II), the concentration C_I of the first state being much higher than that of the second C_{II}. In this case we have the relation

$$D_{II} = D_I \frac{C_I}{C_{II}} \tag{10.1}$$

in which D_I is the formally defined diffusion coefficient for state I. A special case of this kind is that in which D_I is the coefficient of self-diffusion. In the case of a tarnishing reaction one has the analogous relation:

$$D_{II} = k' \frac{C_I}{C_{II}}. \tag{10.2}$$

Processes of this type have not yet been investigated in the diffusion of foreign atoms in zinc oxide. However, they clearly are decisive in the diffusion of radioactive zinc in zinc oxide and in the oxidation of metallic zinc.

[36] F. Seitz, *Acta Cryst.* **3**, 355 (1950).

The investigations of Lindner[29] on the diffusion of radioactive zinc in sintered tablets of zinc oxide may be influenced by diffusion along grain boundaries (cf. Roberts and Wheeler[37]). In contrast, the investigations of Moore and Secco and Münnich indicate that radioactive zinc can enter and leave substitutional positions in the lattice by diffusion. It is not clear on the basis of existing investigations whether the process occurs solely by substitutional diffusion or by interstitial diffusion of an excess of zinc and an exchange with zinc atoms in normal sites. If one assumes that the second mechanism is valid, one can use Eq. (10.1) and the assumptions mentioned above to determine the diffusion coefficient of radioactive zinc from the diffusion coefficient of the excess zinc. The ratio $C_{ZnO}/C_{Zn_0} = 4 \times 10^4$ determined at 1000°C in saturated vapor (Fig. 56) with the assumption that the total excess is interstitial, must correspond to the ratio of the measured diffusion coefficients. Because of the large scattering of the measured values, it does not appear justifiable to use the agreement in a few cases as a proof for this representation of affairs. There seems to be agreement to order of magnitude, however. The investigations of Lindner are excluded in this comparison not only because of the possibility of diffusion along grain boundaries, but also because his specimens were in equilibrium not with zinc vapor but with the oxygen of the air. The concentration of zinc ions in interstitial positions C_{Zn_0} must be substantially lower in this case and is unknown at the present time.

The tarnishing of metallic zinc in oxygen can be described in terms of the following model. A coherent layer of zinc oxide is formed by oxidation of the outermost layers of atoms on the metallic zinc. Excess zinc diffuses through this layer from the metal to the surface and is oxidized there. The thickness of the layer of zinc oxide increases with time as a result of this process. Thus, the transport of zinc produces, first of all, a layer of zinc oxide which cannot diffuse; second, it produces an excess of zinc which can. The concentration of excess zinc decreases from the temperature dependent equilibrium value C_{Zn_0} at the boundary of the metal and the oxide to a value near zero at the boundary of the oxide and the oxygen atmosphere. The diffusion coefficient D_{Zn_0} of the excess zinc is given in terms of the measured tarnishing constant by the relation

$$D_{Zn_0} = k' \frac{C_{ZnO}}{C_{Zn_0}}. \tag{10.3}$$

In any case, the possibility of diffusion of oxygen through the layer of zinc oxide is excluded by the fact that the tarnishing constant is independent of the pressure of oxygen for thick layers. By extrapolation from Fig. 55, one

[37] J. P. Roberts and C. Wheeler, *Phil. Mag.* [8] **2**, 708 (1957).

can obtain the value $C_{Zn_0} = 5 \times 10^{15}$ cm^{-3} for a concentration of excess zinc at equilibrium with saturated vapor at 400°C. Thus in other words, the diffusion constant of the excess zinc should be larger than the tarnishing constant k' by the factor $C_{ZnO}/C_{Zn_0} = 4.2 \times 10^{22}/5 \times 10^{15} \approx 10^7$ at 400°C. In fact, the measured values of the diffusion constant lie between 4×10^{-8} [38] and 10^{-9} cm^2 sec^{-1} or lower;[28] whereas, the tarnishing constant has values between 8×10^{-15} [39] and 1.8×10^{-16} cm^2 sec^{-1}.[26] In other words, the two methods seem to agree in order of magnitude. No space charge effects on the surface have been taken into account in deriving Eq. (10.2). This is permissible according to Hauffe and Engell[40] when the tarnishing layer is thick compared to the exhaustion layer produced by chemisorbed oxygen. They have calculated the influence of adsorbed (not diffusing) oxygen for thin layers and have obtained agreement with the observations of Moore and Lee.[26]

The fact that the concentration of interstitial Zn_0 ions is critical for transport of zinc by diffusion is demonstrated from the interpretation of tarnishing experiments on metallic zinc involving tri- and monovalent metals as admixtures.[41] In general, the reaction governing the formation of Zn_0 is

$$\text{undisturbed ZnO crystal} \rightleftharpoons Zn_0^{\cdot} + e^- + \tfrac{1}{2}O_2 \text{ (gas)}. \qquad (10.4)$$

A high vapor pressure of zinc in the surrounding atmosphere corresponds to a very low concentration of O_2 (gas). The concentration of $Zn_0^{\cdot}$ and e^- is thereby increased. If the ZnO contains aluminum as an addition, one has the relation

$$\text{undisturbed ZnO crystal} + Al_2O_3 \rightleftharpoons 2Al^{+++}_{subst}(Zn) + 2e^- + 2ZnO + \tfrac{1}{2}O_2 \text{ (gas)}. \qquad (10.5)$$

The electron concentration increases with increasing content of Al_2O_3 when the concentration of oxygen pressure is maintained constant (see Section 18c). According to Eq. (10.4), the concentration of $Zn_0^{\cdot}$ must decrease at the same time. This implies a decrease in the tarnishing constant k' according to Eq. (10.3) in agreement with experiment. In the case of monovalent admixtures, such as Li_2O, the following relation is valid:

$$\text{undisturbed ZnO crystal} + Li_2O \rightleftharpoons 2Li^{+}_{subst}(Zn) - 2e^- + 2ZnO - \tfrac{1}{2}O_2 \text{ (gas)}. \qquad (10.6)$$

[38] D. G. Thomas, *J. Phys. Chem. Solids* **3**, 229 (1957).
[39] C. Wagner and K. Grünewald, *Z. physik. Chem.* (*Leipzig*) **B40**, 455 (1938).
[40] H. J. Engell and K. Hauffe, *Metall* **6**, 285 (1952).
[41] K. Hauffe and C. Gensch, *Z. physik. Chem.* **195**, 116 (1950).

The electron concentration decreases with increasing concentration of lithium, if the pressure of oxygen is maintained constant. The concentration of $Zn_0^{\cdot}$ and, hence, the tarnishing constant k' increase in agreement with experiment. A quantitative verification of these principles is difficult because of the large scattering in the experimental results.

IV. Optical Properties

11. Absorption and Refraction

a. Materials without Admixtures

Pure zinc oxide possesses a white color when observed at room temperature in powdered or sintered form. Thin layers and single crystals are colorless and transparent. Zinc oxide becomes colored during heating,

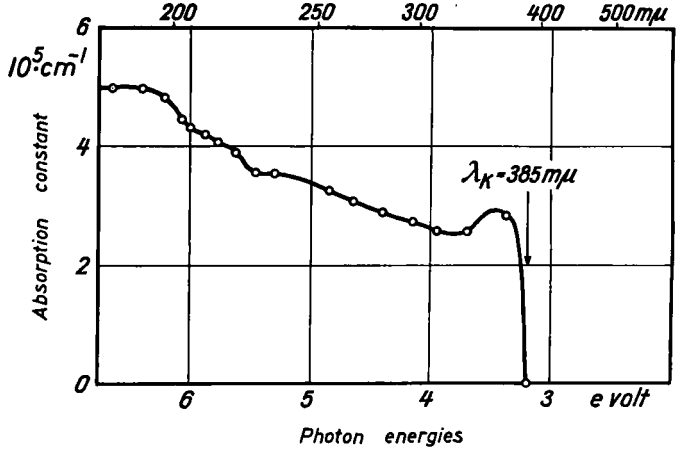

Fig. 14. Thin layer. Absorption spectrum at room temperature. The absorption constant has the value of about 10^5 cm^{-1} for $\lambda_K = 385$ mμ. After Mollwo.[6]

making the transition from light yellow to orange with increasing temperature. The original color is restored, however, when the specimen is cooled again. This coloration is produced by a shift of the fundamental absorption edge which moves from the ultraviolet into the visible part of the spectrum at elevated temperatures. The form of the intrinsic absorption spectrum can be observed only in thin layers because of the very high absorption coefficient. Up to the present time such measurements have been made only on layers formed by evaporation (Fig. 14). A very steep increase in the absorption constant is found at about 385 mμ $\triangleq$ 3.2 ev. One observes a maximum at shorter wavelengths and

then a mildly rising region.[6] The absorption in the region of steep descent toward long wavelengths (the edge) has been investigated as a function of temperature.[42] The shift toward longer wavelengths at elevated temperatures, found in many substances, has been observed (Fig. 15). The energy at which the absorption constant has a value of 1 cm^{-1} has the displacement coefficient -9.5×10^{-4} ev/deg in the range between 300 and 1400°K.

Incidentally, it has been demonstrated[11] that sintered specimens free of additions assume a definite yellow color as a result of mechanical

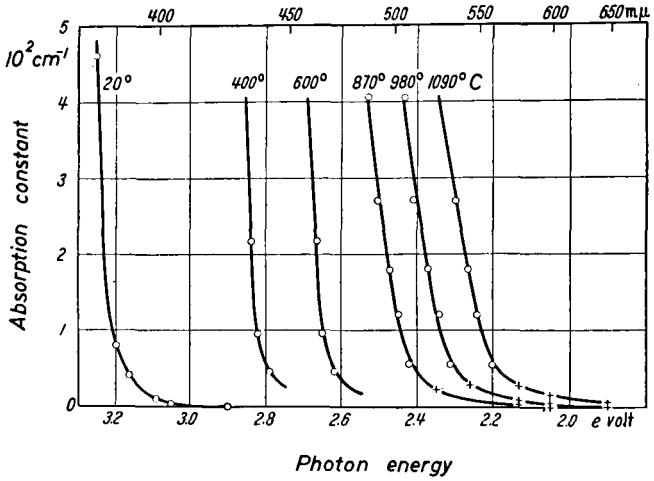

FIG. 15. Crystal. Absorption spectrum on the long wavelength edge of the fundamental band at different temperatures. Light vector $E \parallel c$ axis. The measured points designated with + have been obtained from emission measurements. After Mollwo.[42]

working. This color disappears when the surface is etched. Spectral absorption measurements have not been made yet of the effect. Qualitative observations indicate, however, that such treatment produces a new absorption band in the blue region of the spectrum (compare Sections 11b and c).

Measurements on the absorption of zinc oxide powder in the infrared were made in 1928[43] and in 1937.[44] The first work indicated a sequence of absorption maxima at the positions λ = 15.2, 13.95, 12.35, 11.55, 8.65, 8.1, and 6.7 μ. If interpreted as combinational vibrations, the observations led to the conclusion that the zinc oxide lattice has fundamental

[42] E. Mollwo, *Z. angew. Physik* **6**, 257 (1954).
[43] S. Tolksdorf, *Z. physik. Chem.* **132**, 161 (1928).
[44] M. Parodi, *Compt. rend.* **204**, 1111 (1937).

vibrations at 28, 22, and 15.2 μ. The measurements of Parodi demonstrated the presence of two bands at 30 and 22.4 μ. Observations with thin evaporated layers indicate no absorption peaks in the range from $\lambda = 0.4$ μ to $\lambda = 13$ μ. On the other hand, one does find absorption maxima at $\lambda = 10.1$ μ and 11.5 μ in sintered layers 20 μ in thickness.[27] The same absorption peaks were found in the spectrum of a single crystal of zinc oxide 60 μ thick having leaflet form (Fig. 16).[27] It will be noted that maxima also occur at 8.1 and 6.7 μ.

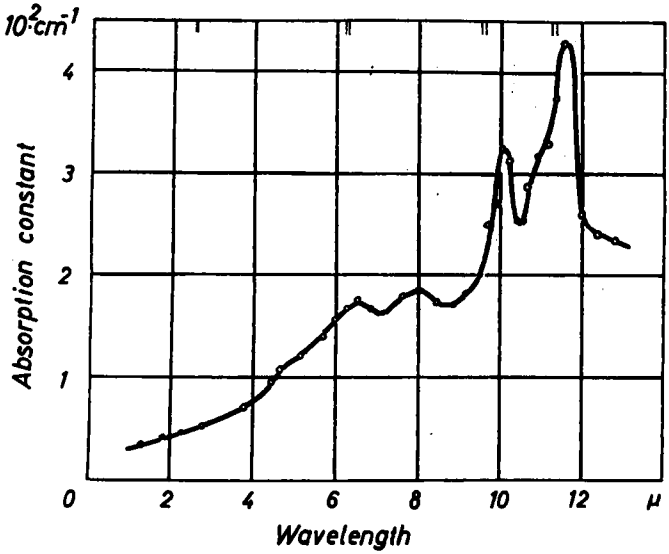

FIG. 16. Crystal, plate 6×10^{-3} cm thick. Absorption spectrum in the infrared spectral range. The double lines on the upper edge give the spectral slit width. After Arneth.[27]

The index of refraction of zinc oxide has been measured in the visible region of the spectrum on natural[45,46] as well as on synthetic single crystals.[42] Table III contains values for the synthetic crystals. The high dispersion in the blue region of the spectrum is noteworthy. The dispersion $dn/d\lambda$ attains the value $-3.5\ \mu^{-1}$ at $\lambda = 405$ mμ. The natural crystals employed were red in color and somewhat impure. Their index of refraction is higher than that of the synthetic material by a few units in the third decimal place. The article by Strong[47] contains a discussion of the reflection of zincite in the infrared.

[45] J. Bermann, *Am. Mineralogist* **12**, 168 (1927).

[46] A. N. Winchell, "Microscopic Characters of Minerals," 2 ed. Wiley, New York, 1931.

[47] J. Strong, *Phys. Rev.* **38**, 1818 (1931).

TABLE III. CRYSTAL
Refractive indices n_ω and n_ϵ at room temperature. Error limits ± 0.002[a]

$\lambda[m\mu]$	$n_\omega(E \perp c)$	$n_\epsilon(E \parallel c)$
405	2.239	2.248
436	2.137	2.151
460	2.097	2.115
492	2.064	2.081
497	2.059	2.076
546	2.025	2.041
578	2.011	2.028
589	2.009	2.024
610	2.001	2.017
671	1.984	2.001

[a] After E. Mollwo, *Z. angew. Physik* **6**, 257 (1954).

b. Crystals with Admixtures

The additions discussed in Section 6, namely, indium, copper, hydrogen, and zinc have a significant effect on the absorption spectrum of zinc oxide crystals. In all four cases the rise of the absorption constant in the transition from the visible to the infrared is changed. No selective peaks characteristic of the individual additions have been observed (Figs. 17, 20). The value of the absorption constant at a definite wavelength increases with the conductivity of the crystal. In the case of a crystal doped with hydrogen, the increase ΔK in absorption constant is proportional to the conductivity σ (Fig. 18). This relation appears to be at least approximately independent of the form of the addition. The absorption in hydrogen-doped crystals at short wavelengths is lower than in crystals containing other additions and the same value of the conductivity. It should be noted that crystals without any admixtures also exhibit an absorption in the infrared which is correlated with their conductivity. In the case of additions which are introduced by diffusion and then removed by subsequent heating, the rise and fall of the conductivity has a corresponding change in the infrared absorption associated with it.[48] Crystals containing a very large addition of copper have a very low conductivity (compare Section 19b) and weak absorption. In contrast, crystals containing a large amount of indium have a very high conductivity. The infrared absorption is so strong that the short wave extension reaches into the visible spectrum and causes the crystals to be colored blue.[25]

The fundamental absorption in the ultraviolet, in particular, the region of the edge, remains nearly unchanged as a result of additions

[48] R. Arneth, Dissertation, University of Erlangen, 1959.

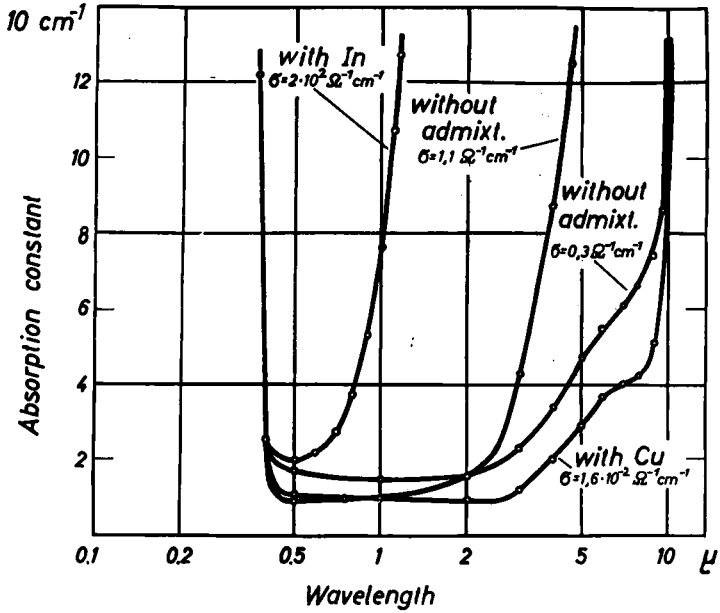

FIG. 17. Crystals without intentional addition, and with additions of indium and copper. Absorption spectrum. The conductivity of the crystals is indicated on the curves. After Arneth.[48]

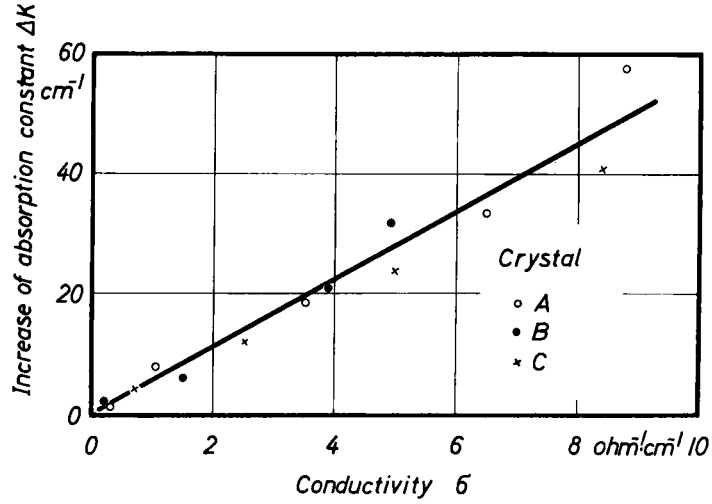

FIG. 18. Crystal heated in H_2. The increase ΔK of the absorption constant ($\lambda = 4\,\mu$) as a function of the conductivity σ. $\Delta K = K_\sigma - K_0$. K_σ is the absorption constant measured at conductivity σ, whereas K_0 is the extrapolated value for conductivity $\sigma = 0$. Crystal A: $K_0 = 42\ \mathrm{cm}^{-1}$. Crystal B: $K_0 = 24\ \mathrm{cm}^{-1}$. Crystal C: $K_0 = 63\ \mathrm{cm}^{-1}$. After Arneth.[48]

of indium, copper, and hydrogen. In contrast, crystals which have been heated in zinc vapor display a new characteristic absorption immediately on the long wavelength side of the ultraviolet edge (*b* absorption, Fig. 19), as well as the increase in absorption in the infrared. The new absorption gives the crystals a yellowish color. Again, it is found that the absorption constant at a given wavelength increases with increasing conductivity of the crystal. This correlation is observed, however, only when the crystal is quenched immediately after being heated in zinc

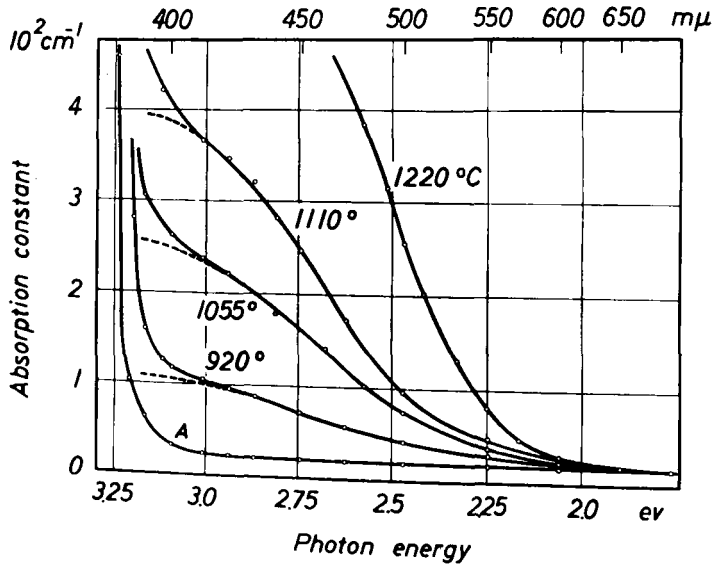

FIG. 19. Crystals. Absorption spectrum (20°C) on the edge of the ultraviolet fundamental band after heating in zinc vapor to different temperatures. *b* absorption. Curve *A* is prior to treatment. After Scharowsky.[23]

vapor.[23] The connection between the absorption and conductivity is not a simple one. In particular, one can diminish the conductivity and the absorption in the infrared by heating the crystal in a vacuum or in air (Section 7) without altering the *b* absorption band observed at the foot of the absorption edge. The latter absorption vanishes only after a long tempering procedure, during the early part of which the conductivity attains its constant low value.

A survey of numerous measurements of the absorption spectrum of zinc oxide is given in Fig. 20. The measurements on thin layers (fundamental absorption in the ultraviolet) and synthetic crystals are presented simultaneously.

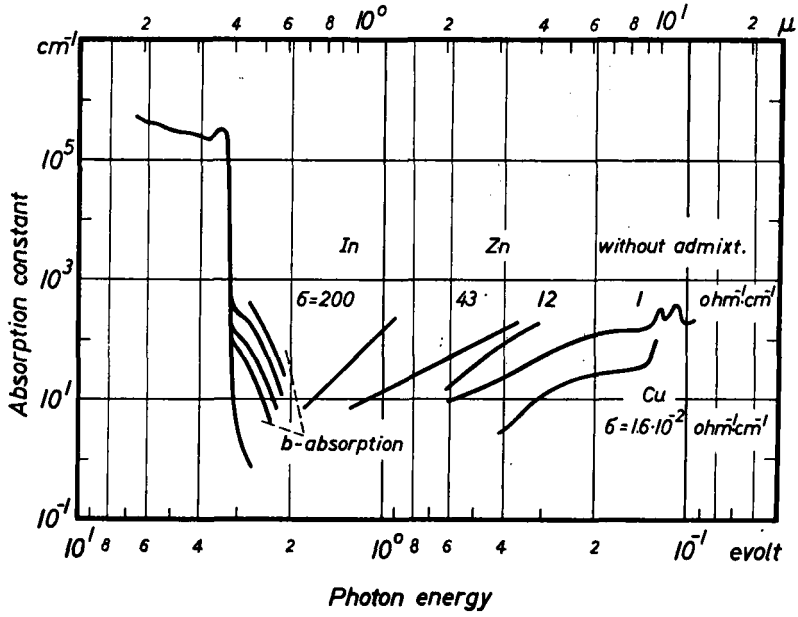

FIG. 20. Survey of the absorption spectrum of zinc oxide with and without additions. The *b* absorption is produced by heating in zinc vapor. The absorption constant is coupled with the conductivity σ in the spectral range at long wavelengths.

c. Discussion of the Absorption

The absorption spectrum of zinc oxide free of additions fits in with the general experience concerning absorption in solids. By extrapolating the position of the absorption edge to 0°K, one obtains a spacing of the order of 3.4 ev between the conduction and the valence band. The extraordinarily rapid rise of the absorption edge is noteworthy. There is no evidence for a secondary shelf having an absorption coefficient of the order of 10^2 cm^{-1}, as is found in germanium and ascribed to indirect transitions. The selective absorption bands found in the infrared may well originate in lattice vibrations (Fig. 16), since they appear to be the same, at least in part, and of comparable intensity in specimens having very different origin. Moreover, the rise in continuous absorption in the infrared which is connected in an obvious way with the electrical conductivity partially is to be explained in terms of transitions involving "free" electrons in the conduction band.[49,50] (See also the additional literature referred to in Jaumann.[49]) However, transitions from high-lying

[49] J. Jaumann and R. Kessler, *Z. Naturforsch.* **11a**, 387 (1956).

[50] H. Y. Fan and M. Becker, "Semiconducting Materials." Butterworths, London, 1951.

discrete states into the conduction band are also possible. This process predominates according to preliminary measurements of the temperature dependence of absorption. Moreover a correlation between conduction and absorption can be expected in this case.

In this connection the additional absorption produced near the edge of the fundamental band by heating the crystal in zinc vapor is very interesting. It seems highly unlikely that the early interpretation of this peak in terms of the absorption of Zn^+ ions is correct. Experimental facts described above make it seem much more likely that the absorption peak is a result of a change in the lattice of the crystal, for example, as a result of the production of lattice defects. These could be produced as a result of the penetration of the zinc. The lattice recovers only slowly when the excess of zinc is removed (compare also Section 7). An explanation in terms of foreign atoms which react with the excess of zinc seems very unlikely in view of the relatively high absorption constant which can be attained in undoped crystals.

12. Light Emission

a. Thermal Excitation

If a zinc oxide crystal is heated, it begins to glow at a temperature between 700 and 800°C with a color in the range from blue-green to yellow-green depending upon the thickness of the crystal. The emission shifts to longer wavelengths as the temperature increases. The emission spectrum approaches that of a black-body more and more nearly with increasing thickness of the crystal. In fact, the crystal emits in a manner closely resembling that of a gray radiator for thickness of a few millimeters. The emission spectrum depends upon the polarization of the light. The difference actually is not great, the emission color for light having the electric vector polarized parallel to the c axis being definitely more yellow than that for light polarized at a right angle ($E \perp c$).

The emission spectrum has been compared on a monochromatic basis with the radiation from platinum, deposited in the form of a thin reflecting layer on a part of the crystal under investigation.[42] At short wavelengths in the region of more intense absorption, the zinc oxide crystal emits somewhat more strongly than the platinum. The situation is inverted at longer wavelengths (Fig. 21). The emissivity of platinum is almost independent of wavelengths and is approximately 0.4 compared to that of a blackbody. Therefore, zinc oxide radiates somewhat less than a blackbody having the same temperature at all wavelengths and temperatures. Thin layers of zinc oxide indicate the same behavior[51] (Fig. 22) if the influence of scattering is neglected.

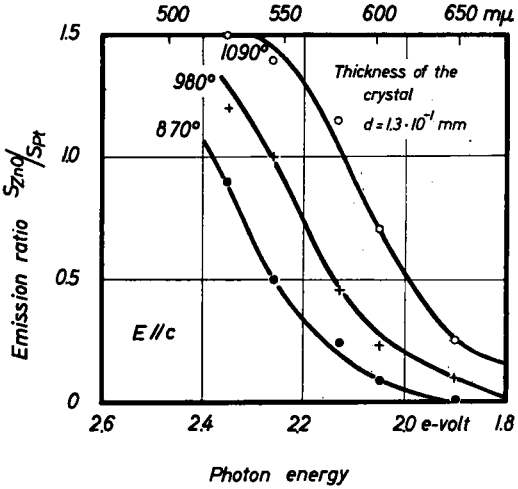

FIG. 21. Crystal thickness 1.3×10^{-2} cm. Spectral distribution of light emission at high temperatures, measured by comparison with the emission of platinum. After Mollwo.[42]

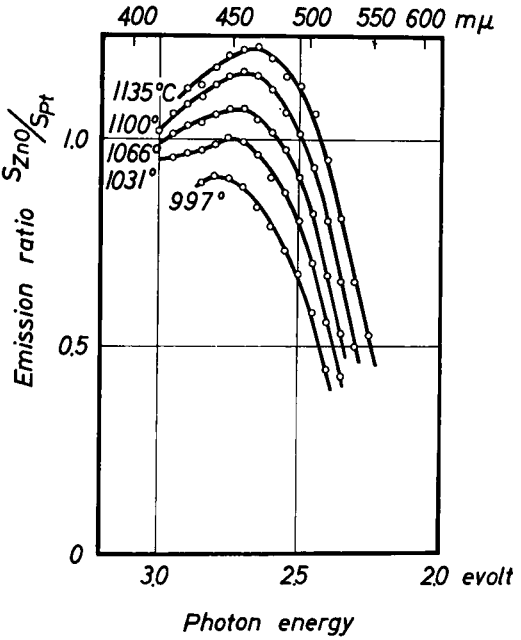

FIG. 22. Thin sintered layer, thickness about 10^{-3} cm. Spectral distribution of the light emission at high temperatures, relative to the radiation from platinum. After H. Rupprecht.[51]

[51] H. Rupprecht, Diplomarbeit, University of Erlangen, 1950.

b. Discussion of Thermal Excitation

Since the thermal glow of zinc oxide deviates from the radiation of a blackbody,[51a] it was regarded as a special form of luminescence for a long period of time. This luminescence, however, was not viewed as identical with the ordinary thermoluminescence obtained by heating phosphors after excitation at low temperatures. The investigations described above and similar Russian work[52] show that this assumption is false. The emission is pure thermal radiation and can be explained completely with the help of Kirchhoff's law.

According to Kirchhoff's law, each body emits in proportion to its absorptivity. It may be seen from Fig. 20 that pure zinc oxide absorbs in the visible part of the spectrum only at short wavelengths. As a result, it can emit only there. This behavior is characteristic only of those substances whose absorption drops sharply on the short wavelength side of the visible spectrum as one moves in the direction of longer wavelengths. Zinc oxide provides one of the few examples of such a substance. With increasing temperature, the absorption shifts toward longer wavelengths. The emission also shifts, in sharp contrast to the behavior of ordinary glowing bodies. Zinc oxide is optically anisotropic; hence, the emission is different for the two directions of polarization and, in fact, is greater at long wavelengths for light having the electrical vector parallel to the c axis than for that having the vector perpendicular to it. This is exactly what one would expect on the basis of the general relationships between dispersion and absorption, if the refractive index n_r is greater for light polarized parallel to the c axis than for that perpendicular to it, as is shown for zinc oxide in Table III. Finally, we may note that it is also a consequence of Kirchhoff's law that the relationships will be somewhat different for polycrystalline specimens which scatter intensely. One must take account of the diminution of light by scattering as well as by true absorption in discussing the absorption in such materials. Nevertheless, Fig. 22 also shows that there is a clear relationship with absorption, particularly the intense decrease at long wavelengths. If one extrapolates the position of the maximum of emission to lower temperatures, one obtains the value for which the absorption maximum occurs at room temperature, as shown in Fig. 14.

If one multiplies the measured values given in Fig. 21 with the relative emissivity of platinum and with Planck's emission curve, one obtains

[51a] Similar deviations are known in ZnS and TiO_2 and, less frequently, in many other materials.

[52] V. M. Kudryatseva and G. J. Sinyapkina, *Doklady Akad. Nauk SSSR* **59,** 1411 (1948); *Phys. Abstr.* **A52,** 1829 (1949).

the absolute value of the emissivity of zinc oxide as a function of wavelength. The result, shown in Fig. 23, is an emission band of the same type as that observed in the recombination of injected carriers. Such recombination has been studied experimentally and theoretically in the case of germanium and silicon.[53] Viewed in this way, one can regard the thermal radiation of zinc oxide as a thermally stimulated recombination radiation,

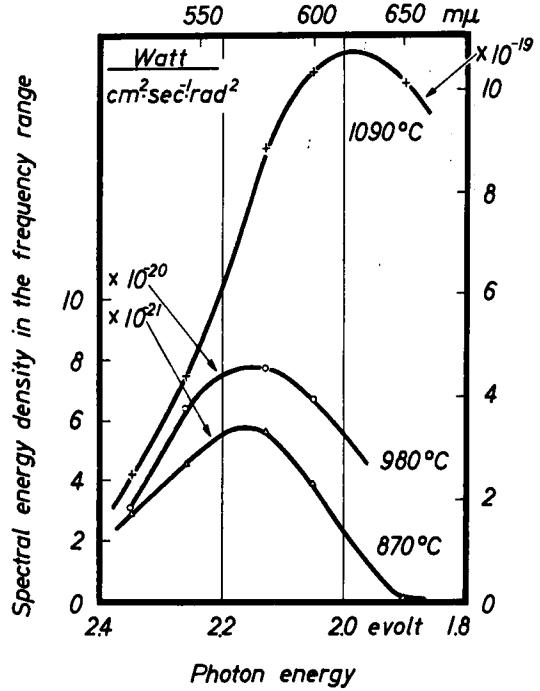

FIG. 23. Spectral energy density in the frequency range as a function of the photon energy. The curves are calculated from those of Fig. 21.

that is, as a result of radiative recombination of electron-hole pairs which are produced by thermally induced band to band transitions.

If one evaluates the curves given in Fig. 23 in this way and takes account of the absorption, one obtains the recombination rate R given by the relation

$$R = \int_0^\infty \frac{4\pi n_r^2 K(\nu)}{1 - e^{-K(\nu)d}} \times \frac{S_\nu}{h\nu} \times d\nu. \tag{12.1}$$

Here S_ν is the quantity represented in Fig. 23; n_r is the refractive index; $K(\nu)$ is the absorption constant given in Fig. 15; and d is the thickness

[53] W. van Roosbroeck and W. Shockley, *Phys. Rev.* **94**, 1558 (1954).

TABLE IV. RADIATIVE RECOMBINATIONS ON THERMAL EXCITATION

Temperature (°C)	Recombination rate R (cm^{-3} sec^{-1})	Optical band gap (ev)	Intrinsic carrier concentration n_i (cm^{-3})	Recombination coefficient $r = R/n_i^2$ (cm^3 sec^{-1})	Recombination cross section $\sigma = r/v$ ($v = \sqrt{3kT/m}$) (cm^2)	Minority carrier lifetime $\tau = 1/rn$ (for $n = 10^{17}$ cm^{-3}) (sec)
870	5.5×10^{15}	2.43	8.4×10^{14}	7.8×10^{-15}	3.4×10^{-22}	1.3×10^{-3}
980	1.2×10^{17}	2.35	4.1×10^{15}	7.1×10^{-15}	3.0×10^{-22}	1.4×10^{-3}
1090	$\approx 2.5 \times 10^{18}$	2.20	2.1×10^{16}	6×10^{-15}	2.4×10^{-22}	1.7×10^{-3}

of the crystal, namely, 0.13 millimeter. From this one obtains the values assembled in Table IV. As is found in the case of other materials, the cross section for recombination of electrons and holes by radiation is extraordinarily small and depends on the temperature almost not at all.

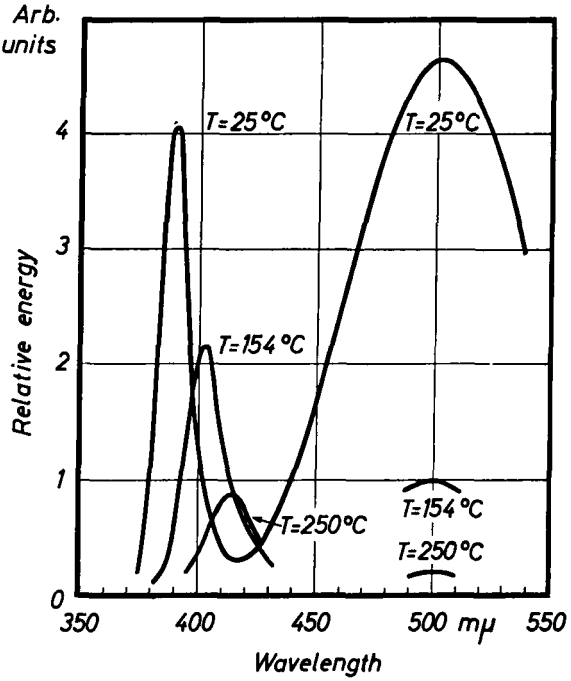

FIG. 24. Zinc oxide powder. Spectral distribution of luminescence at different temperatures. Excitation by electrons with 2×10^4 ev of energy. After Nicoll.[54]

[54] F. H. Nicoll, *J. Opt. Soc. Am.* **38**, 817 (1948).

c. Excitation by Photons and Electrons

Zinc oxide, which has been prepared in an appropriate way, can be made to luminesce by exposing it to radiation of short wavelength or to electron bombardment. The spectrum usually consists of a narrow band in the ultraviolet and a broad band in the green (Fig. 24). The ratio of intensities depends upon the means of excitation and the methods of preparation.

More explicitly, the ultraviolet emission increases relative to the green at higher densities of excitation. It is particularly notable when the zinc oxide has been prepared by burning zinc vapor or by calcining in oxygen, that is, under oxidizing conditions.[55] In contrast, one obtains the green band predominantly when the zinc oxide has been prepared at high temperatures (1200°C) under reducing conditions, for example,[56] by calcining zinc oxide in H_2 or by calcining ZnO + 1% ZnS in an inert atmosphere such as nitrogen. In the latter case the reduction occurs as in accordance with the reaction 2ZnO (lattice) + ZnS (lattice) $\rightarrow$ SO_2 + 3Zn (excess in ZnO). In agreement with this, pure zinc oxide is not reduced on being calcined with N_2 and indicates, accordingly, only the ultraviolet band. Zinc oxide which has been prepared by calcining zinc sulfide or zinc carbonate in air exhibits only the green band.[57] This can be intensified by addition of 0.05% of lead and suppressed by an addition[58] of 0.001% of Mn. The green luminescence can also be destroyed irreversibly by mechanical working of the crystals (pressure quenching). It seems sure to conclude from the method of preparation that neither the ultraviolet or the green luminescence require foreign atoms as activators.

If one permits zinc or hydrogen to diffuse into the crystal at temperatures below 1000°C, the green luminescence is quenched reversibly. The electrical conductivity increases at the same time. There is a clear correlation between the two quantities: the green luminescence is more intense, the smaller the conductivity.[32] The ultraviolet emission is scarcely affected by this process. If anything, it increases with the quenching of the green luminescence. One can recover the initial state completely by heating crystals treated in this manner in air or in a vacuum. This correlation between conductivity and the intensity of the green luminescence is not restricted to the introduction of hydrogen and zinc. Each of the additions which raises the conductivity, for example, indium (see

[55] H. W. Leverenz, "An Introduction to Luminescence of Solids," p. 218, Wiley, New York, 1950.
[56] F. A. Kröger and J. A. M. Dikhoff, *J. Electrochem. Soc.* **99**, 144 (1952).
[57] H. Gobrecht, D. Hahn, and K. Scheffler, *Z. Physik* **139**, 365 (1954).
[58] H. W. Leverenz, *R.C.A. Rev.* **7**, 199 (1946).

Section 19b), weakens the intensity of luminescence. Figure 25 shows an instructive example. An unknown addition was introduced into the crystal under investigation during its growth. The addition had the effect of raising the conductivity. By making measurements with a light probe and a potential probe one can follow the inverse variation of conductivity and luminescence in detail over the cross section of the crystal.[34]

Zinc oxide powder that has been given an intensely oxidizing treatment has an orange luminescence having a wide band, which lies between

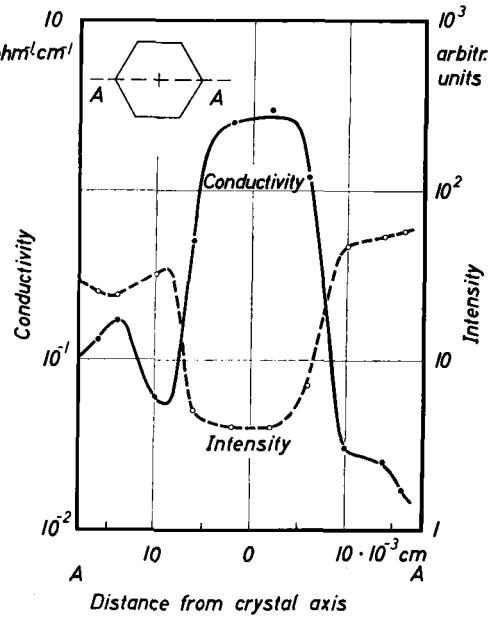

FIG. 25. Crystal. Distribution of the intensity of green luminescence and of the conductivity over the cross section of an inhomogeneous crystal, measured with a potential probe and a light probe. After Mollwo.[34]

500 and 800 mμ, and a maximum near 610 mμ. This band is mentioned frequently in the older literature.[59] One can also obtain[60] it by incorporating Ga, Al, Gd, Cl, or Br in concentrations in the range of 10^{-5} to 10^{-3} which are used as coactivators in zinc sulfide phosphors. The orange luminescence is weak compared with the green and, hence, has not been studied extensively as yet.

The energy efficiency of the luminescence of the green band under

[59] E. Beutel and A. Kutzelnigg, *Monatsh. Chem.* **55,** 158 (1930); **57,** 9, 15 (1931); **61,** 69 (1932); **70,** 297 (1937).

[60] F. A. Kröger and H. J. Vink, *J. Chem. Phys.* **22,** 250 (1954).

ultraviolet excitation is of the order[61] of 20%. In other words, it is of the same magnitude as in other good phosphors. Excitation with electrons gives lower efficiency,[61a] about 7%, and can be produced at the extraordinarily low energy of 3 ev.[62,63] According to new investigations,[64] only a few tenths of an ev are needed. The energy efficiency for the ultraviolet band with electron excitation is about 0.2%.[61a]

At increasing temperatures (Fig. 24), the green band diminishes more rapidly than the ultraviolet band, so that in practice only the latter

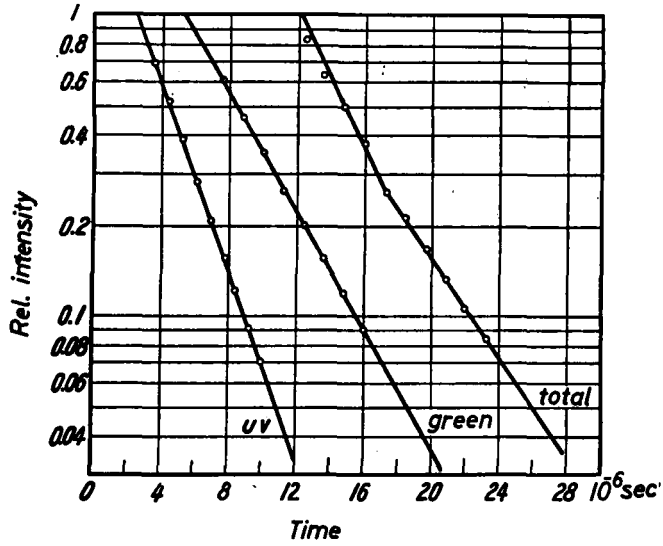

FIG. 26. Zinc oxide powder. The decrease of luminescence with time at room temperature after excitation with electrons. After Gobrecht *et al.*[57]

remains at high temperatures. It is essentially quenched[54] at 500°C. Both bands exhibit a fine structure at low temperatures (90°K). This structure consists of an equally distant sequence of overlapping maxima when energy is used as abscissa. Table V contains the peaks of the ultraviolet emission obtained by different observers. The results are closely reproducible. The structure of the green band is discussed in Litvinowa.[65]

The extraordinarily short afterglow of zinc oxide has been known for a

[61] A. Schleede, *in* "Leuchten und Struktur fester Stoffe" (R. Tomaschek, ed.), p. 158. R. Oldenbourg, Munich, 1943.
[61a] A. Bril and H. A. Klasens, *Philips Research Repts.* **1**, 401 (1952).
[62] S. F. Kaisel and C. B. Clerk, *J. Opt. Soc. Am.* **44**, 134 (1954).
[63] R. E. Shrader and S. F. Kaisel, *J. Opt. Soc. Am.* **44**, 135 (1954).
[64] P. Wachter, *Verhandl. deut. physik. Ges.* p. 115 (1957).
[65] P. S. Litvinowa, *J. Exptl. Theoret. Phys.* (*USSR*) **27**, 636 (1949).

TABLE V. FINE STRUCTURE OF THE ULTRAVIOLET EMISSION BAND, MEASURED AT 90°K

λ_{max} [A]	3708	3753	3830	3927	4011	—	Ewles[a]
	3692	3750	3840	3930	3990	—	Kröger[b]
	3715	3758	3840	3922	4005	4100	Randall[c]
$h\nu_{max}$ [ev]	3.341	3.302	3.232	3.164	3.099	3.027	
$\Delta h\nu$ [ev]		0.039	0.070	0.068	0.065	0.072	

[a] J. Ewles, *Proc. Roy. Soc.* (*London*) **A167**, 34 (1938).
[b] F. A. Kröger, *Physica* **7**, 1 (1940).
[c] J. T. Randall, *Trans. Faraday Soc.* **35**, 1 (1939).

long time. The decay time τ is of the order of 10^{-6} sec for cathode ray excitation. A new measurement is shown in Fig. 26. The decay is purely exponential with $\tau_{uv} = 2.7 \times 10^{-6}$ sec for the ultraviolet and

$$\tau_{gr} = 4.5 \times 10^{-6} \text{ sec}$$

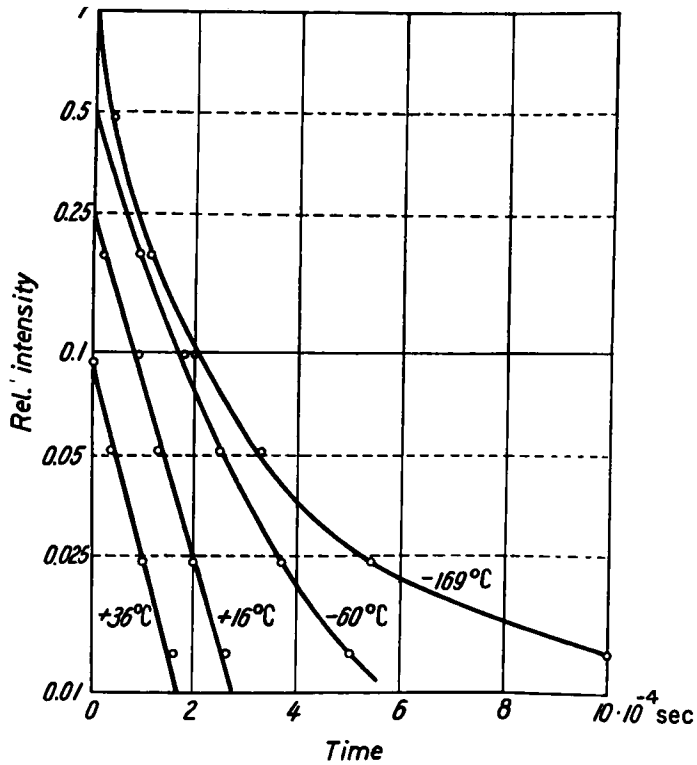

FIG. 27. Zinc oxide powder. Decrease with time of the green luminescence after excitation with light ($h\nu$ = 3.4 ev) at different temperatures. After Gobrecht *et al.*[57]

for the green band. The latter is different for different preparations, and depends upon the temperature and the form of preparation (Fig. 27). In agreement with earlier observations,[66] the decay below $T = -60°C$ is no longer exponential. According to Fig. 27, $\tau_{gr} \approx 9 \times 10^{-5}$ sec at room temperature under excitation with ultraviolet light in the intrinsic absorption region. In contrast, τ_{gr} attains values of the order of magnitude from 10 sec to one minute at $-186°C$ under weak excitation with ultraviolet radiation in the spectral region of the tail of the fundamental

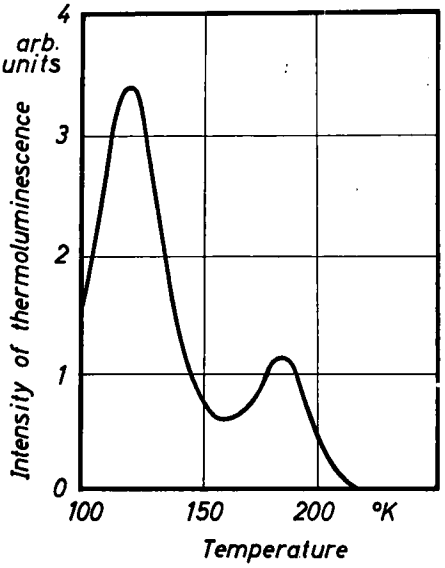

FIG. 28. Zinc oxide powder. Glow curve. After Garlick and Wilkins.[68]

absorption band.[34] There are no systematic investigations of the dependence of the decay time on the conditions of excitation. Similar decay times have been observed in electroluminescence.[67] The thermoluminescence of zinc oxide has been measured many times. The material is excited at low temperatures and is warmed at a constant rate. The emission is measured as a function of time and temperature. Figure 28 shows an example. The results of other investigations agree only in part with the results shown in Fig. 28. Maxima have been found at[10] 150°K and at[69] 470°K, in addition to those shown at 120°K and 185°K in Fig. 28.

[66] J. T. Randall, *Trans. Faraday Soc.* **35,** 1 (1939).
[67] A. Fischer, *Z. Naturforsch.* **8a,** 756 (1953); *Physik. Verhandl.* **3,** 64 (1954).
[68] G. F. Garlick and M. F. H. Wilkins, *Proc. Roy. Soc. (London)* **A184,** 408 (1945).
[69] J. Roux, *Compt. rend.* **236,** 2492 (1953).

For completeness, we should mention the excitation of the luminescence of zinc oxide by alternating electric fields. This is usually observed in the customary arrangement of an electroluminescent cell. Zinc oxide behaves like other electroluminescent phosphors in this respect. As a result, it will be sufficient here to refer to the work of the various investigators.[70] The luminescence can be observed even at potential differences of a few volts[67] and possesses temperature-dependent maxima like those of the glow curves.[71]

In addition to true electroluminescence which can be produced in an unexcited phosphor by an alternating electric field (Destriau effect), it is also possible to observe an optical emission which is induced by a field when the crystal has been excited (Gudden-Pohl effect). This phenomenon presumably will not be observed in the case of luminescence which decays very rapidly, for it presumably is related to the effect of the field on electrons in traps. One might expect a correlation with emission having a long decay time or with the maxima of thermoluminescence observed at elevated temperatures.

d. Discussion of the Mechanism of Luminescence

Although the decay of luminescence of zinc oxide is exponential and possesses a very short decay time, the light presumably is produced by recombination. In support of this are, for example, the photoconductivity of zinc oxide, the deviations from exponential decay at low temperatures, the thermo and electroluminescence, and numerous quantitative observations which cannot be explained in terms of simple excitation of a center. The ultraviolet emission presumably follows from the direct recombination of electrons and holes, perhaps passing through an exciton-like state of binding in the process. Apart from the method of excitation, this glow is similar to the thermal emission of zinc oxide at high temperatures. The maximum of the ultraviolet band, shown in Fig. 24, shifts to long wavelengths with increasing temperatures, the temperature coefficient being 11.5×10^{-4} ev/deg. If one extrapolates this value to higher temperatures, one obtains good agreement with the maximum of the thermal emission curve shown in Fig. 23 (compare Fig. 29).

In view of the small cross section for recombination of electrons and holes with radiation, obtained from an analysis of the thermal glow (Table IV), it seems surprising that one can observe the recombination as a result of a nonthermal excitation. This difficulty can be circumvented if we assume that excitons are formed first with a relatively large cross

[70] H. Gobrecht, D. Hahn, and H. E. Gumlich, *Z. Physik* **136,** 612 (1954); H. Gobrecht, D. Hahn, and F. W. Seemann, *ibid.* **140,** 432 (1955).

[71] H. Gobrecht, D. Hahn, and H. E. Gumlich, *Z. Physik* **136,** 623 (1954).

section. They are responsible for the observed ultraviolet emission obtained at low temperatures in the absence of thermal excitation. The excitons are not effective at elevated temperatures. They dissociate, as a result of thermal excitation, more rapidly than they are able to emit photons.

The green band appears in the presence of a stoichiometric excess of zinc, which apparently serves as the activator. Presumably the excess must be present in the form of defects resembling F centers.[60,72] The

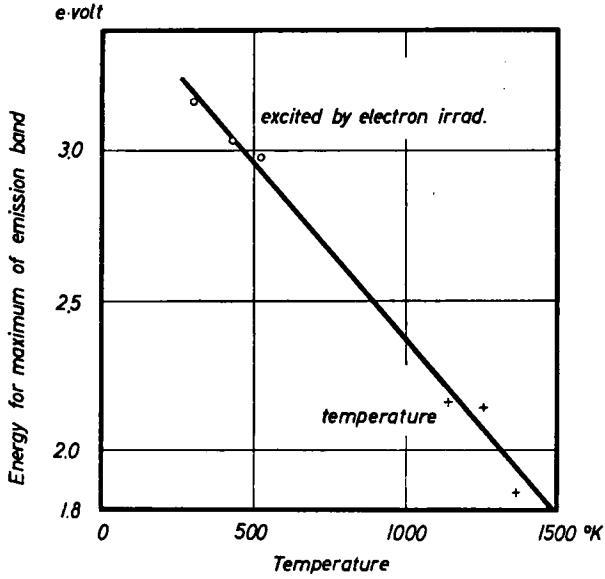

FIG. 29. Position of the maximum of the edge emission bands as a function of temperature on excitation by radiation or temperature. Taken from Figs. 23 and 24.

diffusion of oxygen would be required to form such centers, that is, a high temperature would be required in the preparation of the material. Thus, a reducing treatment at low temperatures should not activate zinc oxide. As was pointed out above, this actually is the case. In fact, a reducing treatment at lower temperatures destroys the green luminescence.

The fine structure of the two emission bands, which can be resolved only at low temperatures, may be interpreted in terms of the superposition of a vibrational structure.[73] One should not expect the differences in energy of the fine structure pattern to agree with the infrared spectrum, for one must note that the optically active infrared vibrations correspond to transverse waves in the lattice. In contrast, one should expect longi-

[72] N. Riehl and H. Ortmann, *Z. Elektrochem.* **60**, 149 (1956).
[73] F. A. Kröger and H. J. G. Meyer, *Physica* **20**, 1149 (1954).

tudinal waves to be associated with a change in charge of the luminescent center. As far as one can estimate, the energy of such waves corresponds to the measured fine structure (compare Table V).

The orange band also requires an activator. It is generated as a result of an intense oxidizing treatment or as a result of the introduction of coactivators, which, when viewed from the standpoint of charge balance, is equivalent to an oxidation process. The assumption that the activator is a zinc deficiency, perhaps in the form of imperfections resembling V centers, is in good agreement with this observation and the few other facts which are known about the orange band.

An exponential decay law is only possible during recombination if the concentration of one of the recombining partners remains practically constant during the decay. In contrast to the situation for phosphors of the ZnS type, this condition is fulfilled in zinc oxide in the sense that it contains an appreciable density of free electrons which are responsible for the high electrical conductivity observed in the luminescent form. According to this point of view, the decay time should be inversely proportional to the density of electrons. There has been no systematic experimental investigation of this question, so that the entire matter remains undecided at the present time. Since the concentration of free electrons decreases with decreasing temperature, one would expect deviations from the exponential decay to be observed most prominently at low temperatures, as is, in fact, the case. The observation of thermoluminescence and slowly decaying phosphorescence having weak intensity demonstrates the presence of deep lying traps for electrons or holes. Nothing is known about the atomistic structure of such traps. They must depend to a substantial degree upon the method by which the specimens are prepared, for the partly contradictory results obtained in studies of thermoluminescence can be interpreted in this way.

One can understand other details of the decay process if one postulates that the formation of excitons precedes the ultraviolet emission. An exponential decay law necessarily follows from this picture. The initial bimolecular recombination occurs very rapidly in a time normally not measured. The observed decay time corresponds to the lifetime of the exciton and is, as observed, substantially independent of external influences. In the case of the green band, on the other hand, the dependence upon the electron concentration, described above, remains. Perhaps further investigations will lead one to a better understanding of the experimental fact that the decay time τ_{gr} depends upon the method of preparation, the temperature, and the means of excitation.

To summarize, one can construct the following picture of the luminescent processes. Free electrons and holes are produced as a result of excitation. The first are relatively unimportant for luminescence, since

many electrons are already present even in the dark. The holes either recombine directly with the free electrons, forming excitons which then radiate in such a way as to produce exponential decay, or are captured by the activators which produce the green bands. In the second case, the light emission follows a bimolecular recombination of the activators and free electrons. The decay is exponential in the second case, since the electron concentration is practically constant. The larger the electron concentration, that is, the larger the conductivity, the larger is the probability that the hole will combine with an electron to form an exciton. For this reason, assuming all other factors remain the same, the green band retrogresses more and more relative to the ultraviolet band when the conductivity of the specimen grows or when the electron concentration increases as a result of very intense excitation. In all cases, however, an appreciable fraction of the excited electrons make the transition to the grounds state as a result of radiationless processes.

In general, the ultraviolet emission does not increase with increasing conductivity as rapidly as the green emission decreases. This observation can be explained in terms of impact recombination, which has been discussed in a number of new investigations concerning the lifetime of minority carriers in germanium and other semiconductors and photoconductors.[74,75] In this process the energy which is released in a transition involving an electron at a defect does not appear in the form of a photon, but, as in the Auger effect, emerges as the kinetic energy of a free electron. This form of recombination is the inverse of ionization by collision. The relative frequency of such radiationless transitions increases with increasing concentration of electrons. In zinc oxide the green luminescence is affected more than the ultraviolet by the competition of the new process. The latter is affected practically not at all, for the probability that an electron combines with a hole to form an exciton increases in proportion to the electron concentration, just as the relative frequency of impact recombination. According to the theory, the probability that an exciton is dissociated by impact recombination is very small.

Studies of the photoconductivity of zinc oxide indicate that one must consider additional ways of binding holes. One cannot explain the properties of photoconductivity by considering only processes which play an important role in producing luminescence radiation.

V. Adsorption and Catalysis

The conductivity characteristics of many preparations of zinc oxide depend significantly upon the state of the surface (compare Sections 19c,

[74] H. Y. Fan, *Solid State Phys.* **1,** 356 (1955).

[75] L. Bess, *Phys. Rev.* **105,** 1469 (1957).

20 to 23, and 25). It has been shown that gases have a strong influence on the conductivity at room temperature and lower temperatures where a variation in the volume conductivity as a consequence of diffusion is excluded. The gases alter the density of defects on the surface as a result of a reaction or chemisorption. In the sections quoted above, the variations of the conductance are always related to such processes. As a result, it seems reasonable to give a brief presentation of other types of observations concerning the interaction of the surface of zinc oxide with gases.

We shall be concerned either with the variations in the pressure in a closed volume as a result of adsorption or desorption on the surface, or with the velocity and the activation energy of a reaction when zinc oxide serves as a catalyst.

13. Adsorption

a. Oxygen

If thin layers of zinc oxide are heated in a vacuum and oxygen is then introduced at room temperature, the decrease in the pressure of oxygen can be observed, along with the decrease in conductivity, if the volume of the vessel is small enough. It is found that substantially more oxygen molecules than conduction electrons[76] disappear. The details of this investigation will be found in Section 21.

The adsorption of oxygen at high temperatures has been investigated[77] with the use of zinc oxide powder having grains of the order of 2.5×10^{-5} cm in linear dimensions. The pressure attained when a definite amount of oxygen is admitted into a chamber which has a constant, small volume and contains the previously annealed specimen is measured. The amount of gas adsorbed attains a maximum value at 425°C for a specimen which has been given a previous heat treatment in a vacuum at 600°C for one minute. The amount of adsorbed oxygen depends both on the temperature and the duration of the previous annealing.

b. Hydrogen

The adsorption of hydrogen on zinc oxide was investigated most prominently by H. S. Taylor and his co-workers.[14,78] Such observations were possible only after appropriate "activation" of the zinc oxide. The treatment consisted in heating the specimen in a vacuum or in hydrogen to temperatures in the vicinity of 400°C. Powdered and sintered materials

[76] E. Mollwo, *Forsch. u. Fortschritte* **26,** Suppl. 3, 13 (1950).
[77] S. R. Morrison and P. H. Miller, Jr., *J. Chem. Phys.* **25,** 1064 (1956).
[78] H. S. Taylor and C. O. Strother, *J. Am. Chem. Soc.* **55,** 586 (1934).

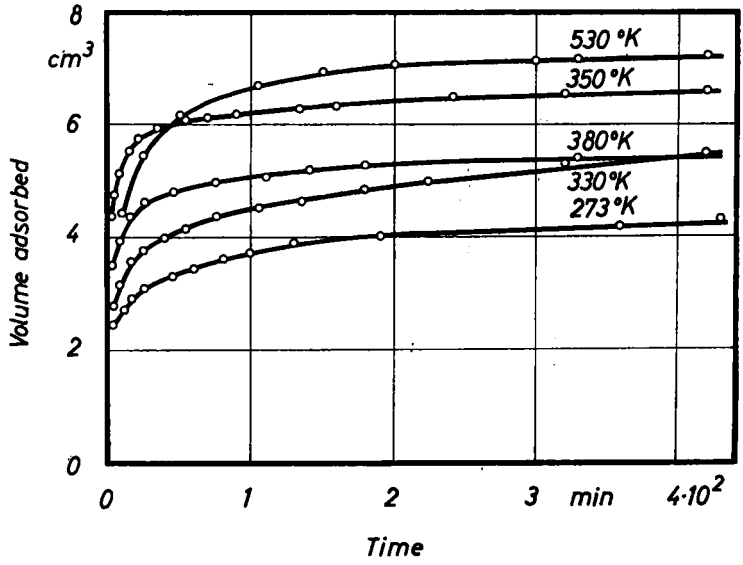

FIG. 30. Zinc oxide powder made from zinc oxalate (26.4 gram). Adsorbed amount of hydrogen given as a function of time for different temperatures. Pressure 1 atmos. Before each run with a new adsorption temperature, the powder was heated in a vacuum at 400°C. After Taylor and Strother.[78]

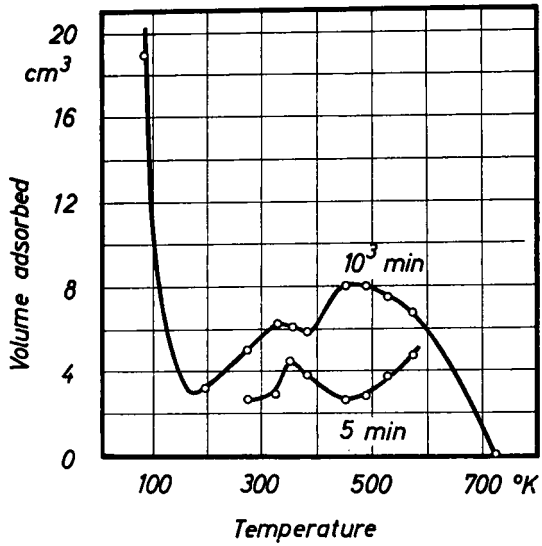

FIG. 31. Zinc oxide powder prepared from zinc oxalate (26.4 gram). Adsorbed amount of hydrogen as a function of temperature. Two different times of exposure. Pressure 1 atmos. Before establishing a new adsorption temperature, the specimen was always heated in a vacuum at 400°C. After Taylor and Strother.[78]

were used preferentially because of the large surface. Figure 30 illustrates the time dependence of the adsorption process at different temperatures. After a rapid increase, the curve tends towards saturation slowly. Figure 31 indicates an example in which the amounts of H_2 adsorbed in 5 min and 10^3 min are shown as functions of temperature. Two maxima are observed above room temperature, namely, at 80° and 218°C. The amount of adsorbed hydrogen increases steeply at low temperatures. At 77°K and a hydrogen pressure of one atmosphere, about 80% of the surface which would be effective in nitrogen absorption[20] is covered.[79]

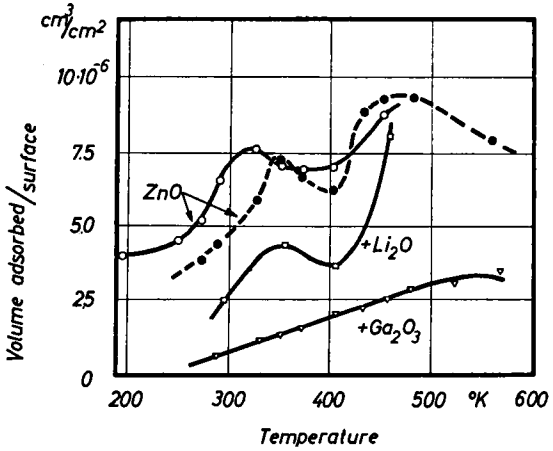

FIG. 32. Sintered samples. Adsorbed amount of hydrogen as a function of temperature (p_{H_2} = 715 torr, time = 900 min). ○, ZnO prepared from zinc oxalate at 450°C; ●, ZnO sintered at 900°C; ▼, ZnO + 0.35 mole % Ga_2O_3 sintered at 900°C; □, ZnO + 0.5 mole % Li_2O sintered at 900°C. Before each measurement the specimen was heated in a vacuum at 450°C for four hours. After Cimino *et al.*[80]

The amount of hydrogen that may be adsorbed in the temperature range from 290° to 560°K is decreased strongly by the addition of Ga_2O_3 (Fig. 32).[80] The influence of an addition of Li_2O is less clearly defined. In these experiments, doping was achieved by impregnating the ZnO with a nitrate solution followed by sintering. The surface area of the specimens was determined by nitrogen adsorption.[20] The two upper curves possess maxima similar to those shown in Fig. 31.

14. CATALYSIS

Research in the field of heterogeneous catalysis has obtained a new stimulation in recent years as a result of knowledge and principles derived

[79] H. S. Taylor and S. C. Liang, *J. Am. Chem. Soc.* **69**, 1306 (1947).
[80] A. Cimino, E. Cipollini, and E. Molinari, *Naturwiss.* **43**, 58 (1956).

from the physics of solids. The most prominent investigations center about the influence of the semiconducting properties of an oxide contact upon gas reactions and the interpretation of such investigations in terms of the principles of the theory of semiconductors.[81,82] The following topics are closely related to these studies: adsorption of gases (Section 13) and surface conductivity (Sections 19c, 20 to 23, and 25). As a result, a brief discussion of catalysis appears to be essential in this article in order to provide a suitable picture of the surface properties of zinc oxide.

One deals with *heterogeneous catalysis* whenever adsorption permits a reaction which either would not occur at all in the gas state at the used temperature or would occur only slowly. Such catalysts not only make it possible to carry out reactions at lower temperature, but also to control the reaction. In preparing such catalysts one always seeks, by suitable preparation, to obtain a large specific surface (cm^2/g) and a form of surface which favors the desired reaction most. Treatment under reducing and oxidizing conditions as well as the addition of foreign agents may play a significant role. In order to achieve a high stationary reaction velocity, it is necessary not only to have adsorption but also to have suitable desorption of the products of reaction. The slowest process in the reaction is always critical in determining its rate. A substance which absorbs a given gas very strongly is not necessarily a good catalyst for reactions involving the gas.

Zinc oxide has been used as a catalyst for a very long time. An extensive summary of the applications may be found in Gmelin's Handbuch.[2] A few examples may be mentioned: the dissociation of methanol into CO and H_2; the synthesis of methanol; the dehydriding and dehydrating of alcohols; the synthesis of ketons and aldehydes from alcohol.

In order to investigate the surface reactivity on zinc oxide, it is appropriate to have simple test reactions. Examples are the decomposition of nitrous oxide and the oxidation of carbon monoxide (oxidation reactions) as well as hydrogen-deuterium exchange (hydriding reactions).

a. The Decomposition of Nitrous Oxide

C. Wagner[15] investigated the influence of the decomposition of nitrous oxide on the electrical conductivity of zinc oxide catalysts, on one hand, and the action of an addition of Ga_2O_3 upon the velocity of reaction on the other. The catalytic material was prepared by precipitation from the solution of the nitrate with NaOH. At a given pressure of oxygen, the resistivity was increased by the presence of N_2O; that is, the concentration of the conduction electrons was decreased. In order to

[81] K. Hauffe, "Reaktionen in und an festen Stoffen." Springer, Berlin, 1955.
[82] K. Hauffe, *Z. angew. Chem.* **67**, 189 (1955).

measure the catalytic activity a stream containing 10 mole % of N_2O and 90% of O_2 was passed over the catalyst, and the temperature was increased slowly. The degree of decomposition was determined from the thermal conductivity of the resulting gas mixture. The reaction first began at a notable rate above 600°C. An addition of one mole % of Ga_2O_3 produced an increase in the conductivity by a factor of 50, but increased the rate of decomposition by only a small amount. In contrast, an increase in the amount of oxygen hindered the reaction.[15] Additions of lithium had also only a minor influence.[16] Schwab and Block,[19] in a similar sequence of experiments, found a definite variation in the activation energy for the decomposition of nitrous oxide as a result of additions to the zinc oxide catalyst. Although Ga_2O_3 produced a slight increase in activity, Li_2O produced a slight decrease when present in small quantity. In other words, foreign additions which influence the volume conductivity by orders of magnitude alter the catalytic properties by a small amount, at least as far as a decomposition of N_2O is concerned. Actually ZnO is a poor catalyst for this decomposition (the reaction begins at 600°C) and is greatly surpassed by *p*-conducting oxides, such as NiO for which the reaction begins at 300°C. The homogeneous reaction begins in the range from 700 to 800°C.

b. The Oxidation of Carbon Monoxide

Schwab and Block[19] investigated the influence of foreign additions, which alter the conductivity, upon the catalytic activity of ZnO in the oxidation of CO. The catalysts were prepared by mixing ZnO powder with Li_2CO_3 or Ga_2O_3 and sintering the result in air for three hours at 850°C. The course of the reaction was determined by measuring the total pressure in a closed volume. A gross value of the activation energy was determined from the initial velocity of the reaction at temperatures near 500°C. Figure 33 shows this activation energy as a function of the content of foreign oxide. A comparison with Fig. 44 shows that the conductivity is increased and the activation energy for the oxidation of CO is decreased as a result of the addition of oxides of trivalent metals, whereas the reverse behavior is found with additions of lithium. Prior treatment with CO (reduction) produces a definite increase in the reaction velocity. In other words, an increase in electron concentration favors the oxidation of carbon monoxide.

c. The Hydrogen-Deuterium Exchange

The hydrogen-deuterium exchange process provides a particularly appropriate reaction for testing the action of the catalyst for hydriding.

The activation of hydrogen can be investigated without the interference of accessory reactions.

Investigations of the hydrogen-deuterium reaction in accordance with the equation $H_2 + D_2 = 2HD$ were carried out by Smith and Taylor[83] using ZnO as a catalyst. Molinari and Parravano[18] continued and extended the investigation with the use of zinc oxide catalysts containing additions of Li_2O and Ga_2O_3. Figure 34 shows an example. The specimens were composed of powder and were sintered for three hours at 800°C in air. The additions were introduced by impregnating the

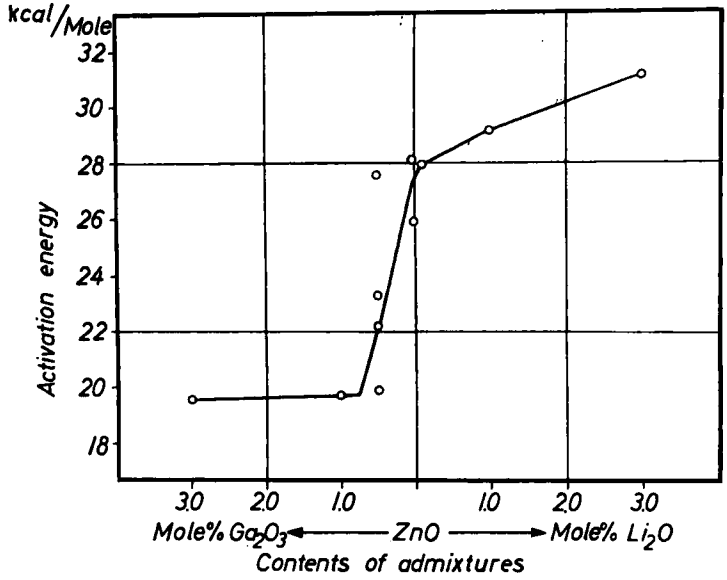

FIG. 33. Sintered samples with admixtures. Activation energy for the CO-oxidation at 440 to 560°C. After Block and Schwab.[19]

powder with solutions of the nitrate before sintering. An exchange could be observed only after sufficient activation of the material. In general, this meant that the specimens had to be heated in hydrogen to a temperature between 230° and 350°C or to 450°C in a vacuum. The activity could be disturbed by exposure to oxygen; however, it could be restored by reactivation in the manner described above. The activity, measured in terms of the quantity q appearing in the caption of Fig. 34, increased rapidly as a result of the influence of the H_2-D_2 mixtures at constant temperatures; it then increased more slowly over a period of hours and finally remained constant. Figure 34 shows that the rate of exchange is

[83] E. R. Smith and H. S. Taylor, *J. Am. Chem. Soc.* **60**, 362 (1938).

enhanced by additions of gallium and diminished by lithium. In other words, an increase in the density of conduction electrons in ZnO as a result of the addition of gallium increases the velocity of reaction. Prior treatment with hydrogen (reduction) has the same effect. It also produces an increase of conductivity in the surface layer (see Section 19c).

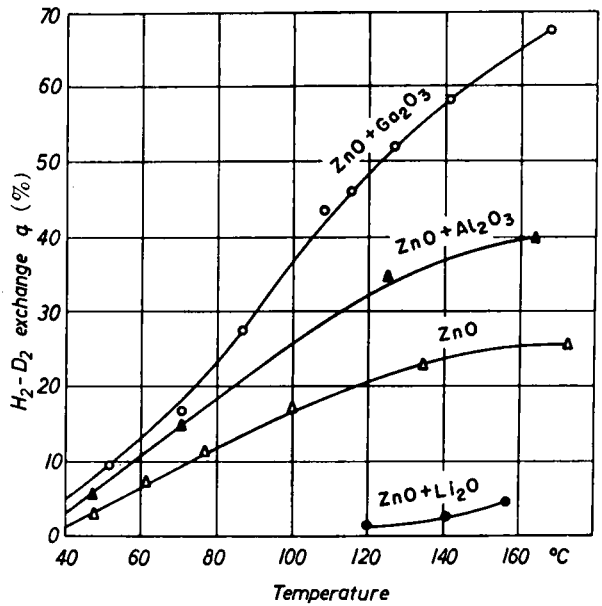

FIG. 34. Sintered samples with admixtures. H_2-D_2 exchange on the surface of ZnO samples, pretreated in hydrogen at 350°C, BET surface[20] 0.1 m^2. Flow rate 0.238 cm^3/sec. $q = \alpha_t/\alpha_{t\to\infty}$, α = (number of HD molecules/number of H_2 molecules); $\alpha_{t\to\infty}$ = equilibrium ratio. After Molinari and Parravano.[18]

d. Photocatalytic Properties of ZnO

ZnO exhibits special catalytic properties when radiated with ultraviolet light lying in the region of fundamental absorption. The activity is found only during the irradiation.[2] The reactions catalyzed by ZnO in this way are, for the most part, oxidation reactions. Examples are the formation of O_3 from O_2, of H_2O_2 from H_2O and O_2, of NO_2 from air, of formaldehyde (H_2CO), from H_2 and CO, and many others. Details of the course of the reactions are not known exactly in any of the cases. For this reason the photocatalytic properties of ZnO are merely mentioned in passing. We shall return to this point in the discussion of photoelectric phenomena in Section 25e, for the viewpoints presented there may provide a basis for understanding.

15. Discussion of Adsorption and Catalysis

The phenomenon of chemisorption is far more important for understanding the electrical properties of zinc oxide than is the physical adsorption of gases. The latter corresponds to the weak bonding of molecules to the surface by van der Waals forces, whereas typical chemical bonding forces act between molecules of the absorbed gas and the surface in chemisorption. A transfer of charge occurs frequently, although homopolar bonding is not excluded. Each reaction on a heterogeneous catalyst is preceded by chemisorption. The process of desorption must occur sufficiently rapidly. The slowest step in the sequence determines the reaction velocity.

The chemisorption of oxygen on ZnO plays an influential role in oxidation reactions, such as the decomposition of nitrous oxide and the oxidation of carbon monoxide. Unfortunately, only a few quantitative facts are known about such adsorption. One can conclude from observations of the influence of oxygen on the conductivity of thin films at low temperatures (see Section 21) and of the rectifying characteristics of crystals covered with oxygen (see Fig. 63) that the oxygen binds electrons on the surface and thereby produces a depletion layer (Sections 19c and 21). In the adsorption measurements of Morrison,[77] the heating and adsorption were carried out at such a high temperature that it is quite possible the excess zinc was able to diffuse significantly (Section 7). Under these circumstances one finds that the oxygen produces a decrease in the amount of excess zinc in the interior of the crystals. In other words, a combination of adsorption and diffusion is observed in these experiments. Therefore a discussion seems to be difficult.

The chemisorption of N_2O on ZnO can be regarded as the first step in the decomposition of N_2O, the molecule binding one or more electrons of ZnO on the surface. The desorption of chemisorbed oxygen is the second step. There does not appear to be any strong influence of additions. In contrast, *p*-conducting oxides such as CoO and NiO are much better catalysts for these reactions.

In the case of the oxidation of CO, the chemisorption of oxygen on ZnO represents the first step. This is followed by a second, time determining step consisting of the reaction of the adsorbed oxygen with the carbon monoxide. The concentration of conduction electrons in ZnO is increased by the addition of Ga_2O_3 (Section 18c). As a result, more oxygen can be adsorbed, and the second step is accelerated. The acceleration of the reaction observed as a result of prior treatment with CO can be understood in the same way. There is a partial reduction and a consequent increase in the electron density on the surface. According to Fig. 44, Li_2O

additions decrease the concentration of conduction electrons when present in quantities that are not too large. As a result, such additions are unfavorable for the oxidation of CO.

Thus, the chemisorption of oxygen on ZnO appears to play an important role both in the decomposition of N_2O and in the oxidation of CO. Only an oxidizing gas acts upon the surface in the first reaction, whereas both an oxidizing and a reducing gas are in contact with the catalyst in the second.

Zinc oxide is difficult to reduce and, as a result, can also be used as a catalyst for *hydriding reactions*. Examples of different types of hydrogen adsorption are given in Figs. 31 and 32. Physical absorption may be assumed at very low temperatures. This retrogresses with increasing temperature. The renewed increase, with two maxima, is to be ascribed to processes having an appreciable activation energy, that is, to chemisorption. The uptake of hydrogen above room temperature occurs sluggishly (Fig. 30) and, according to Taylor and Thon,[84] can be described in terms of a logarithmic time dependence given by the Elovich equation.[84a] The action of additions of gallium can be understood if one assumes that electrons are given to the ZnO during the adsorption of hydrogen. This step is made more difficult when a high concentration of free electrons is already present in the ZnO, such as when it has additions of gallium. The observations concerning the exchange of hydrogen and deuterium can be explained in a similar way. The reaction velocity increases with the electron concentration. Here again it is necessary to assume that desorption occurs as a result of a transfer of electrons from ZnO to hydrogen and that this is the rate-determining step. The restricting influence of additions of Li_2O also can be understood in this way, for, as is shown in Section 18c, such additions decrease the conductivity.

The position of the Fermi level, that is, the electron concentration, at the surface, is important for adsorption and catalysis. The concentration of electrons at the surface can be varied by orders of magnitude relative to the values obtained by doping in the interior of the crystal, as a result of the development of exhaustion or accumulation boundary layers at the surface. Under certain conditions such changes can occur as a result of the reaction being studied. Many apparent contradictions in the experiments carried out with doped semiconducting catalysts can be explained in this way. Moreover, it is by no means certain that the additions are always distributed atomically throughout the lattice. If not, the catalyst is of mixed type, containing two substances. In view of these difficulties it would be highly desirable to carry out measurements of the surface

[84] H. A. Taylor and N. Thon, *J. Am. Chem. Soc.* **74,** 4169 (1952).

[84a] S. Y. Elovich and G. M. Zhabrova, *J. Phys. Chem.* (*U.S.S.R.*) **13,** 1761, 1775 (1939).

conductivity and of the adsorption and catalytic properties on the same set of specimens. Such a procedure faces very great difficulties for experimental reasons. It is possible to measure the surface conductivity only on single crystals (Section 19c), whereas the observations of adsorption and catalysis require large surfaces which are obtained most readily with polycrystalline specimens.

VI. Conductivity in Thermal Equilibrium

16. Methods of Measurement

The conductivity of thin films can be measured in a simple way in terms of the current and applied voltage. The film thickness is estimated by interference colors. Zinc electrodes formed by evaporation are frequently used at low temperatures, whereas electrodes made of evaporated gold or platinum are employed for measurement at higher temperatures. The platinum electrodes are usually burned into the glass or quartz base prior to depositing the zinc layer.

The contacts on sintered specimens are prepared by nickel-plating the ends and soldering leads[12] or by graphitizing and pressing on platinum contacts.[17] Pressed silver contacts are also used.[11] The evaporated zinc layers possess a much lower contact resistance than evaporated silver layers.[21] The measured conductivities can be spurious in the case of layers and sintered specimens, as a result of the polycrystalline structure.

In the case of single crystals, electrodes which are satisfactory for measurement of the conductivity and Hall effect can be obtained with the use of liquid gallium and soldered indium contacts.[23,85] It is possible to obtain contacts of evaporated gold or platinum which are free of contact resistance by removing the adsorbed oxygen (Section 19c). This can be done either by prior heating in a vacuum to temperatures above 600°K[86] or by the action of atomic hydrogen (obtained from a gas discharge or from an incandescent strip of tungsten heated in hydrogen at about 0.1 torr). The hydrogen treatment produces an accumulation layer which provides a good contact.[97] The rod-like form of the single crystals makes it possible to carry out four probe measurements with spring-impressed platinum contacts in a very good way.[87] It is often useful to apply the voltage from a small, highly charged condenser to a contact which conducts poorly because of a surface layer in order to break down the contact resistance. Most of the measurements of conductivity described in the following were made on crystals with the use

[85] H. Rupprecht, *J. Phys. Chem. Solids* **6**, 144 (1958).
[86] G. Heiland, *Z. Physik* **142**, 415 (1955).
[87] G. Heiland, *Z. Physik* **138**, 459 (1954).

of potential probes. A vibrating reed electrometer was used to measure the potential.

17. Thin Layers

a. Temperature Dependence of the Conductivity. Hall Effect and Thermoelectric Power

Figure 35 provides an example of the conductivity of thin evaporated layers in the region of low temperatures.[88] The lowest curve was obtained from a layer which had been introduced into a vacuum without any other treatment. As is discussed in Section 22a, it is possible to increase the

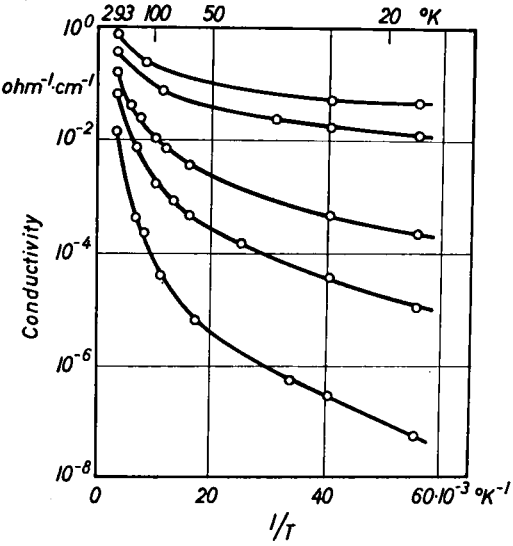

Fig. 35. Thin layer. Conductivity at low temperatures measured in a vacuum. The transition to the next highest curve is obtained by light or electron radiation in a vacuum at room temperature. After Weiss.[88]

conductivity in the vacuum irreversibly, for example, by use of electron radiation. One then obtains the upper curves in Fig. 35. The lower curve may be obtained again by allowing air or oxygen to act upon the specimen. The curves are bent; in other words, they cannot be represented in terms of relation of the form $\sigma = \sigma_0 \times e^{-\epsilon/kT}$ with a constant value of ϵ (compare Section 25d and Fig. 96).

Figure 36 provides an example of the conductivity of the thin layers at high temperature, as measured in air. The arrow indicates the course of the measurement as a function of time. The curves are reversible with

[88] H. Weiss, private communication.

time in the range of temperature A; however, one obtains irreversible changes if one heats to the range B. There is a very rapid rise of conductivity in range C, coupled with an energy $\epsilon \cong 1$ ev which is related to a very strong and irreversible decrease of the conductivity during cooling.[89,90]

The Hall mobility found in thin layers is about 10 cm²/volt sec when measured in air after weak oxidation (large conductivity) and in the range of temperature from 20 to 200°C. Values smaller than 1 cm²/volt sec are found[91] after heavy oxidation (small conductivity).

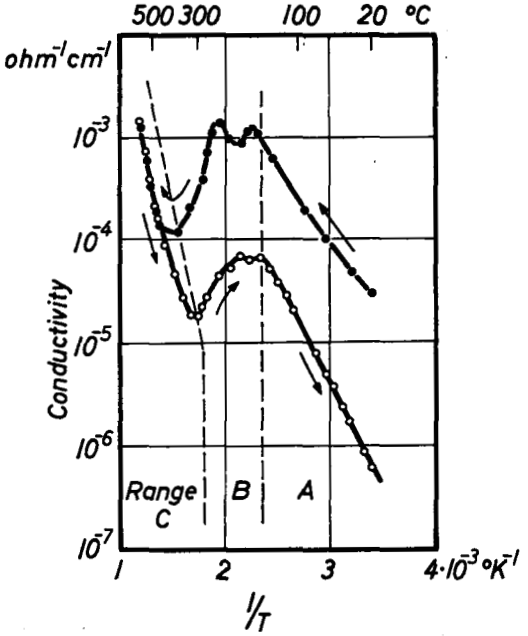

FIG. 36. Thin layer. Conductivity at high temperatures, measured in air. Upper curve, heating. Lower curve, cooling. After Tischer.[90]

The thermoelectric power of thin layers is found[21] to be 0.25 mv/deg in the range from −30 to +70°C. The sign always corresponds to n-type conductivity. In other words, the electrons always flow from the metal to the zinc oxide at the contact with the higher temperature.

b. Influence of Additional Foreign Metals on the Conductivity

It is possible to evaporate silver and aluminum along with zinc on quartz plates. The layers can then be oxidized in the usual way in air.

[89] F. Stöckmann, *Z. Physik* **127**, 563 (1950).
[90] G. Tischer, Dissertation, University of Erlangen, 1954.
[91] K. Intemann and F. Stöckmann, *Z. Physik* **131**, 10 (1951).

The measurements of conductivity indicate, however, that the influence of oxidation and of adsorbed oxygen is so strong that it is not possible to obtain a clear picture of the influence of the admixed metals.[90]

18. Sintered Specimens

a. The Influence of Oxygen on Conductivity and Thermoelectric Power

The conductivity of a sintered specimen depends upon the atmosphere, just as in the case of a thin layer. Whereas the influence of oxygen was observed primarily in the region of low temperatures in thin layers,

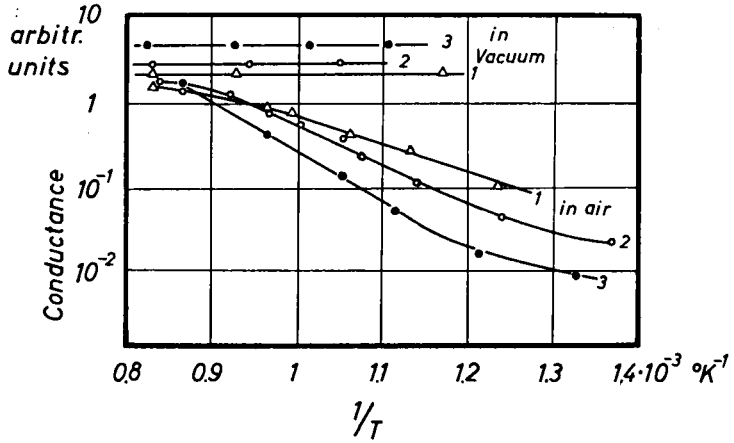

Fig. 37. Sintered samples. Conductivity at high temperatures measured in air or in a vacuum. Sample 1 from ignition of ZnC_2O_4. Sample 2 from ignition of metal. Sample 3 from ignition of basic zinc carbonate. After Bevan and Anderson.[92]

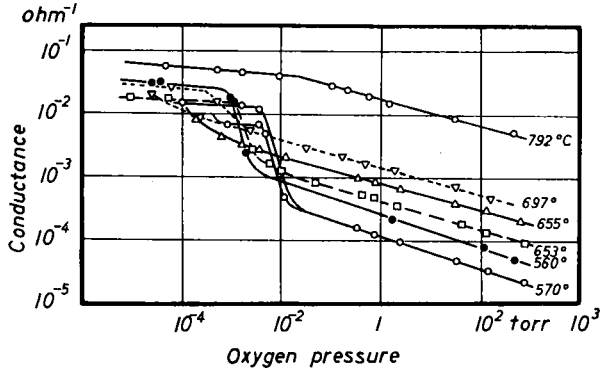

Fig. 38. Sintered samples. Conductivity as a function of oxygen pressure at different temperatures. After Bevan and Anderson.[92]

[92] D. J. M. Bevan and J. S. Anderson, *Discussions Faraday Soc.* **8**, 238 (1950).

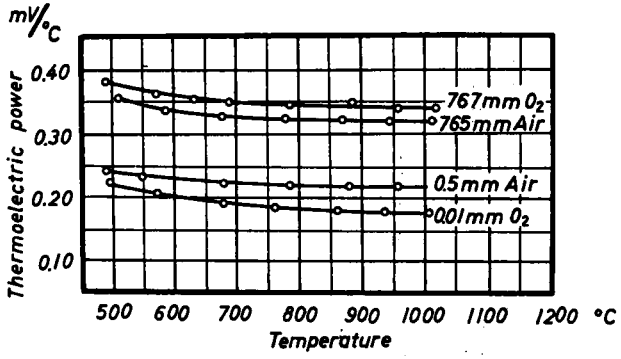

FIG. 39. Sintered samples. Thermoelectric power as a function of temperature at various air and oxygen pressures. After Hogarth.[94]

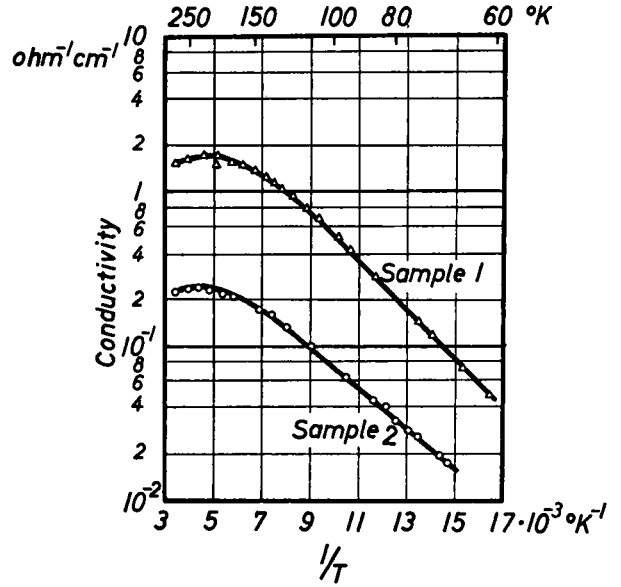

FIG. 40. Sintered samples. Conductivity at low temperatures. Sample 1 was sintered at 1325°C and sample 2 at 1050°C for 18 hr in air. After Harrison.[13]

the effects are most evident at high temperatures in the sintered specimens. Figures 37 and 38 show an example. The dependence of the conductivity on the pressure of oxygen at constant temperature can be expressed in terms of the relation $\sigma \sim p^{-1/m}$. It follows from Fig. 38 that $m = 4$. The influence of oxygen on the conductivity disappears at pressures below 10^{-4} torr. Von Baumbach and Wagner[93] found values of m

[93] H. H. von Baumbach and C. Wagner, *Z. physik. Chem.* (*Leipzig*) **B22**, 199 (1933).
[94] C. A. Hogarth, *Phil. Mag.* [7] **39**, 260 (1948); *Nature* **161**, 60 (1948); *Z. physik. Chem.* (*Leipzig*) **198**, 30 (1951).

in the range $m = 4.1$ (630°C) to 4.5 (530°C); Hogarth[94] found that m lies in the range from 3.6 (977°C) to 4.6 (560°C); Hauffe and Block[95] found $m = 5.5$ (665°C) (see Section 24b).

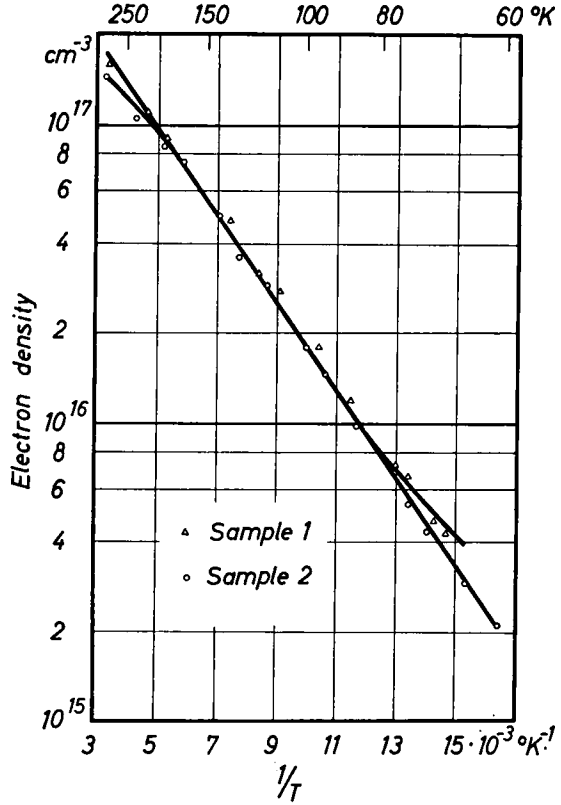

FIG. 41. Sintered samples. Electron concentration obtained from the Hall effect at low temperatures. After Harrison.[12]

Measurements of the thermoelectric power at different pressures of oxygen are reproduced[94] in Fig. 39. The sign always corresponds to n-type conductivity. If in accordance with the relation

$$Q \sim \frac{k}{e} \ln n_0/n + f_1(T) \sim \frac{k}{em} \ln p/p_0 + f_2(T) \qquad (18.1)$$

one plots the thermoelectric power Q linear and the pressure of oxygen p logarithmically, one obtains the value $m = 6$ from the slope. n is the electron concentration.

[95] K. Hauffe and J. Block, *Z. physik. Chem.* (*Leipzig*) **196**, 438 (1951).

b. Temperature Dependence of Conductivity and Hall Effect

An example of measurements in the range of low temperature is given in Figs. 40 to 42. The conductivity, the electron density (determined from the Hall effect) and the mobility are represented for two samples, sintered at different temperatures.[12] Although the electron densities of the two specimens are approximately equal, the specimen sintered at higher temperature has a higher mobility. The relation $\mu \sim T^{-\frac{3}{2}}$ is approximately valid above 150°K. The Hall mobility of coarsely crystalline,

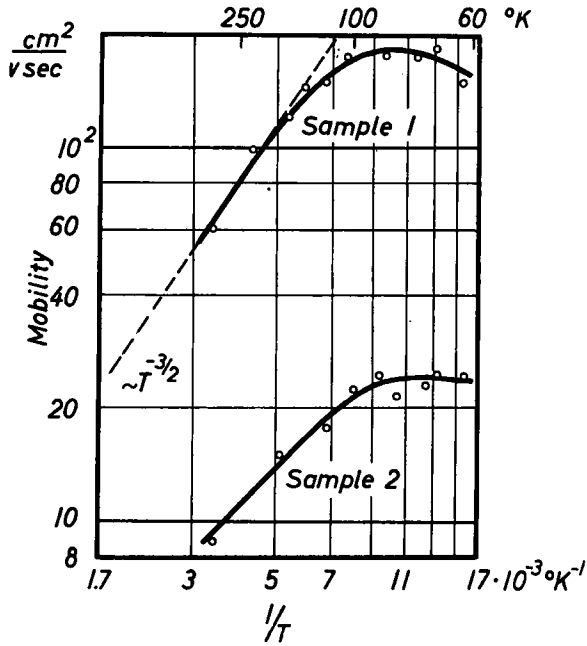

FIG. 42. Sintered samples (the same as for Figs. 40 and 41). Hall mobility at low temperatures. After Harrison.[12]

sintered specimens is found to vary[21] between 5 and 37 cm²/volt sec in the range between 90 and 300°K. The measurements of conductivity in the region of higher temperatures, as determined by various investigators,[11,91,96] are indicated in Fig. 43. A steep rise in conductivity is found, as in thin layers. If one expresses the results in terms of the relation $\sigma = \sigma_0 e^{-\epsilon/kT}$, one finds that ϵ has values between 0.5 and 1.3 ev. All the curves with number 1 were measured on the same specimen. *A* and *B* were obtained after sintering at 1270°C by heating the specimen from room

[96] W. Jander and W. Stamm, *Z. anorg. u. allgem. Chem.* **199**, 165 (1931).

temperature to 530°C and cooling it again. Curve J was obtained after several repetitions of the heating to 530°C. The temperature was raised to values as high as 700°C in this measurement. Curve L was obtained after cooling to room temperature. An irreversible variation of the conductivity was found after each heating of the specimen, particularly in the conductivity region of low temperatures where the curves are flat.

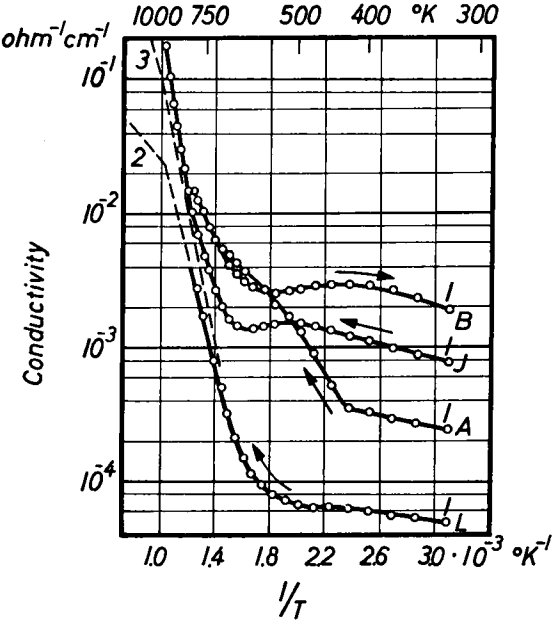

FIG. 43. Sintered samples. Conductivity at high temperatures, measured in air. After Hahn,[11] 1; after Jander and Stamm,[96] 2; after von Baumbach and Wagner,[93] 3.

These variations are less marked in the steep portion of the curve. A well-defined influence of oxygen pressure was found in this region (Section 18a).

c. Influence of Added Foreign Oxides on the Conductivity

The influence of additions of oxides of mono- and trivalent metals on the conductivity is represented[17] in Fig. 44. The trivalent metals chromium, gallium, and aluminum produce an increase in the conductivity, whereas monovalent lithium decreases the conductivity when not present in too large a concentration. It is difficult to determine the actual fraction of the foreign atom which is in solution in the lattice because of the method used to prepare the specimens. Whereas the additions of

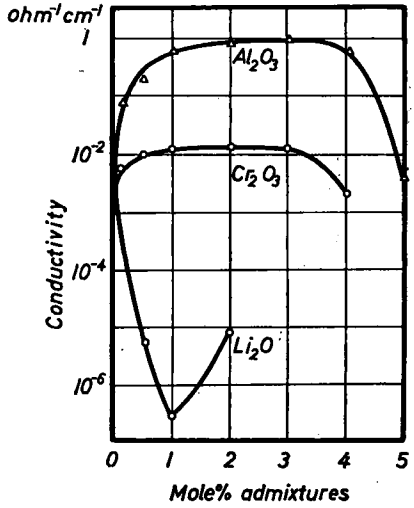

FIG. 44. Sintered samples. Conductivity at 400°C as a function of the quantity of admixed foreign oxide. After Hauffe and Vierk.[17]

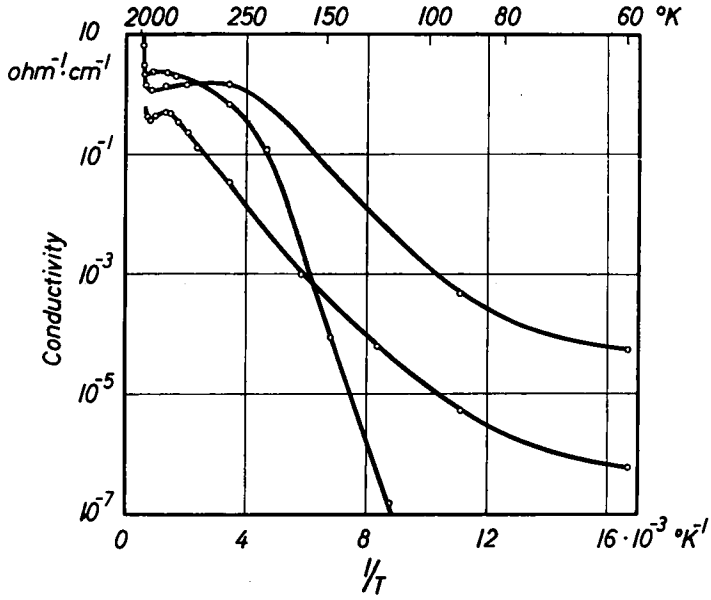

FIG. 45. Crystals, without intentional addition. Before the measurement the specimen was heated 20 min in air at 1400°K. The conductivity as a function of temperature. Two curves coincide at 1950°K in the steep branch. After Heiland[97] and Pohl.[98]

[97] G. Heiland, *Z. Physik* **148**, 15 (1957).
[98] R. Pohl, private communication.

lithium do not alter the influence of oxygen on the conductivity in the region of high temperatures, gallium or aluminum additions have a strong effect on this influence.[95] The quantity m varies between 10 and 12 at 800°C in the equation $\sigma \sim p^{-1/m}$.

19. Single Crystals

a. Without Arbitrary Additions. Dependence of the Conductivity on the Temperature and Pressure of Oxygen. Thermoelectric Power

The electrical conductivity can vary significantly from specimen to specimen at low temperatures in the synthetic crystals which do not contain intentional additions as well as in the exceedingly impure natural and "seminatural" specimens. This fact is indicated in Fig. 45 by measurements of conductivity for three different crystals (extreme examples).

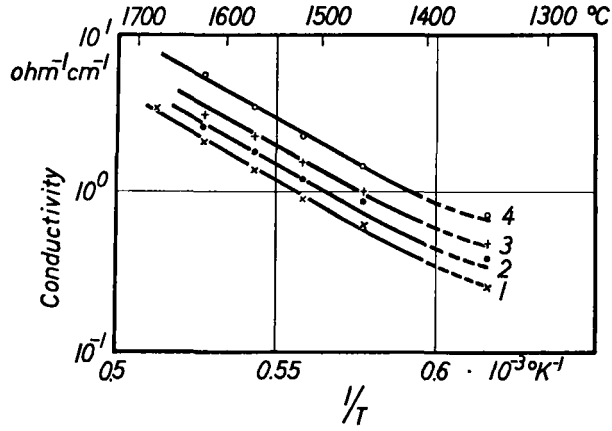

FIG. 46. Crystal. Conductivity at very high temperatures (steep branch in Fig. 45) after subtraction of the impurity conductivity. Atmosphere: a mixture of oxygen and argon. 1: $p(O_2)$ = 40 atmos; p(Ar) = 0 atmos; 2: $p(O_2)$ = 20 atmos; p(Ar) = 20 atmos; 3: $p(O_2)$ = 5 atmos; p(Ar) = 35 atmos; 4: $p(O_2)$ = 0 atmos; p(Ar) = 40 atmos. From $\sigma \sim \exp(-\epsilon/kT)$ one obtains ϵ = 2.3 ev. After Pohl.[99]

In these cases the behavior of the curves is independent of the direction in which the temperature is varied. The crystals are tempered at 1400°K in air for 20 minutes before the measurements in order to decrease the erratic effects of additions of hydrogen or zinc introduced during growth as much as possible.

As in the case of thin layers and sintered specimens, there is a rapid rise of the curves representing conductivity as a function of temperature

[99] R. Pohl, Diplomarbeit, University of Erlangen, 1955.

at high temperatures. This effect is nearly independent of the particular specimen.[99] In order to inhibit the vaporization of the crystals at these high temperatures, the measurements were carried out in a high pressure of argon or oxygen or a mixture of the two gases (Fig. 46). In this the

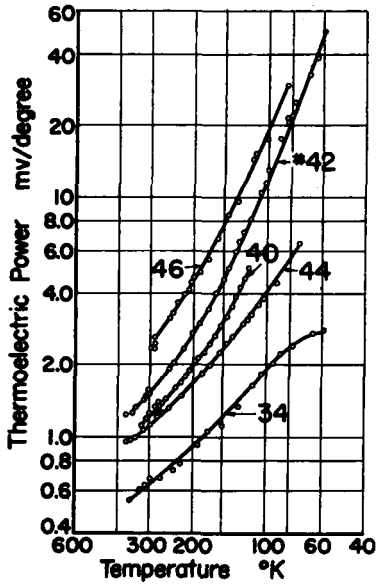

FIG. 47. Crystals without intentional addition. Thermoelectric power as a function of temperature.

Crystal no.	Carrier concentration at 300°K (Hall effect)
46	1.2×10^{15} cm^{-3}
42	1.8×10^{16}
40	6.7×10^{16}
44	8.2×10^{16}
34	3.3×10^{17}

After Hutson.[100]

relation $\sigma \sim p_{O_2}^{-\frac{1}{6}}$ was found at a given temperature. The slope of the curve in the representation of the logarithm of the conductivity as a function of $1/T$ was a constant and had the same value at all pressures of oxygen. The activation energy $\epsilon = kT \ln (\sigma/\sigma_0)$ was 2.3 ev, that is, was essentially larger than in the case of sintered specimens

[100] A. R. Hutson, *Bull. Am. Phys. Soc.* [2] **2**, 56 (1957); private communication.

(compare Section 18b). In contrast to the behavior found with sintered specimens (Section 18a), an influence of oxygen on the conductivity was established only above 1350°C. However, the influence of oxygen appeared in a range of temperature in which the conductivity varies more steeply than at low temperatures in both cases. This range begins at

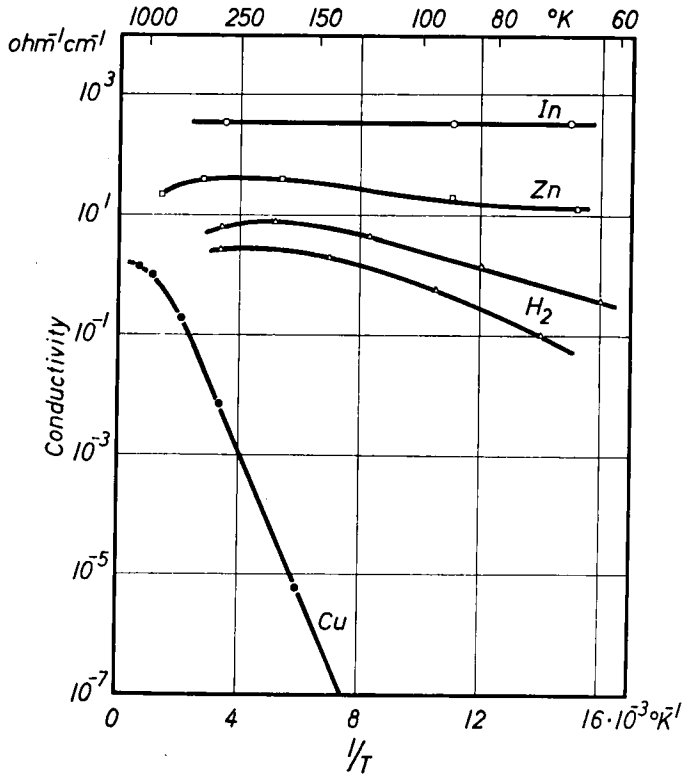

FIG. 48. Crystals with different additions. Conductivity as a function of temperature. In: 10^{20} atoms/cm³. Zn: after heating in saturated zinc vapor at 1320°C. H_2: after heating in H_2 at 40 atmos, 700°C or 50 atmos, 600°C. Cu: 10^{19} atoms/cm.³ After Heiland,[97] Pohl,[98] H. Rupprecht.[85]

lower temperatures in the measurements on sintered specimens (Figs. 37, 38, and 43) [compare Section 24b(1)].

Measurements of the thermoelectric power have been carried out on single crystals recently (Fig. 47).[100] The thermoelectric power increases very rapidly at low temperatures and decreases with increasing electron concentration. (Compare Section 24c and Fig. 94.)

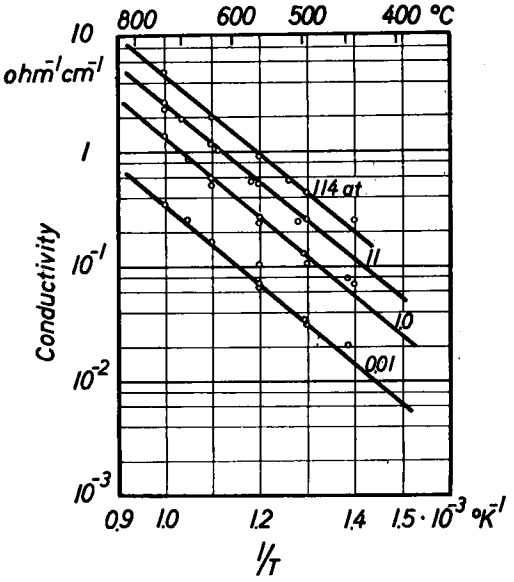

FIG. 49. Crystal. Contribution to conductivity made by hydrogen at different pressures and temperatures. After Thomas and Lander.[33]

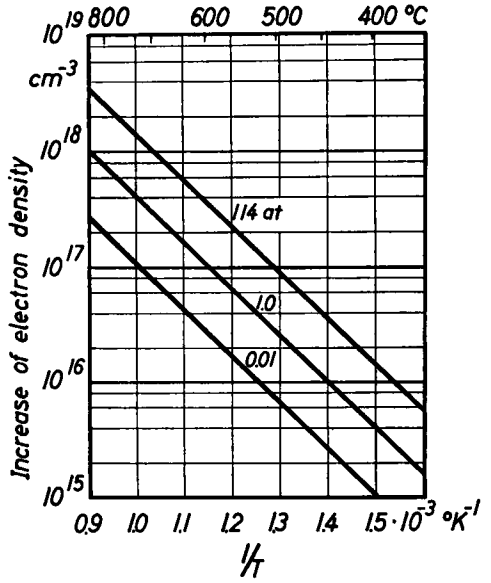

FIG. 50. Crystals. Increase of the concentration n of conduction electrons induced by different pressures of hydrogen as a function of temperature. From $n \sim \exp(-\epsilon/kT)$ one obtains $\epsilon = 0.8$ ev. After Thomas and Lander.[33]

b. Crystals with Additions. Dependence of Conductivity and Hall Effect on Doping and Temperature

Whereas the conductivity of crystals that do not contain intentional additions can scatter over a wide range, the conductivity can be stabilized arbitrarily by doping. An indication of the influence of doping on the conductivity is shown in Fig. 48 as a function of the temperature. In this figure the curves for the highest attainable values of the conductivity obtained with indium, zinc, and hydrogen are shown in addition to those for the lowest conductivity attainable with copper. The collection also contains a curve corresponding to weak doping with hydrogen. The following particular comments regarding the various additions can be made.

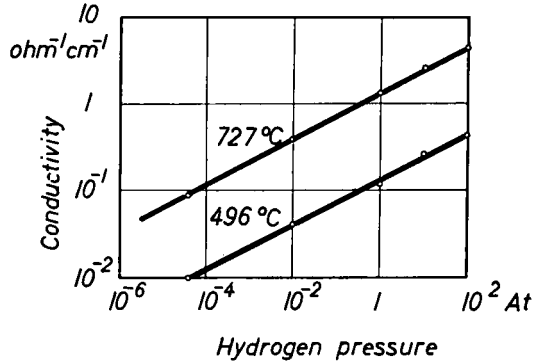

FIG. 51. Crystals. Increase of conductivity σ as a function of hydrogen pressure for two different temperatures. The slopes give $\sigma \sim p(H_2)^{\frac{1}{4}}$. After Thomas and Lander.[33]

(*1*) *Hydrogen.* Crystals which are heated in hydrogen exhibit an increase in conductivity which progresses by diffusion from the surface toward the inside.[32,33] Figure 49 indicates the equilibrium values attainable for different pressures of hydrogen as a function of temperature. The electron densities calculated from these curves are shown in Fig. 50. The mobility is assumed to be proportional to $T^{-\frac{3}{2}}$; the absolute value at room temperature is about 200 cm²/volt sec. Finally, Fig. 51 shows the equilibrium value of the conductivity as a function of hydrogen pressure at two fixed temperatures. As long as the additional conductivity is large compared to the initial value, the relation $\sigma \sim p_{H_2}^{\frac{1}{4}}$ is observed. On the other hand, the relation $\Delta\sigma \sim p_{H_2}^{\frac{1}{2}}$ is found if the additional conductivity $\Delta\sigma$ is small compared to the initial conductivity. If one cools the crystal heated in hydrogen quickly, the conductivity remains enhanced.

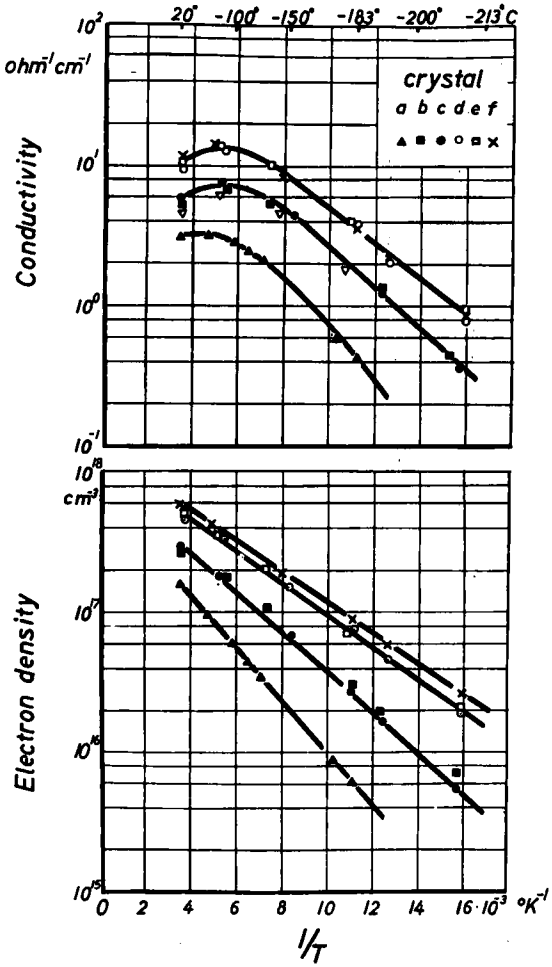

FIG. 52. Crystals, heated in hydrogen. Conductivity and electron density (Hall effect) measured at low temperatures in a vacuum. The hydrogen treatment is as follows: Crystal *a*: 50 atmos, 600°C, 20 min; Crystals *b* and *c*: 40 atmos, 700°C, 5 min; Crystals *d*, *e*, *f*: 70 atmos, 700°C, 5 min. After H. Rupprecht.[85]

The enhancement can be removed completely by renewed heating in a vacuum or in air. One can obtain a far higher concentration of hydrogen donors in the crystal in the temperature range from 200 and 400°C by a procedure in which the crystal is heated and bombarded with hydrogen ions at the same time.[101]

[101] J. J. Lander, *J. Phys. Chem. Solids* **3**, 87 (1957).

The conductivity, the electron concentration determined from the Hall effect, and the electron mobility are shown[85] in Figs. 52 and 53 at temperatures below 300°K for specimens heated in hydrogen. The logarithm of the electron concentration is proportional to $1/T$ in the temperature range between 63 and 300°K. The electron mobility increases from the lower to the higher temperatures, passes through a maximum, and then falls in a manner proportional to $T^{-\frac{3}{2}}$.

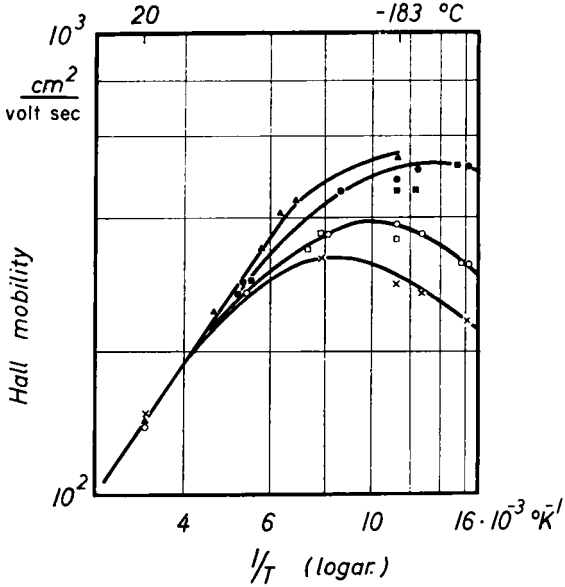

FIG. 53. Crystals, treated with hydrogen as in Fig. 52. Hall mobility at low temperatures. After H. Rupprecht.[85]

(*2*) *Zinc.* If one heats a crystal along with a supply of metallic zinc in a closed quartz bomb, one obtains an increase in conductivity after cooling the specimen rapidly. This increased conductivity can be driven out by heat to yield a residual conductivity of the magnitude of 1 ohm^{-1} cm^{-1}. The relationship between the temperature of heating in the saturated zinc vapor and the additional "reversible" conductivity, measured at room temperature, is shown[28] in Fig. 55.

The chemical analysis of zinc crystals that have been treated in zinc vapor indicates the presence of excess zinc. The crystals may be dissolved in hydrochloric acid containing an addition of iodine and

potassium iodide and titrated with sodium thiosulfate.[30,102] The concentration of excess zinc atoms found in this way is in good agreement with the electron density obtained from measurements of the Hall effect at high temperatures (400°C). The conductivity, the electron density deter-

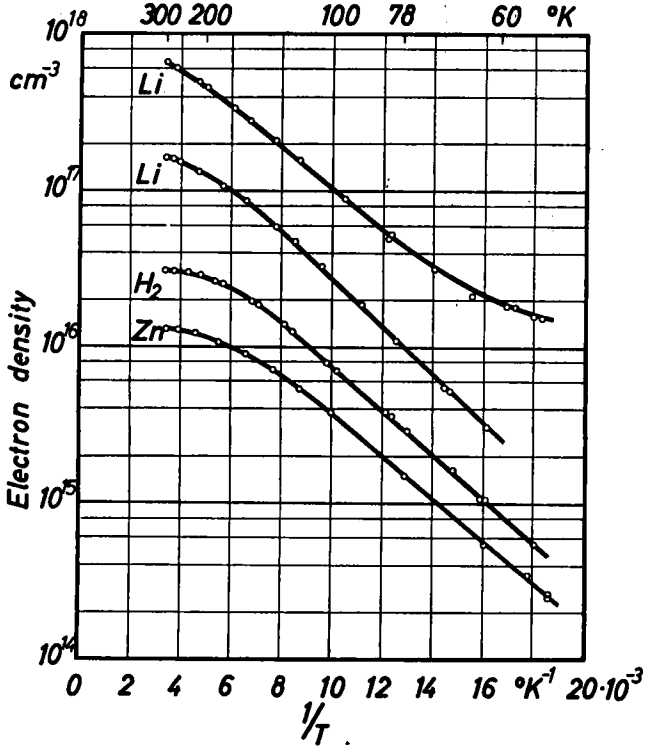

FIG. 54. Crystals, containing a small amount of H_2 and Zn. Electron density obtained from Hall effect as a function of temperature. The two upper curves are measured after treating the crystals with molten zinc containing a small amount of lithium. At the present time it seems doubtful if the lithium introduces donors, or if there are also just zinc donors. Hydrogen treatment: 1 atmos, 500°C, 10–15 min. Zinc treatment: 450°C, 5 min. After Hutson.[101a]

mined from measurements of the Hall effect, and the electron mobilities in the range of temperature between 60°K and 700°K are displayed in Figs. 56 and 57 for crystals heated in zinc vapor.[85] The relationships are very similar to those found for crystals heated in hydrogen.

[101a] A. R. Hutson, *Phys. Rev.* **108**, 222 (1957).
[102] G. Bogner, Diplomarbeit, University of Erlangen, 1956.

(3) *Indium.* Crystals in which an addition of indium is made during growth exhibit considerably larger increases in conductivity than those heated in hydrogen or zinc vapor (Section 6). The interrelationships between the electron density, the content of indium atoms, and the conductivity of such crystals are shown[25,85] in Fig. 58. As one can see, the concentration of electrons and of indium atoms are practically equal

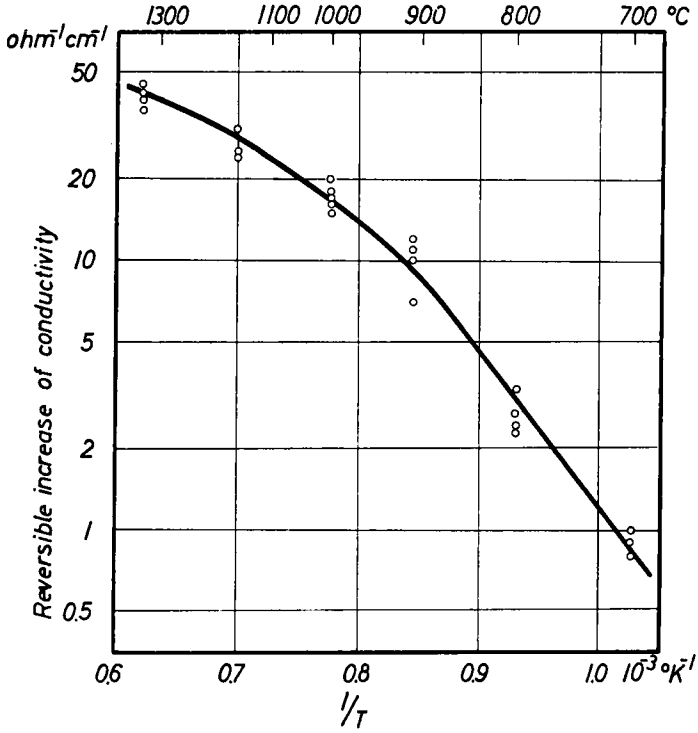

FIG. 55. Crystals. Increase of conductivity at room temperature after sufficiently long heating in saturated zinc vapor and quenching to room temperature. The heating temperature is given as the abscissa. After Pohl.[28]

for the same values of the conductivity. Initially, however, the conductivity increases approximately proportionately to these two quantities. The conductivity saturates at sufficiently high concentrations of indium. Presumably the solubility limit is exceeded in this range.

The conductivity and the electron concentration determined from the Hall effect are shown in Fig. 59 for temperatures below 300°K. Both are practically independent of the temperature. The same relation is

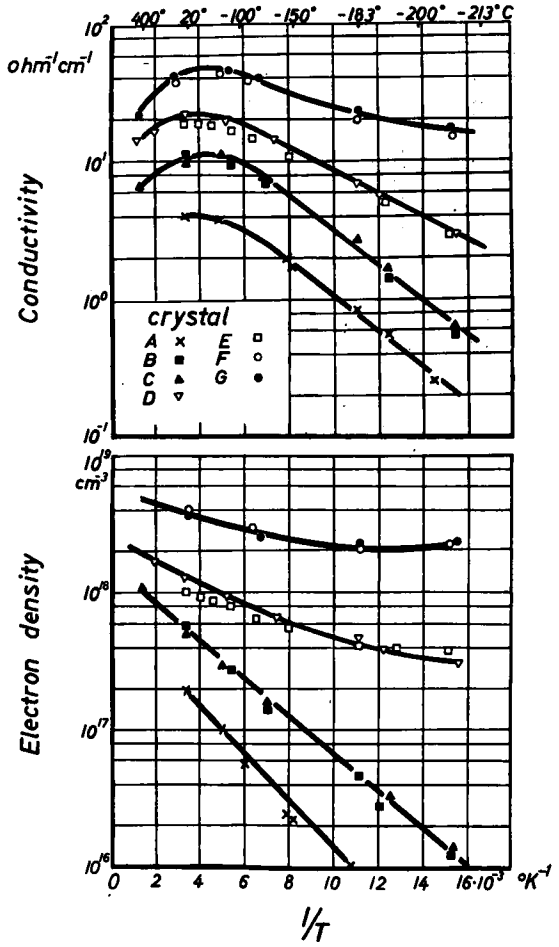

FIG. 56. Crystals heated in zinc vapor. Conductivity and electron density as a function of temperature. Zinc treatment: Crystal *A*: 850°C, 8 hr; Crystals *B* and *C*: 950°C, 50 hr; Crystals *D* and *E*: 1200°C, 4 hr; Crystals *F* and *G*: 1320°C, 1 hr. After H. Rupprecht.[85]

valid for the electron mobility. The latter quantity is shown in Fig. 60 as a function of the electron concentration. One finds a very slight decrease with increasing concentration of electrons.[85]

(*4*) *Copper.* In contrast to the behavior of the above-mentioned additions, doping with copper induces a decrease rather than an increase in conductivity when performed during growth of the crystals. Figure 61 shows the relationship[25] between the conductivity at room temperature

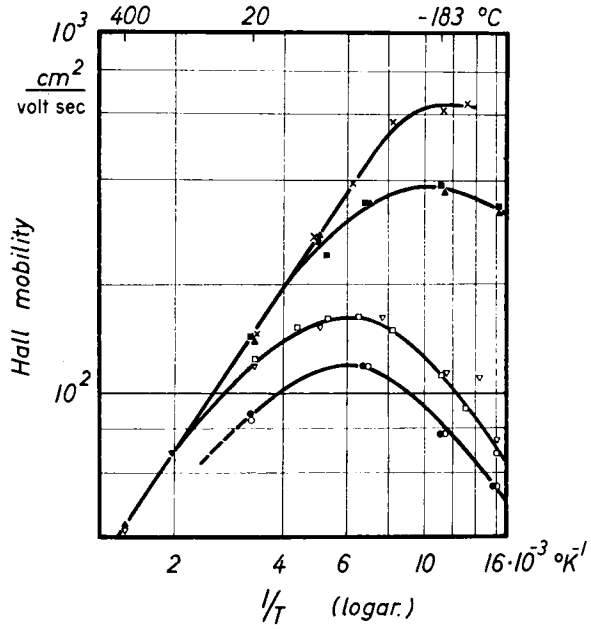

FIG. 57. Crystals treated in zinc vapor in the manner of those in Fig. 56. Hall mobility as a function of temperature. After H. Rupprecht.[85]

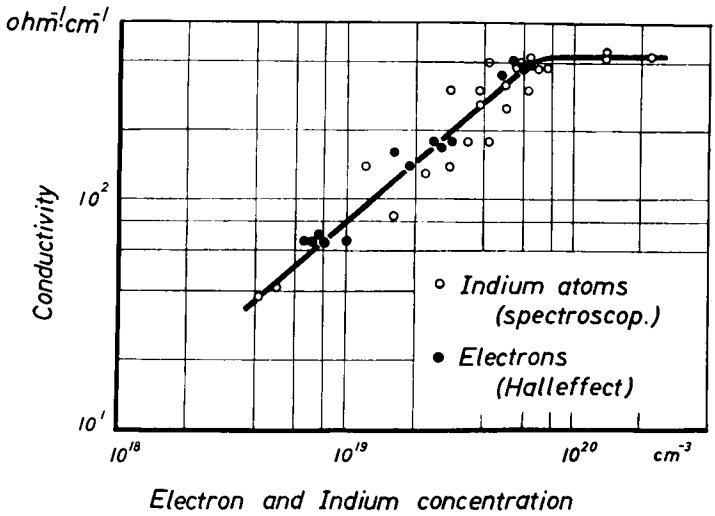

FIG. 58. Crystals with addition of indium. Conductivity at room temperature as a function of electron density (from Hall effect) or indium content (from spectral analysis). After Bogner and Mollwo,[25] and H. Rupprecht.[85]

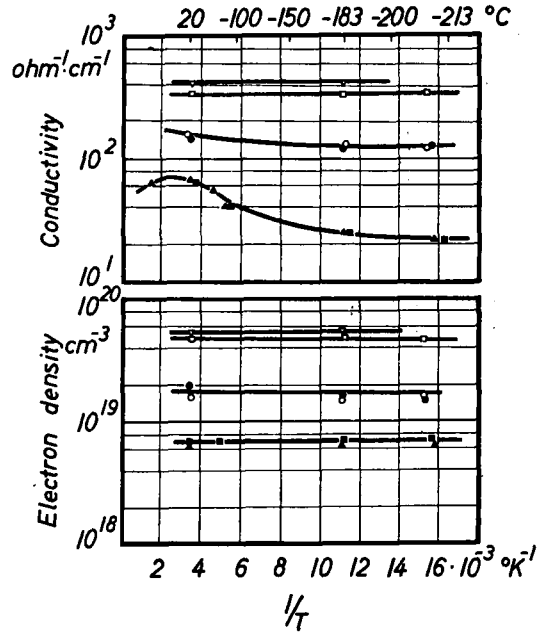

FIG. 59. Crystals with indium additions. Conductivity and electron density as a function of temperature. After H. Rupprecht.[85]

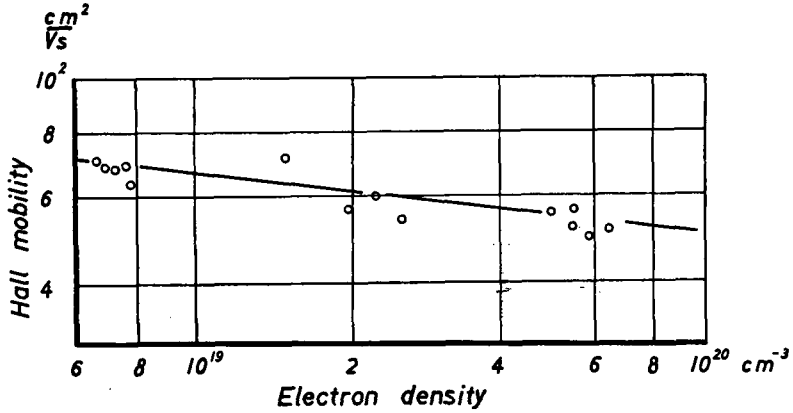

FIG. 60. Crystals with indium addition. Hall mobilities at room temperature as a function of electron density. After H. Rupprecht.[85]

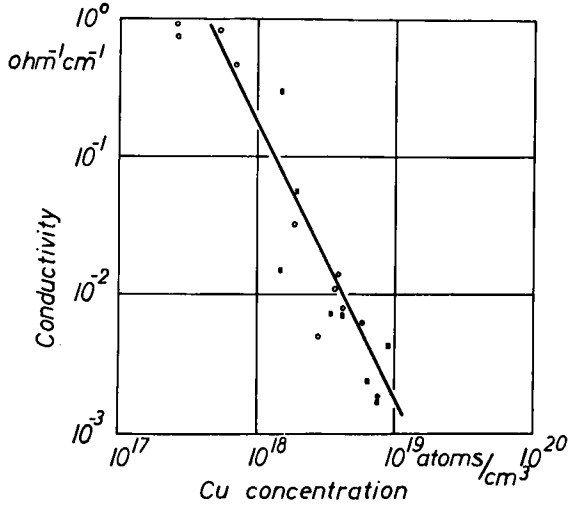

FIG. 61. Crystals with copper addition. Conductivity at room temperature as a function of copper concentration (from spectral analysis). After Bogner and Mollwo.[25]

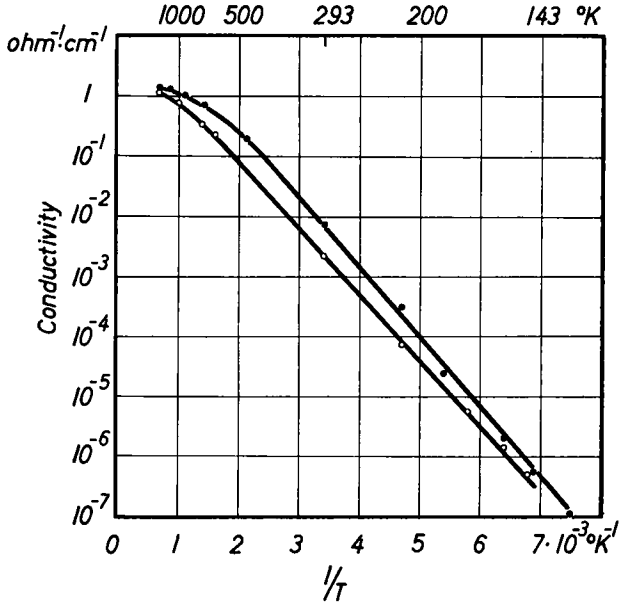

FIG. 62. Crystals with copper addition (5×10^{18} to 1×10^{19} Cu atoms/cm^3). Conductivity as a function of temperature. After Heiland[97] and Pohl.[98]

and the copper content as determined by spectral analysis. According to this, the conductivity is approximately proportional to the inverse of the square of the concentration of copper. Figure 62 shows[97,98] a typical example of the temperature dependence of the conductivity for two such crystals. Measurements of the concentration of electrons and of the mobility are not yet available. Up to now it has not been possible to obtain p-conducting zinc oxide by the addition of a large amount of copper, or, in fact, by any other addition.

c. Surface Conductivity of Single Crystals

Although a separation of the volume and surface effects is very difficult for thin layers and sintered specimens, one can delimit the volume and well-defined surface effects in single crystals. The surface conductivity of zinc oxide crystals was discovered in the course of investigations of the influence of hydrogen and oxygen on the conductivity of crystals.[86,87,97] Clear and reflecting growth surfaces have been used in such investigations. Since the volume conductance is always connected in parallel to the surface conductance, it is convenient to carry out the measurements at low temperatures where the volume conductance is very small. In general, the temperature dependence of the surface conductance is smaller than that of the volume conductance.

In carrying out the measurements, a current is passed in the direction of the length of the needle-like crystals, and the potential drop is measured at two platinum probes separated by a distance of about 0.1 cm. If the observed conductance g is due to surface conduction, one can calculate a characteristic "surface conductivity" defined as the conductance of a square piece of the surface. In the following the surface conductivity G (ohm^{-1}) will be expressed in the form

$$G = e\mu\nu \tag{19.1}$$

in which μ is the mobility and ν the surface density of the carriers (having the dimension cm^{-2}). The separation of probes and the crystal circumference were about the same in Figs. 64, 65, and 66. Thus, the conductance g, insofar as it is determined by the surface, can be interpreted in terms of the surface conductivity G without recalculation.

Crystals often have a surface layer which conducts well from the time of growth. Such cases can be recognized by the influence of oxygen upon the conductance at low temperatures as will be discussed later. The layer which conducts well can be removed easily by heating the crystals for a short time in air or in a vacuum at about 1000°K. An oxygen atmosphere has no influence upon the conductance of such a crystal except at very high temperatures (Section 19a).

Nevertheless, oxygen can exert an influence upon the crystal surface. This is indicated by the behavior of the rectification observed with a platinum point contact (Fig. 63). This rectification disappears when the specimen is heated in a vacuum at 600°K; it reappears when oxygen is introduced. The crystal has a positive voltage relative to the contact in the blocking direction. This indicates that the conductivity is *n*-type.

In contrast, a very intense influence of oxygen on the conductance of the crystal can be observed at low temperatures when a surface layer which conducts well is present. Such a layer can be produced either by the action of atomic hydrogen (surface conduction of type *A*) or by

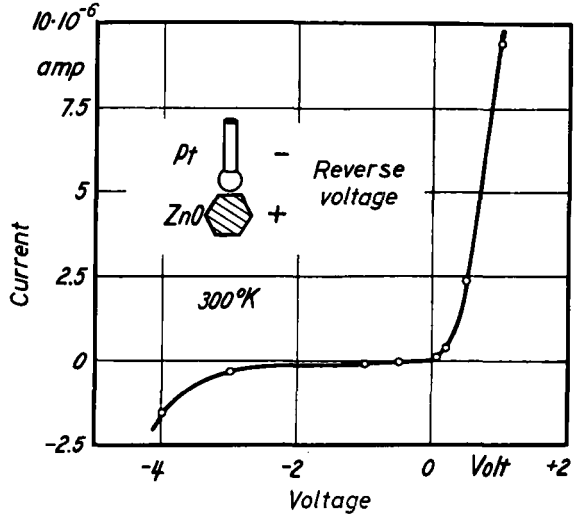

FIG. 63. Crystal. Current-voltage-relation of a platinum contact on a crystal covered with adsorbed oxygen. The rectification disappears after heating in a vacuum. After Heiland.[97]

heating for a short time in molecular hydrogen; for example, at 800°K for 15 min in 5 atmos of H_2 (surface conduction of type *B*). The atomic hydrogen can be produced either with a gaseous discharge or with a heated tungsten ribbon. The crystal may be at a temperature between 86°K and 500°K during the process. In contrast, molecular hydrogen produces no observable change in surface conductivity at these temperatures in times as long as six hours.

An example of the surface conductivity of type *B* is shown[87] in Fig. 64. The diagram demonstrates that the conductance of such a crystal can be decreased by orders of magnitude as a result of the action of oxygen at room temperature. Moreover, this decrease in the conduct-

ance persists in a vacuum. The effect of the oxygen can be reversed only by heating in a vacuum to 600°K (curves 6 and 7). A treatment with hydrogen at high temperatures and pressures leads to an increase in the conductivity in the entire volume (Sections 8 and 19b). The surface conductivity and the influence of oxygen subside at the same time (curves

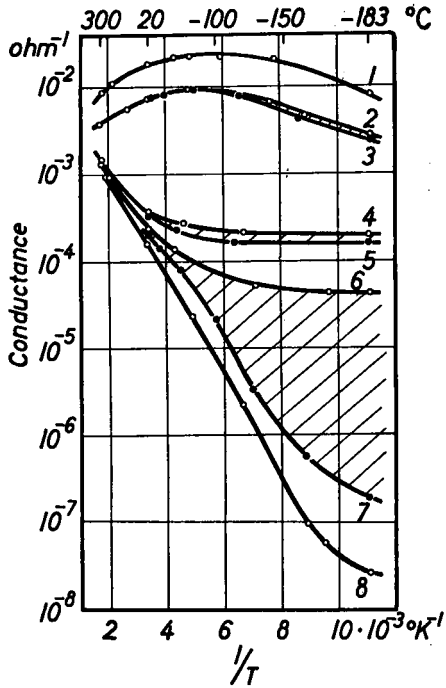

FIG. 64. Crystals. Conductance measured in a vacuum as a function of temperature after different treatments. 1: 50 atmos hydrogen, 600°C, 15 min. 2: 25 atmos hydrogen, 500°C, 15 min. 4: 1 atmos hydrogen, about 800°C, 3 sec. 6: 6 atmos hydrogen, 500°C, 15 min. 8: Vacuum, about 800°C, 10 sec. 1, 2, 4, 6, 8 measured after heating in a vacuum at 300°C, 10 min. 1, 3, 5, 7 result from 1, 2, 4, 6 after the action of oxygen (3 torr, 20°C, 3 min). Separation of probes about the same as the crystal circumference. Thus, the surface conductivity is equal to the surface conductance. After Heiland.[87]

4–5, 2–3, and 1). Curve 8 was obtained on the crystal after heating to incandescence (volume conductance). The surface conductivity of type *B*, generated by heating in hydrogen, is only temporarily masked by oxygen and is finally removed completely only by heating the crystal at 1000°K in air or in a vacuum. The electron diffraction pattern observed in reflection exhibited the structure of a single crystal[7] in the case of these crystal surfaces.

The surface conductivity of type A produced by atomic hydrogen at low temperatures[97] is less stable than that of type B. It subsides even when the specimen is warmed to 500°K in a vacuum. It disappears in the presence of oxygen just as the surface conductivity of type B does; however, it does not reappear after the oxygen treatment when the specimen is heated to 600°K in a vacuum. The increase of conductance with time as a result of the action of atomic hydrogen appears to follow a logarithmic law (Fig. 65). Figure 66 gives an example of surface conductivity of type A. The doping of the volume of the crystals has no significant influence upon the magnitude of the surface conductance as long

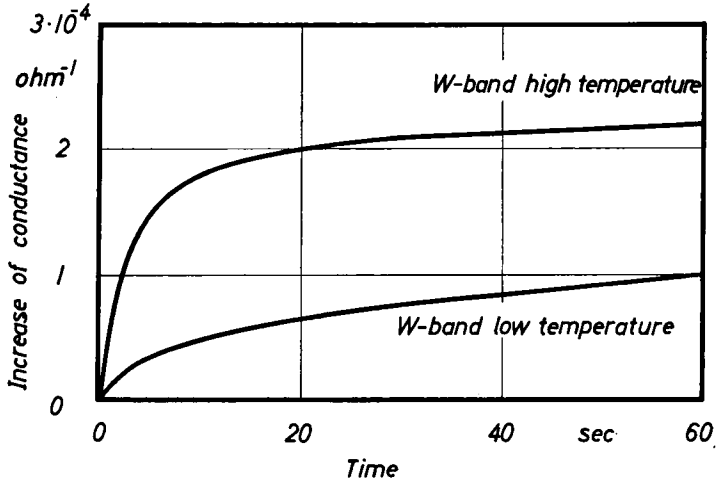

FIG. 65. Crystal. Increase of the conductance $g - g_v$ during the action of atomic hydrogen as a function of the time at 300°K. Volume conductance $g_v = 3.7 \times 10^{-5}$ ohm^{-1}. $p(H_2) = 1.6 \times 10^{-2}$ torr. $g - g_v \approx$ surface conductivity. After Heiland.[97]

as the parallel connected volume conductance does not become so large that the surface conductance can no longer be observed The same can be said about the influence of increasing temperature. The highest surface conductance is nearly independent of temperature, just as in Fig. 64.

The formation of a well-conducting surface layer on zinc oxide crystals provides a new, very sensitive test for atomic hydrogen. In order to regenerate the detector one must either heat the crystal in vacuum for a short time at 600°K, for example, directly by passing a current, or by permitting oxygen or air to act upon the specimen at room temperature. Conversely, the crystal with surface conduction provides a sensitive test device for oxygen.

It has been reported recently that surface conduction can be produced by the action of zinc vapor.[103] In this work the vapor density is kept below the saturation value at the temperature of the crystal, which lies between 300 and 800°K. The diffusion of excess zinc into the interior of the crystal can be excluded for the temperatures and times employed. The saturation value of the surface conductivity, namely, 1.5×10^{-4}

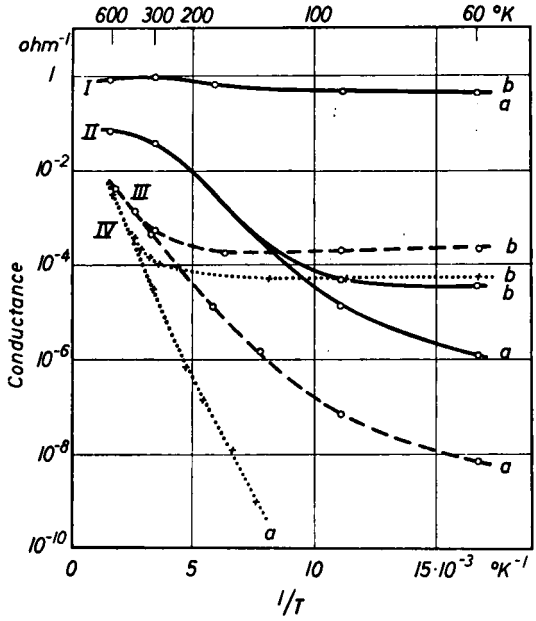

FIG. 66. Four different crystals. Influence of atomic hydrogen on conductance for very different volume conductivities (vacuum). (a) After heating in a vacuum, volume conductance. (b) After treatment with atomic hydrogen. After exposure to oxygen at 300°K curve a reappears. The probe spacing was of the order of the crystal circumference. Hence, the surface conductivity is equal to the surface conductance. After Heiland.[97]

ohm^{-1}, was about the same as that obtained by the action of atomic hydrogen (Figs. 65 and 66). When measured in a vacuum, this conductivity displays the same lack of dependence upon temperature down to 4°K. The introduction of oxygen decreases the surface conductivity in the same way as in the specimens of types *A* and *B*. The vapor pressure of zinc and the crystal temperature have practically no effect upon the saturation value of the surface conductivity attained with the zinc treatment over a wide range of conditions (see Section 25b).

[103] D. G. Thomas and J. J. Lander, *J. Phys. Chem. Solids* **2**, 318 (1957).

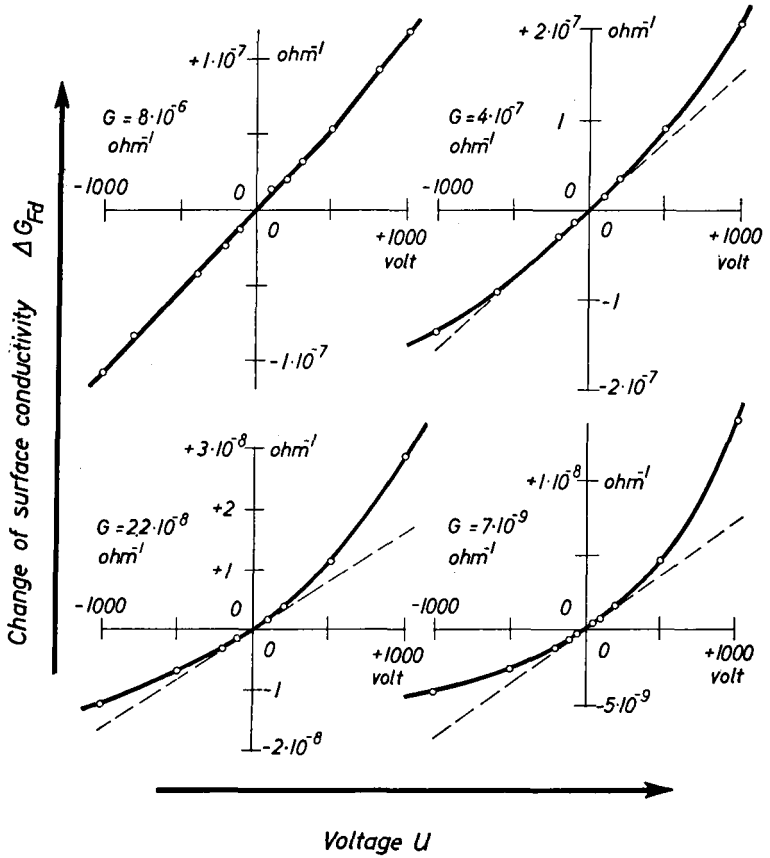

FIG. 67. Crystal (thin plate). Field effect. Variation of surface conductivity ΔG_{Fd} as a function of the voltage between the field electrode and the crystal (vacuum). G is the surface conductivity at zero voltage. Thickness of mica 7.4×10^{-3} cm. 90°K. After Heiland.[104]

VII. The Variation of the Conductivity as a Result of Various Influences

20. FIELD EFFECT ON CRYSTALS

The surface conductivity of crystals can be varied as a result of the influence of an electric field which is applied in the direction perpendicular to the flow of current and the crystal surface.[104] The crystals (plates) were provided with evaporated platinum electrodes, separated by 0.5 mm, after being heated in a vacuum. They were then treated with atomic hydrogen in vacuum apparatus before measurements were made

[104] G. Heiland, *J. Phys. Chem. Solids* **6**, 155 (1958).

in a vacuum (Section 19). The surface conductivity generated in this way can be diminished during the measurements by heating in a vacuum for a short time or by introducing small amounts of oxygen. Cooling to 90°K has the effect of reducing the volume conductance to a value that is small compared to the surface conductance. The field electrode and an insulating sheet of mica lying between the crystal and the electrode can be removed in the process of heating and treating with gas.

Figure 67 shows the variation ΔG_{Fd} of the surface conductivity resulting from the field effect as a function of the potential U between the field

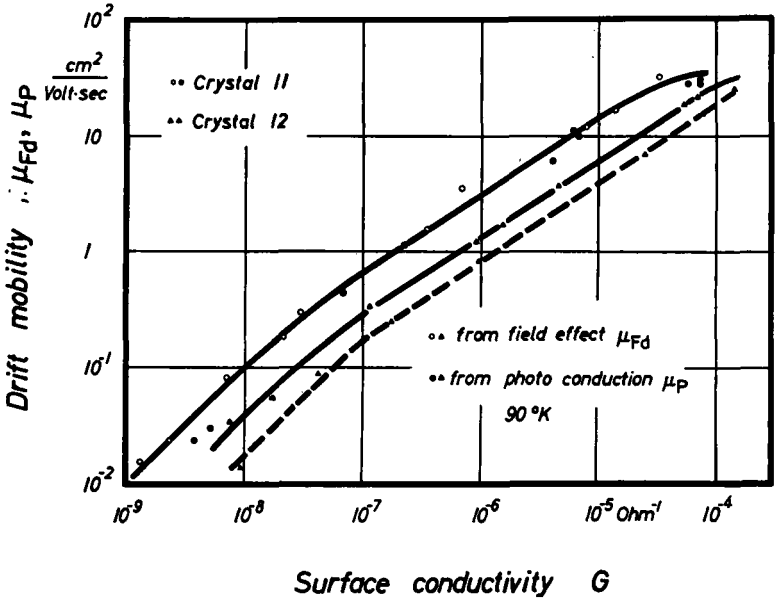

FIG. 68. Crystals (thin plates). Drift mobility as a function of surface conductivity Two independent methods of measurement: field effect and photoconductivity (chopped light). 90°K. After Heiland.[104]

electrode and the crystal for four different initial values of the surface conductivity G. The conductivity decreases if a positive surface charge is induced on the crystal, whereas it is increased by induction of a negative charge. It follows from this that the crystal surface exhibits n-type conduction, as one might suppose from knowledge of the influence of hydrogen and oxygen.

We have the relation $\Delta G_{Fd} \sim U$ at sufficiently small potentials U when $\Delta G_{Fd} \ll G$. With the induced charge density $e\Delta\nu_{Fd}$ one can define a "field effect mobility"

$$\mu_{Fd} = \Delta G_{Fd}/e\Delta\nu_{Fd}. \tag{20.1}$$

In using this expression for the drift mobility it is assumed that all the induced charge carriers are contributing to the surface conductivity. Figure 68 illustrates the field-effect mobility as a function of the surface conductivity G. This is changed by previous treatment of the surface with H, O_2, or heating in vacuum. Along with G, μ_{Fd} increases by four orders of magnitude. At small values of the surface conductivity one has the relation

$$\mu_{Fd} \sim G. \tag{20.2}$$

At larger values of the surface conductivity μ_{Fd} varies approximately as $G^{\frac{2}{3}}$. The largest value attained is 30 cm²/volt sec.

Sluggish changes in the surface conductivity, such as those produced by radiation with light (Section 22), are not observed in conjunction with the field effect in crystals which have been treated with atomic hydrogen. An inertial effect is not observed when the conductance is measured with a device having a time constant of one second when the field was turned either on or off. Slow effects were observed at very small conductances. However, these can be explained in terms of the large time constant of the electrical circuit. Further discussion of the field effect is given in Section 25c.

21. Influence of Oxygen on the Conductivity of Thin Layers

The conductivity of thin layers can be increased by orders of magnitude in a vacuum, for example, by previous heating to temperatures above 400°K. During these processes one observes nonstationary conductivity curves[8,86] (Fig. 69). In the dashed portion of the curve, the conductivity increases slowly even at constant temperature. An increase of the conductivity by several powers of ten can also be obtained by radiating in a vacuum with electrons or light in the spectral range of the fundamental band. This increase remains as long as the system is maintained in a vacuum even after turning off the radiation. Details of the process will be given in Section 22. The increased conductivity falls to its initial low value, however, when oxygen is admitted at room temperature.

It has been established with the following arrangement that gases are given off[76] when thin evaporated layers of zinc oxide are heated to about 500°K in a high vacuum. The layers were deposited on a quartz rod in a glass tube which was evacuated and sealed off from the pump with a mercury lock. Variations in the gas pressure were measured with a hot wire manometer placed in the glass tube. The same arrangement was used to observe the decrease of conductivity in an atmosphere of a zinc oxide layer which had been heated previously in a vacuum at 500°K. Figure 70 shows the variation with time of the current through the layer

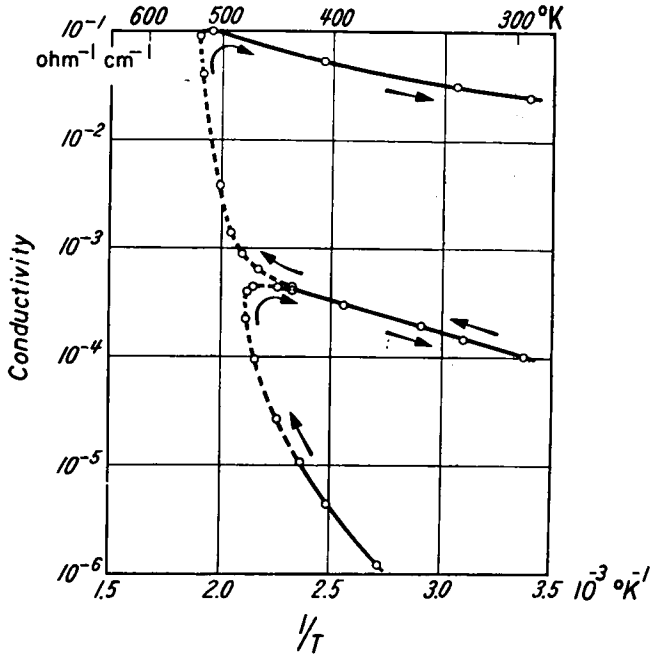

FIG. 69. Thin layer. Nonstationary conductivity in a vacuum at temperatures above 400°K. After Heiland.[86]

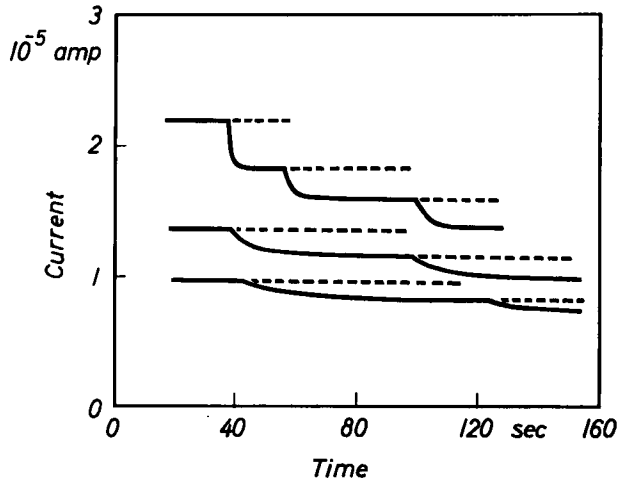

FIG. 70. Thin layer (1 × 1 cm²). Variation with time of the current at constant voltage (50 volts) for the introduction of equal quantities of oxygen (5×10^{-2} torr) in the volume of the chamber ($\approx$ 1 cm³). 1×10^{-5} amp corresponds to a conductivity of 7×10^{-2} ohm^{-1} cm^{-1}. Room temperature. After Mollwo.[76]

at constant voltage when the glass tube was filled seven consecutive times with the same pressure of oxygen. An interval was allowed to elapse before each filling to attain a constant value of the conductivity. The decrease in the current or conductivity for a given addition of oxygen is greater the higher the conductivity. This relationship could be followed continuously by simultaneous measurement of the current i and the oxygen pressure p. The following relationship was found to be valid over one power of ten

$$di/dp \sim i. \tag{21.1}$$

Assuming an electron mobility of 10 cm^2/volt sec (see Section 17a), it is possible to compare the number of adsorbed oxygen molecules with the number of conduction electrons which vanish simultaneously in the layer.

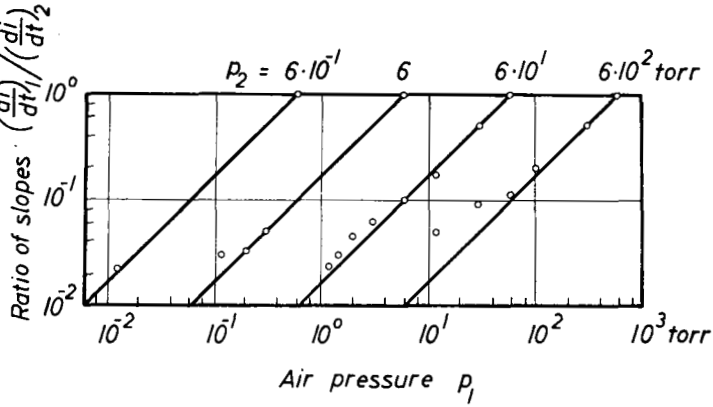

FIG. 71. Thin layer, after heating in a vacuum. Connection between the slope of the current-time curve and the pressure of the admitted air p_1 at different reference pressures p_2. The initial conductivity was 2×10^{-1} ohm^{-1} cm^{-1} in all cases. After Kefeli.[105]

There are many more oxygen molecules than conduction electrons bound. The ratio decreases from 7×10^5 to 10^5 with increasing conductivity of the layer.

If one exposes a zinc oxide layer which has been given a previous heating at 500°K in a high vacuum to oxygen at a constant pressure, the conductivity falls very rapidly initially and more slowly later. If one then increases the oxygen pressure suddenly, the current or the conductivity exhibits a kink when plotted as a function of the time. In this change the slopes immediately before and immediately after the kink point are proportional to the pressure of the atmosphere of oxygen.

[105] A. Kefeli, Diplomarbeit, University of Erlangen, 1957.

That is,

$$\left(\frac{di}{dt}\right)_1 \Big/ \left(\frac{di}{dt}\right)_2 = \frac{P_1}{P_2}. \tag{21.2}$$

One can use this effect to relate a known and an unknown concentration of oxygen often even under conditions in which one has a mixture of gases[105] (Fig. 71).

Powdered samples of ZnO consisting of very small particles become excellent insulators as the result of a negative surface charge of adsorbed oxygen ($\sigma = 10^{-17}$ ohm^{-1} cm^{-1}). The charge is stored for hours[106] in the dark. The special action of oxygen is shown by the following experiments. A corona discharge in air or oxygen provides an efficient negative surface charge. On the contrary, it seems to be impossible to produce a persistent positive surface charge (see "Electrofax," Section 23c). Further discussion is given in Section 25d.

22. Variation of the Conductivity by Radiation with Light or Electrons. Slow Processes

Irradiation with light or electrons generally increases the conductance of layers, sintered samples, and crystals. The conductance drops under the action of radiation only in exceptional cases. If one examines the time dependence, one can distinguish a slow and a fast process. The slow process is associated with a sluggish rise (or in special cases fall) of the conductance. This increase in the conductance endures in a vacuum until oxygen is introduced. The decrease of the conductance which then sets in starts fast but can be detected in air at room temperature over months as a slow drift. The slow process will be discussed in Section 22. In contrast, the fast process corresponds to a rapid rise of the conductivity to a constant value under radiation and to a rapid fall to the initial value when the light is turned off, even when the studies are made in a vacuum. Thus the fast process is found to be reversible, in contrast to the slow process which is irreversible in a vacuum. Section 23 deals with the fast process.

a. Thin Layers

Figure 72 shows[107] an example of the variation of the slow process with time in air. The conductivity rises linearly with time over many orders of magnitude for an astonishingly long period and ultimately attains a saturation value. The conductivity decreases rapidly at first when the radiation is turned off. This drop is then followed by a sluggish decrease.

[106] W. Ruppel, H. J. Gerritsen, and A. Rose, *Helv. Phys. Acta* **30**, 495 (1957).
[107] H. Mahr, Dissertation, University of Erlangen, 1957.

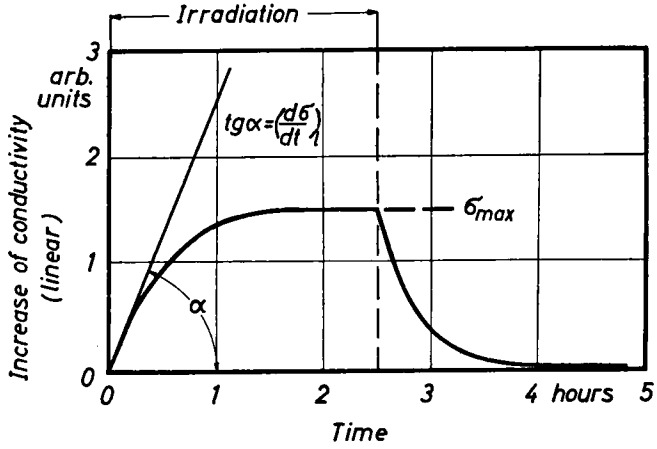

FIG. 72. Thin layer. Variation with time of conductivity during light irradiation in air. Slow process. After Mahr.[107]

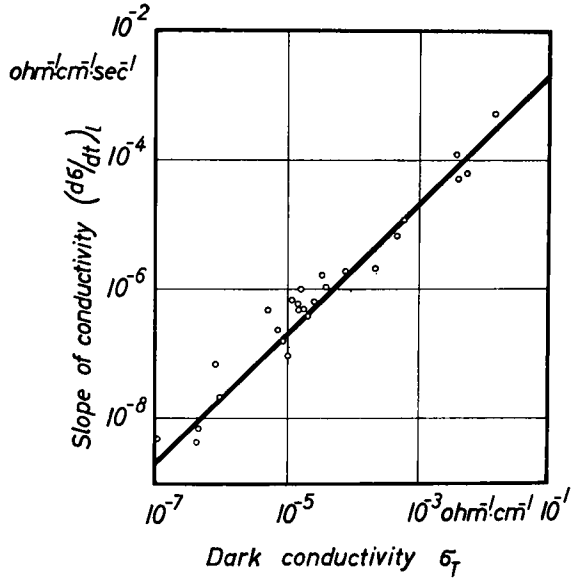

FIG. 73. Thin layer. Slow rise of conductivity $(d\sigma/dt)_t$ during irradiation with light as a function of the lowest dark conductivity σ_T. The rise is independent of oxygen pressure. After Tischer.[90]

Since the properties of different thin films scatter considerably, an attempt was made to coordinate the results by means of an experimentally determined quantity. For this purpose the "lowest conductivity" σ_T was regarded as a proper parameter. This is the conductivity attained after about a week in air in the dark. The conductivity actually falls somewhat more; however, this occurs very slowly. As a consequence of oxidation, σ_T can vary over six orders of magnitude. Additions of copper and heavy oxidation (compare Sections 4 and 17b) lead to a small value of σ_T, whereas additions of indium and weak oxidation lead to large values.

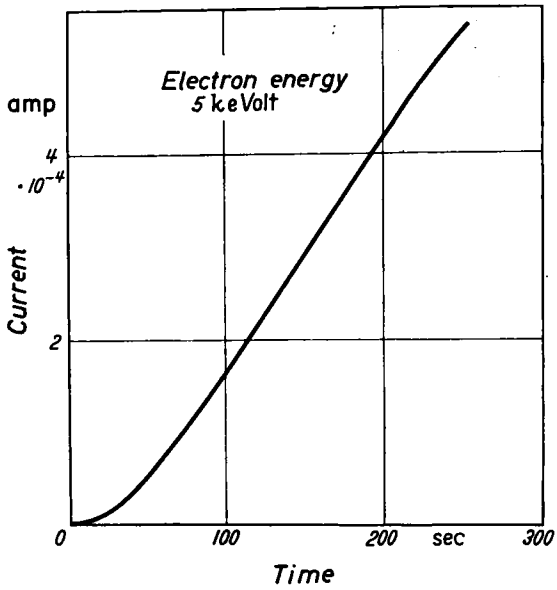

FIG. 74. Thin layer. Current as a function of time during electron bombardment in a vacuum. Bombarding current 3.2×10^{-10} amp. Intensity: 1.6×10^{-4} watt/cm^2. After Heiland.[108]

The following relations[90] are found to govern the initial slope of the conductivity $(d\sigma/dt)_i$ when the radiation is turned on and the saturation conductivity σ_{max}

$$\left(\frac{d\sigma}{dt}\right)_i = C_1 I \sigma_T \qquad \text{(independent of oxygen pressure)} \qquad (22.1)$$

$$\sigma_{max} = C_2 I^{\frac{1}{2}} p^{-\frac{1}{4}} \sigma_T. \qquad (22.2)$$

Here I is the intensity of radiation.

Even in a vacuum the conductivity appears to tend toward a saturation value. At small intensities of radiation an initial linear rise extending

[103]G. Heiland, *Z. Physik* **132**, 354 (1952).

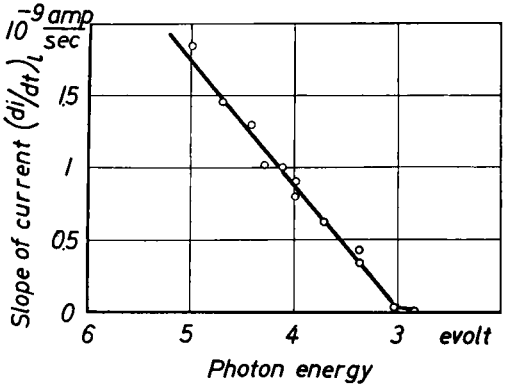

FIG. 75. Thin layer. Slow rise of current $(di/dt)_l$ during irradiation with light in a vacuum as a function of the photon energy, referred to the photon number 4.5×10^{13} cm^{-2} sec^{-1}. Dark current 2.2×10^{-6} amp. After Weiss.[109]

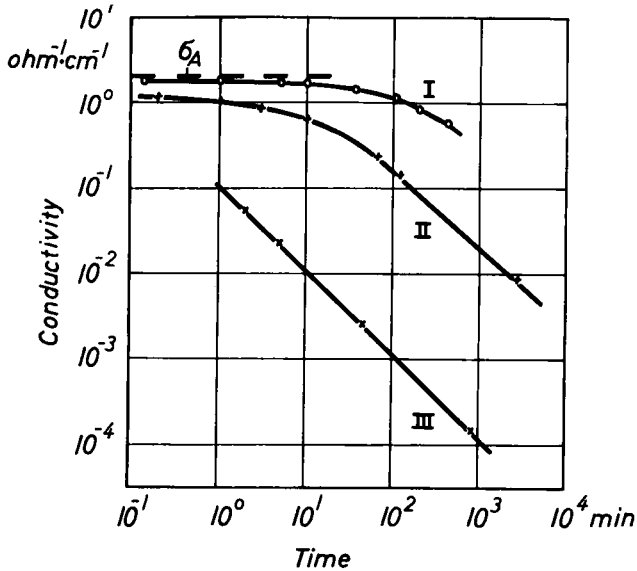

FIG. 76. Thin layer. Decay of conductivity at different pressures of air. I: 6×10^{-6} torr. II: 10^{-2} torr. III: 760 torr. The preceding irradiation occurs in a vacuum and produces the same initial conductivity σ_A for all curves. After Mahr.[107]

over several orders of magnitude is observed. If the radiation is interrupted during the linear rise and then re-established, the same slope $(d\sigma/dt)_l$ is resumed in spite of the increased conductivity. The magnitude of this slope is not determined by the conductivity attained by radiation, but by the characteristic lowest value σ_T associated with the layer.

[109] H. Weiss, *Z. Physik* **132**, 335 (1952).

Figure 73 indicates the slope as a function of σ_T during irradiation with light in air. Figure 74 gives the current, which is proportional to the conductivity through the layer, under electron bombardment in a vacuum. Here the linear rise is preceded in general by a parabolic variation.

The spectral variation of the slope of the current which is proportional to $(d\sigma/dt)_i$ is shown in Fig. 75 (vacuum). The slow process begins at the absorption edge and increases linearly with increasing quantum energy.[109]

The velocity of decay after termination of the radiation depends both on the pressure of oxygen (Fig. 76) and upon the previous history.[107] If a given initial conductivity is attained with a high intensity of radiation, it is followed by a rapid decay. The converse is true if the rise is slow because the irradiation is weak. If the layer is irradiated in a vacuum at low temperatures, the irreversible additional conductivity attained retrogresses almost completely when the specimen is heated to room temperature.[109]

b. Sintered Specimens

Sintered specimens exhibit a slow process similar to that found in thin layers. Figure 77 shows in a schematic way the influence of the

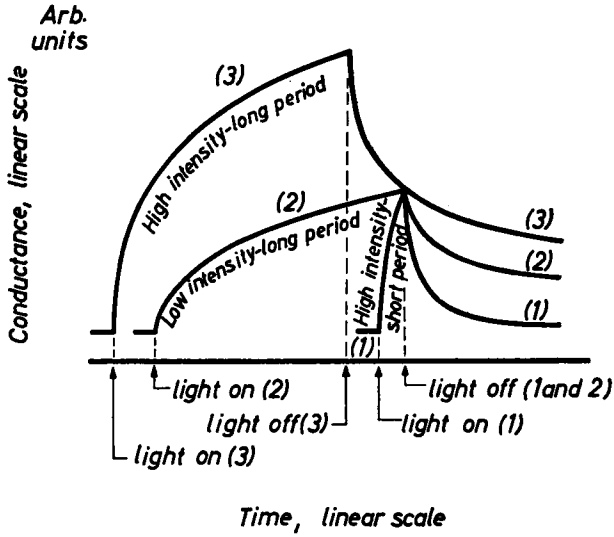

FIG. 77. Sintered samples. Schematic representation of the variation with time of the conductance in air during irradiations with light of different periods and intensities. After Miller.[110]

[110] P. Miller, "Conference on Photoconductivity, Atlantic City." Wiley, New York, 1956.

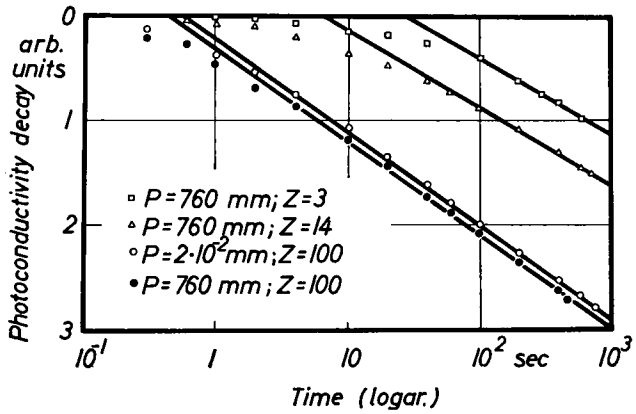

FIG. 78. Sintered sample (2.5×10^{-3} cm thick). Decay of photoconductivity from saturation for three intensities Z of illumination and two pressures P of O_2. After Melnik.[111]

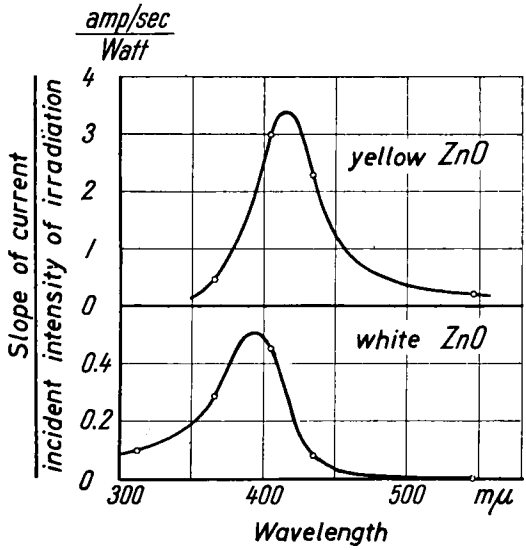

FIG. 79. Sintered layers. Slope of current during irradiation with light in air as a function of wavelength, referred to the same incident intensity. Area about 1 cm². After Mollwo and Stöckmann.[9]

previous history (radiation intensity) upon the course of the decay.[110] The decrease of the conductivity after the radiation is turned off is shown in Fig. 78 on a logarithmic time scale for a number of intensities of radiation and for two different pressures of oxygen. A logarithmic time

[111] D. A. Melnik, *Phys. Rev.* **94**, 1438 (1954).

law seems to be valid here.[111] Comparison with Fig. 76 indicates, however, that the observed variations of the conductivity were too small and the observation times too short to establish this rule with certainty.

The spectral distribution for the slope of the current through sintered specimens is shown in Fig. 79. In the case of white zinc oxide, the maximum lies in the vicinity of the absorption edge, whereas it is at somewhat longer wavelengths for the yellow oxide.[9]

c. Single Crystals

Phenomena similar to those found during observations with thin layers and sintered specimens can be observed on single crystals.[86] This is found to be the case when the conductance of the crystals is determined primarily by a good conducting surface layer (compare Section 19c).

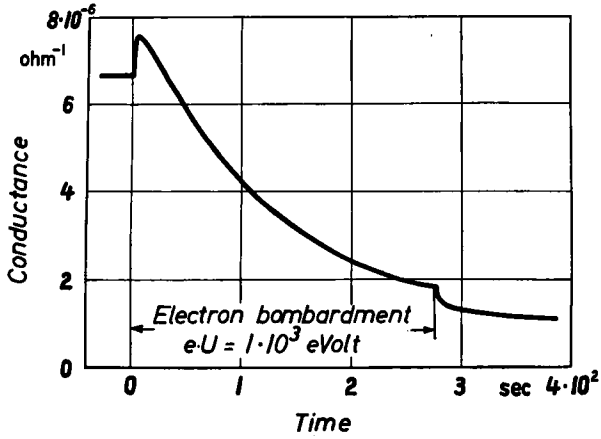

FIG. 80. Crystal. Variation with time of conductance during electron irradiation in a vacuum. Intensity 3.3×10^{-2} watt/cm². After Heiland.[86]

Under these conditions light and electron irradiation can induce a slow irreversible increase in the conductance observed in a vacuum. If the irradiation takes place at liquid air temperature, a substantial part of the irreversible increase of conductance is found to have vanished after the crystal has been warmed to room temperature and cooled again. The effect of oxygen on the increased conductance is similar to that for thin layers. More explicit measurements are not available. A slow decay of the conductance is also observed in the case of weak electron irradiation. This can vary over orders of magnitude for sufficiently extended radiation. Figure 80 shows an example. The simultaneous occurrence of two different processes is shown particularly clearly in this figure. The slow process leads to a sluggish decay of the conductance on which is

superimposed a fast rise when the radiation is turned on or a rapid fall when the radiation is turned off. Further discussion of Section 22 is given in Section 25e.

23. Variation of the Conductance by Irradiation with Light or Electrons. Fast Processes

a. Thin Layers

The fast process can be observed frequently along with the slow process. To be sure, the variations in the conductance produced in this way are usually considerably smaller. Figure 81 shows schematically

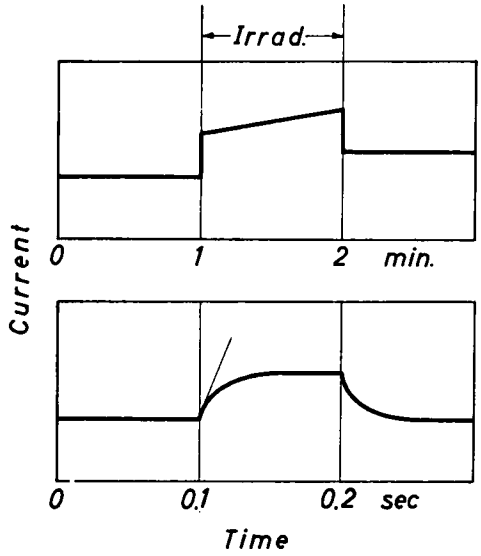

Fig. 81. Thin layer. Schematic variation of photocurrent with time.

the variation with time of the current in the case of the fast process in a vacuum. The radiation is turned on for a longer time in the case corresponding to the upper curve so that the irreversible increase associated with the slow process is quite notable. This increase can vary over a wide range for the same intensity of radiation $(d\sigma/dt)_I \sim \sigma_T$ (compare Section 22a). Separation of the fast process is very difficult if the slow attains a large value. In the case of the fast process, one can establish a number of regularities with an essentially higher degree of reproducibility and a smaller amount of scattering from specimen to specimen than in the case of the slow process.[112]

[112] E. Mollwo, *Ann. Physik* [6] **3**, 230 (1948).

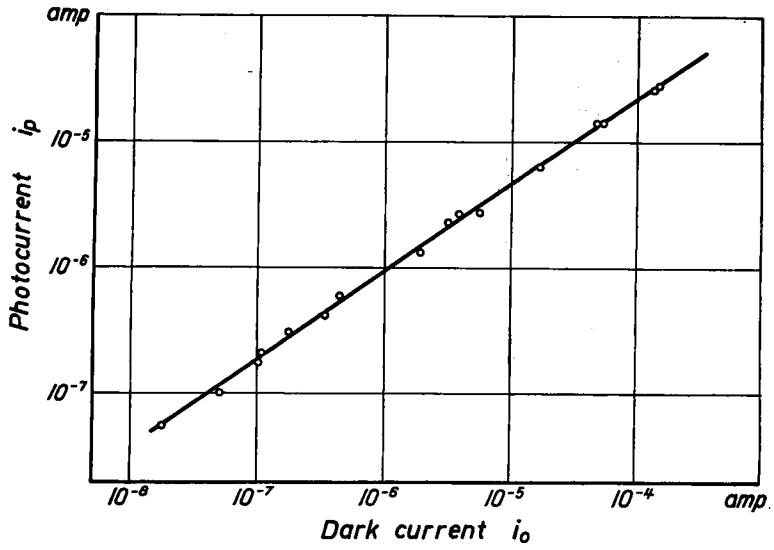

FIG. 82. Thin layer. Photocurrent as a function of dark current. Intensity $I = 2.9 \times 10^{15}$ quanta/cm² sec, $h\nu = 3.4$ ev. After Mollwo.[112]

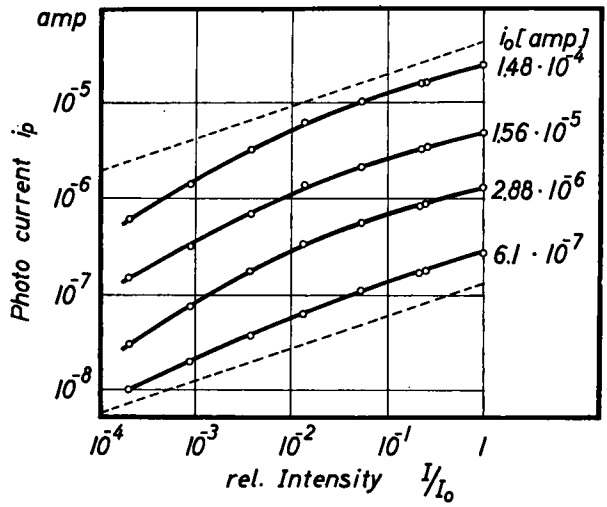

FIG. 83. Thin layer. Photocurrent as a function of intensity of radiation I. $I_0 = 2.9 \times 10^{15}$ quanta/cm² sec, $h\nu = 3.4$ ev. After Mollwo.[112]

All the measurements discussed in this section were made in a vacuum. The dark current can be varied by electron irradiation or the introduction of oxygen. Then the photocurrent i_p increases with the dark current i_0 for several orders of magnitude (Fig. 82). The following relationship is valid

$$i_p \sim i_0^{\frac{2}{3}}. \tag{23.1}$$

The dependence on the intensity of the radiation I (Fig. 83) can be

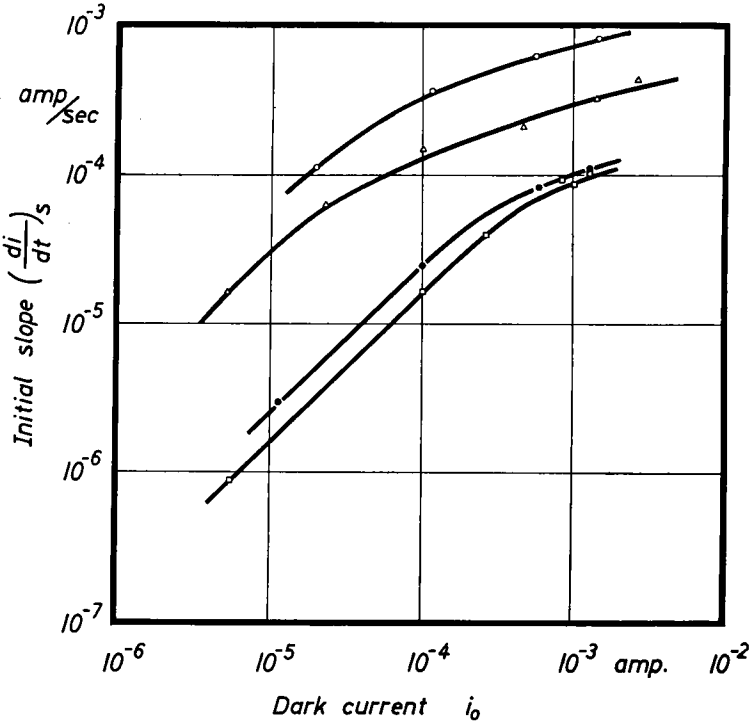

FIG. 84. Thin layers. Initial slope of photocurrent $(di/dt)_S$ as a function of dark current i_0. Vacuum. Intensity of irradiation $I = 4.5 \times 10^{13}$ quanta/cm² sec (1.5×10^{-5} watt/cm²). $h\nu = 3.4$ ev. The two upper curves correspond to small additions of copper, the two lower curves to large additions. (Compare Section 4.) After Weiss.[109]

represented in the manner

$$i_p \sim I^{\frac{1}{3}} \tag{23.2}$$

over several orders of magnitude. Larger exponents are observed in Eqs. (23.1) and (23.2) when the dark currents and the intensity of radiation are small.

The stationary value of the photocurrent is determined by the establishment of equilibrium between the freeing of carriers and their

recombination. Measurements of the initial rise of the photocurrent $(di/dt)_s$ were carried through with the objective of investigating the freeing of carriers by absorbed light without the interference of recombination (compare Fig. 81). The relationship between the initial slope and the dark current is given in Fig. 84 for various layers. At low currents we have

$$\left(\frac{di}{dt}\right)_s \sim i_0 \tag{23.3}$$

whereas the increase occurs more slowly for high dark currents. In addition the relation

$$\left(\frac{di}{dt}\right)_s \sim I \tag{23.4}$$

is always valid. Attempts have been made to obtain information about the quantum yield from both these relations.[108,109,113,114]

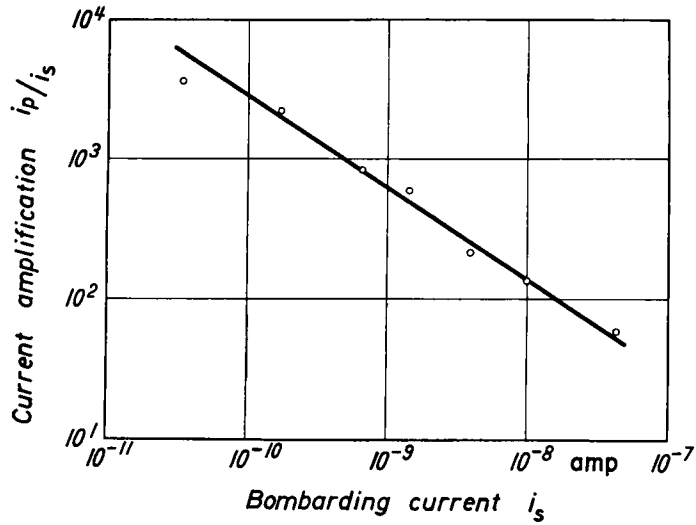

FIG. 85. Thin layer. Current amplification (induced current/bombarding current) as a function of the intensity of irradiation with electrons. Dark current (before irradiation) $i_0 = 10^{-5}$ amp. Electron energy 5×10^3 ev. After Heiland.[108]

All of the relationships described previously in this section were also found under irradiation with electrons[108] having energies in the range of 1 to 5 kev. The intensity of radiation I is replaced by the density of the bombarding electron current i_s. In this study it is possible to define the

[113] E. Mollwo, *Z. physik. Chem. (Leipzig)* **198**, 258 (1951).
[114] G. Heiland, *Z. Physik* **132**, 367 (1952).

current amplification in terms of the increase i_p of the current through the layer relative to the current i_s of the electron beam. Figure 85 shows this current amplification as a function of the bombarding current. The decrease of the amplification corresponds to the relation (23.2), namely, $i_p \sim i_s^{\frac{1}{3}}$. Figure 86 shows an example of the dependence of the initial slope upon the dark current.

The initial slope of the decaying photocurrent, when the irradiation is turned off[111] has been measured for thin layers. This slope is always

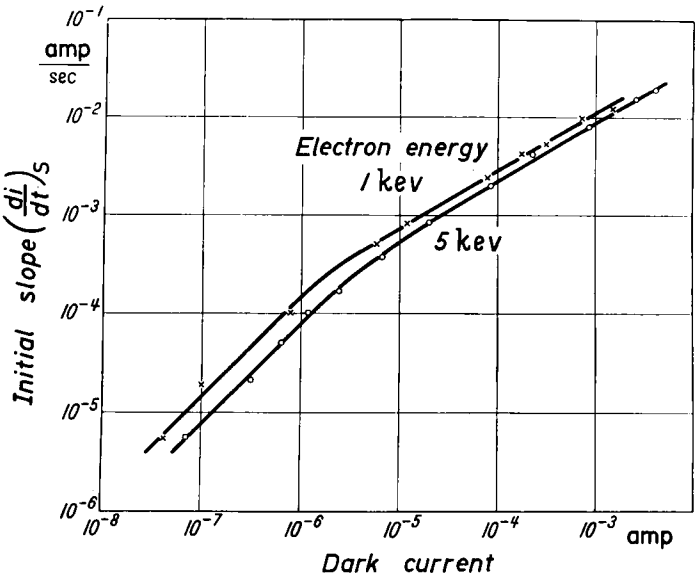

FIG. 86. Thin layer. Initial slope of induced current $(di/dt)_S$ during electron bombardment as a function of dark current i_0. Intensity of irradiation $I = 1.6 \times 10^{-3}$ watt/cm^2. After Heiland.[108]

smaller than the slope obtained when the radiation is turned on. The two slopes are the same only in the limiting case in which i_p is much less than i_0.

The temperature dependence of the photocurrent for different values of the dark current is reproduced in Fig. 87.[109] The spectral distribution of the photocurrent (Fig. 88) follows the absorption spectrum closely (Fig. 14). In contrast to the slow process, photoconduction (fast process) is also observed using irradiation of longer wavelength than that at the absorption edge. A comparison of Figs. 88 and 75 indicate, completely generally, that the spectral distributions of the fast and the slow processes are very different.[109]

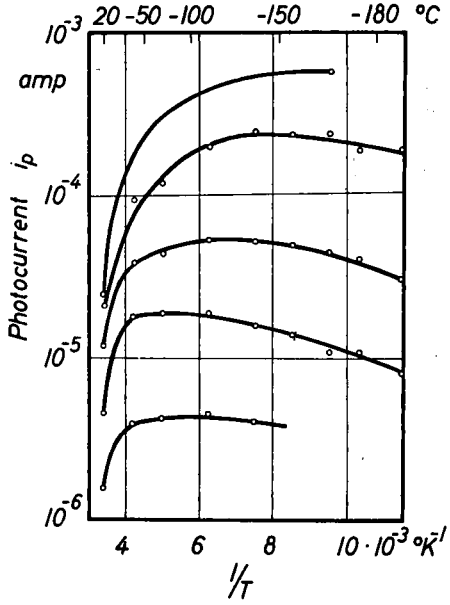

FIG. 87. Thin layer. Temperature dependence of photocurrent for different values of dark current. Intensity of radiation $I = 1.5 \times 10^{13}$ quanta/cm^2 sec. $h\nu = 3.4$ ev. Compare Fig. 35. After Weiss.[109]

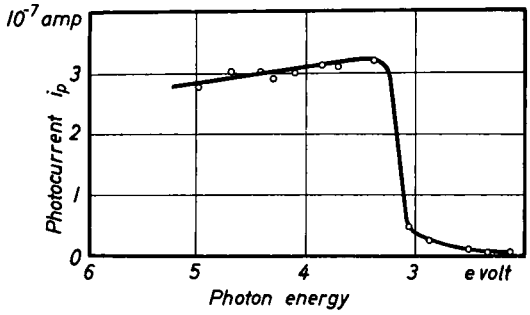

FIG. 88. Thin layer. Photocurrent as a function of photon energy referred to incident photon number 4.5×10^{13} cm^{-2} sec^{-1}. $h\nu = 3.4$ ev. Dark current 2.2×10^{-6} amp. After Weiss.[109]

Investigations of the fast processes have not been carried out on sintered specimens.

b. Single Crystals

There is a very close relationship between the surface conductivity and the photo-surface-conductivity in the case of single crystals (see

Section 19c). The latter quantity is defined as the increase of the surface conductivity during irradiation with light and is, therefore, the increase of the conductance of a square area [compare Eq. (19.1)]. It has not yet been possible to demonstrate photoconduction in the volume of single crystals. The investigation of photoconductivity was carried out in a vacuum at 90°K.[86,104] No effect could be observed at room temperature. Light of wavelength 366 mμ was employed except in the case shown in Fig. 92. The penetration depth was of the order of 10^{-5} cm (Fig. 14).

Figure 89 indicates the photo-surface-conductivity ΔG_p as a function of the surface conductivity G_0 for four different specimens after various

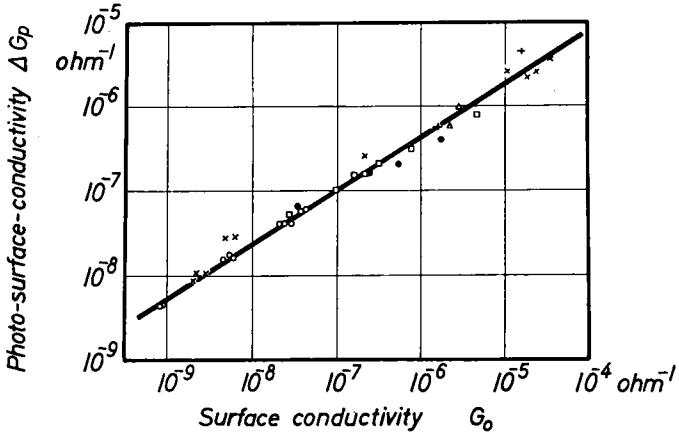

FIG. 89. Crystals. Photo-surface-conductivity ΔG_p as a function of dark-surface-conductivity G_0 (type B, Section 19c). Intensity of radiation 6.3×10^{14} quanta/cm² sec. $h\nu = 3.4$ ev. 90°K. After Heiland.[86]

treatments such as heating in a vacuum, heating in hydrogen (surface conductivity of type B), and the action of oxygen. The following relation is valid over more than 5 orders of magnitude of G_0

$$\Delta G_p \sim G_0^{\frac{2}{3}}. \tag{23.5}$$

This relationship goes over into the relation $\Delta G_p \sim G_0$ for small values of G_0 and small intensities of radiation I. This is shown in Fig. 90 for a crystal with a surface conductivity of the type A.

The influence of the intensity of radiation (Fig. 91) is given approximately by the following law

$$\Delta G_p \sim I^{\frac{1}{3}}. \tag{23.6}$$

The dependence on the intensity of radiation involves a larger exponent at small values of I and G_0. It is possible to have ΔG_p greater than G_0 at large values of the radiation intensity.

The relations (23.5) and (23.6) correspond to the Eqs. (23.1) and (23.2) for thin layers, and are valid for crystals with a surface conductivity of the type A[104] as well as of type B.[86]

The initial slope of the photoconductivity was investigated for thin layers in order to exclude the influence of recombination. Instead, the amplitude $G_\sim$ of the photo-surface-conductivity was measured with chopped light in the case of the single crystals.[104] The problems which are

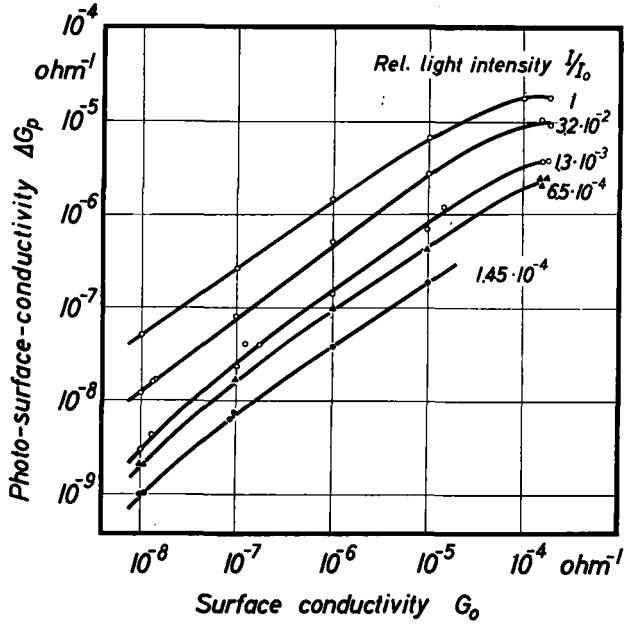

FIG. 90. Crystal 12. Photo-surface-conductivity ΔG_p as a function of dark-surface-conductivity G_0 (type A: atomic hydrogen, Section 19c) for different intensities of irradiation I. $I_0 = 4.8 \times 10^{15}$ quanta/cm^2 sec. $h\nu = 3.4$ ev. 90°K. After Heiland.[104]

encountered in this type of measurement are discussed extensively by Niekisch.[115] Corresponding to $(di/dt)_s \sim I$, one finds

$$G_\sim \sim I. \tag{23.7}$$

Moreover, one finds that

$$G_\sim \sim 1/\omega \tag{23.8}$$

approximately.

It is possible to determine a drift mobility μ_p of the carriers (electrons) as in the case of the field effect if one assumes that each absorbed light quantum frees an electron. The chopping frequency is high enough, if the relations (23.7) and (23.8) are valid. Then the following formula can be

[115] E. A. Niekisch, *Ann. Physik* [6] **15**, 279 (1955).

used when $G_\sim \ll G$:

$$\mu_p = \frac{G_\sim \omega}{eI_\sim}. \tag{23.9}$$

Here G is the total mean surface conductivity during irradiation; ω the circular frequency of the chopped light; $G_\sim$ the amplitude of the photoconductivity; $I_\sim$ the amplitude of the absorbed radiation (this quantity

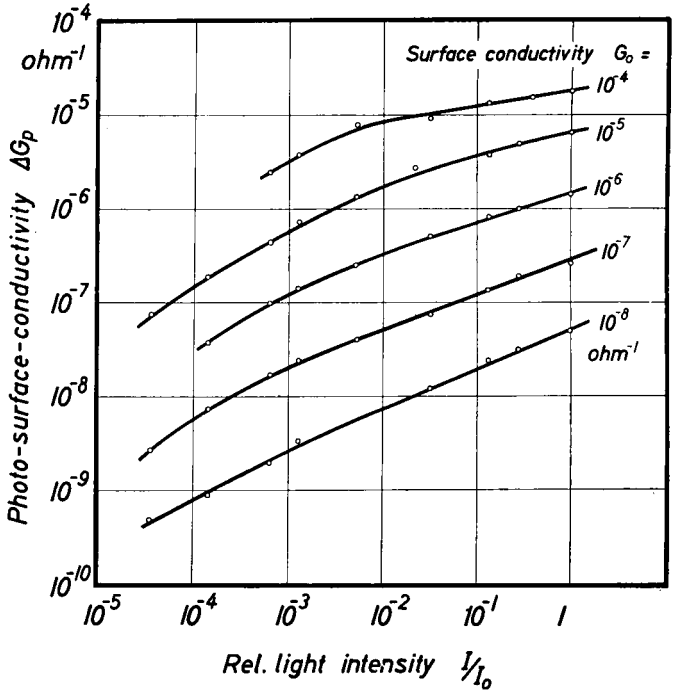

FIG. 91. Crystal 12. Photo-surface-conductivity ΔG_p as a function of the intensity of radiation I for different dark-surface-conductivities G_0 (type A). $I_0 = 4.8 \times 10^{15}$ quanta/cm² sec. $h\nu = 3.4$ ev. 90°K. After Heiland.[104]

is expressed in numbers of quanta per area and time; modulation by a rotating diaphragm). A comparison with the corresponding formula for the field effect mobility

$$\mu_{Fd} = \frac{\Delta G_{Fd}}{e\Delta\nu_{Fd}} \tag{20.1}$$

indicates that the amplitude of the photoelectric modulated carrier density $I_\sim/\omega$ takes the place of the induced carrier density $\Delta\nu_{Fd}$. The drift mobility determined from the photoconductivity and the field effect

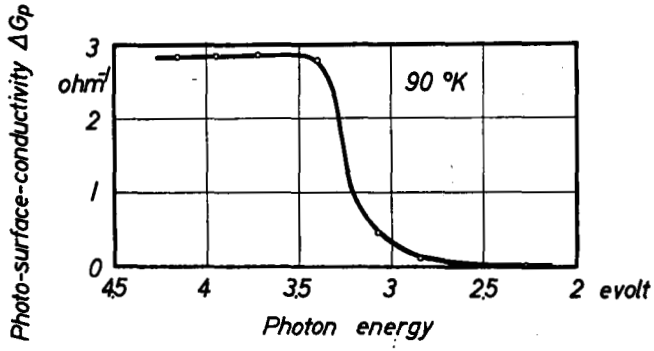

FIG. 92. Crystal. Photo-surface-conductivity as a function of photon energy referred to the incident photon number 3.1×10^{15} cm^{-2} sec^{-1}. Dark-surface-conductivity $G_0 = 2 \times 10^{-8}$ ohm^{-1}. Add an ordinate factor 10^{-8}. After Heiland.[104]

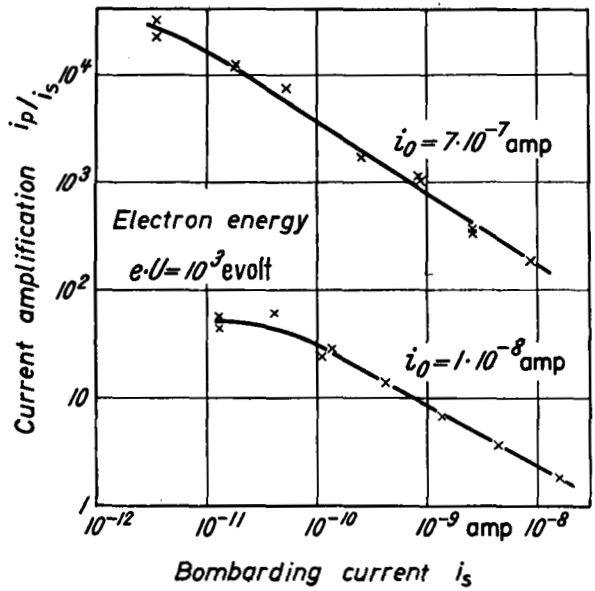

FIG. 93. Crystal. Current amplification (induced current/bombarding current) as a function of bombarding current; 90°K; i_0 = dark current. After Heiland.[86]

is shown in Fig. 68 as a function of the surface conductivity G for two different crystals. The results obtained by very different methods agree quite well. The drift mobility increases with increasing surface conductivity through many orders of magnitude. Initially one has the relation $\mu_p \sim G$ and then the approximate relation $\mu_p \sim G^{\frac{3}{4}}$. Finally the drift mobility approaches to within a factor 2 the value determined in the

volume on strongly doped material with the use of the Hall effect and the conductivity (see Fig. 60 for example).

The spectral distribution of photo-surface-conductivity is reproduced in Fig. 92. As in the case of thin layers, there is a close correlation with the absorption spectrum (Fig. 20).

Electron bombardment acts in much the same way as light irradiation. Figure 93 shows the current amplification, defined in Fig. 85, as a function of the bombarding current.[86]

The photoconductivity of single crystals obeys laws similar to that observed in thin layers. This all goes with the provision that one has a surface layer which conducts well initially. It is characteristic of both thin layers and single crystals that the fast effects can be followed over many orders of magnitude of the dark conductivity and the surface conductivity and are strongly influenced by them. The situation is much the same in the case of the field effect (Section 20). A discussion of the fast process is given in Section 25f.

c. "Electrofax"

An interesting application of photoconductivity of zinc oxide which may achieve a great deal of practical importance is contained in an optical reproduction process known under the designation of "Electrofax."[115a] It is similar to xerography in many respects. In the case of Electrofax, however, the paper on which the final print appears is photosensitive. The Electrofax paper is ordinary paper having a thin flexible white coating of special zinc oxide in a resin binder. The basic Electrofax process can be described by following a simple four-step procedure for making a direct print.

1. The paper is first made sensitive to light by giving it a blanket negative electrostatic charge on the coating side in the dark. One way of doing this is with the use of ion transfer from a corona discharge.

2. The sheet, now sensitive to light, is exposed by any of the conventional photographic procedures. The electrostatic charge is retained in the masked areas, but is lost or reduced in the exposed areas where a photocurrent which possesses all criteria for a "primary current" has been observed: it saturates with increasing voltage and its quantum yield is unity.[116] Thus a latent electrostatic image is formed on the surface of the paper.

3. The latent imagine is developed by applying a pigmented resin powder which carries a positive electrostatic charge. The powder is attracted and held by the negatively charged areas of the image. One

[115a] C. J. Young and H. G. Greig, *R.C.A. Rev.* **15**, 469 (1954).

[116] H. J. Gerritsen, W. Ruppel, and A. Rose, *Helv. Phys. Acta* **30**, 504 (1957).

effective and practical method for bringing properly charged toner particles to the surface which is to be developed is called the magnetic brush development. The "brush" is simply a mass of iron filings mixed with toner and attached to the end of a permanent magnet. The iron particles take on negative charges and the toner particles positive charges when they are mixed.

4. The powder image is fixed by melting the resin powder so it fuses to the paper surface to produce a durable light-fast image.

The light which is effective in this process lies in the spectral range between 320 and 420 mμ which correspond both to the region of absorption of zinc oxide and the spectral distribution of the photoelectric processes. In considering the practical application, however, one might hope for an extension of the sensitivity to longer wavelengths. This can be achieved by sensitizing the photoconductivity of zinc oxide with the use of adsorbed organic dyes, as mentioned in older Russian literature.[117] In this way, much as in the case of the photographic processes using the silver halides, one can obtain light sensitivity throughout the visible part of the spectrum that is not substantially smaller than the sensitivity at short wavelengths.

VIII. Discussion of the Conductivity (Parts VI and VII)

24. Volume Effects

a. Electron Mobility

All the experimental investigations carried out to the present time indicate that zinc oxide is n-type. For example, this is demonstrated by the following facts, discussed in Parts VI and VII: (a) the increase in conductivity resulting from treatment in a reducing atmosphere or from doping with metals in the third group of the periodic system and the decrease of conductivity resulting from treatment in an oxidizing atmosphere or from doping with metals of the first group; (b) the sign of the following four effects: Hall effect, thermoelectric power, rectification, and field effect.

The electron mobility μ in zinc oxide is of the order of magnitude 100 cm^2/volt sec at room temperature. The following relationships are valid for the temperature dependence: at high temperatures ($T > 300$°C) μ is independent of the conductivity and is proportional to $T^{-\frac{3}{2}}$; at low temperatures, in contrast, μ decreases with decreasing temperature and is smaller the larger the concentration of imperfections. This dependence

[117] E. K. Putseiko and A. N. Terenin, *Doklady Akad. Nauk SSSR* **90** (6), 1005 (1953).

is quite reproducible in single crystals (Figs. 53 and 57). It can be interpreted in a way similar to the corresponding behavior in the semiconducting elements, namely, in terms of lattice scattering of the electrons at high temperatures and scattering by charged imperfections at low temperatures.[118]

An explicit discussion of the electron mobility in zinc oxide which takes into account the scattering by optical lattice vibrations was given recently by A. R. Hutson.[119]

We are concerned with a degenerate electron gas in the case of crystals which are strongly doped with indium (Fig. 59). One can understand the temperature dependence of the electron density from this fact. It also follows from Fig. 59 that the Hall mobility is almost independent of the temperature. Since the energy of the conduction electrons is independent of the temperature in the highly degenerate case, the scattering by charged defects is also independent of temperature. According to Fig. 60, the mobility depends only slightly upon the electron concentration, which, according to Fig. 58, is equal to the concentration of indium atoms, that is, to the concentration N_I of ionized centers. Since the energy of the conduction electrons increases with increasing electron density in the degenerate range, one may expect the mobility to decrease more slowly than $1/N_I$. Indeed, the observed dependence, shown in Fig. 60, is even more gradual than the calculated one,[120] which varies as $1/N_I^{\frac{2}{3}}$, extending the Conwell-Weisskopf formula into the region of Fermi-Dirac statistics. An improved calculation takes into account the screening of the ion potential.[121]

In older measurements on thin layers and sintered specimens, for example those shown in Fig. 42, the dependences were not indicated so clearly. Polycrystalline materials possess irregularities arising from crystal boundaries. On the one hand, these irregularities decrease the mobility as a result of an additional, essentially temperature independent scattering; on the other, they can introduce space-charge layers and, thereby, inhomogenities of conductivity. Therefore, the evaluation of the mobility from conductivity and Hall effect seems to be unreliable for polycrystalline samples.

Thus, the results of the measurements of mobility can be explained by use of known principles. In the following discussion of the conductivity it is not necessary to take explicit account of the influence of the mobility.

[118] E. Conwell and V. F. Weisskopf, *Phys. Rev.* **77**, 388 (1950).
[119] A. R. Hutson, *Phys. Rev.* **108**, 222 (1957).
[120] V. A. Johnson and K. Lark-Horovitz, *Phys. Rev.* **71**, 374 (1947).
[121] E. Conwell, *Phys. Rev.* **103**, 51 (1956).

b. Volume Conductivity and Thermoelectric Power at High Temperatures

According to the experimental observations which have been described in the previous sections, one must distinguish between the volume and surface conductivity of zinc oxide. It is possible to separate the two parts of the conductivity experimentally in the case of single crystals. On the other hand, an unambiguous separation is often not easy to achieve for thin layers and sintered specimens. Furthermore, in addition to the distinction between volume and surface effects it is possible to put the conductivity measurements in order at low and high temperatures. One can achieve equilibrium among the imperfections at high temperatures, whereas a nonequilibrium situation may be quenched-in at low temperatures. Only characteristic examples will be discussed in the following. A description of all the details of conductivity measurements would lie outside the scope of this summarizing review.

(1) Zinc oxide in equilibrium with oxygen at high temperatures. At sufficiently high temperatures, the conductivity of zinc oxide crystals obeys the Boltzmann relation $\sigma = \sigma_0 e^{-\epsilon/kT}$ with an activation energy $\epsilon \cong 2.3$ ev (Fig. 46), independent of doping and previous history. For discussions of the results on sintered samples see Section 25d. In spite of this, one is not dealing with an ordinary intrinsic conductivity. This is demonstrated convincingly by two observations: (1) the thermal activation energy $2\epsilon \cong 4.6$ ev is definitely larger than the value obtained by extrapolating the optical values to absolute zero temperature, namely, 3.4 ev; (2) the conductivity σ of zinc oxide is a function of the pressure of oxygen in the surrounding atmosphere at fixed temperature. In the case of single crystals (Fig. 46) and sintered specimens (Fig. 38) there is close agreement with the relationship of the form $\sigma \sim p^{-1/m}$ in which $3.6 < m < 5.5$. Temperatures above 1400°C are necessary in the investigation of single crystals in order to establish these relations clearly. In contrast, temperatures over 600°C are sufficient for sintered specimens and thin layers.

The dependence of the "apparent" intrinsic conductivity upon the pressure of oxygen demonstrates the presence of an underlying imperfection-determined conductivity, the imperfections being in equilibrium with the environment. Two different interpretations of the results have been discussed in the literature.[93,122] According to one, the imperfections are generated on the surface of the crystal as a result of a dissociation reaction and become distributed uniformly through the entire crystal as a result of diffusion. According to the other interpretation, they are generated at the surface and establish an adsorption equilibrium there.

[122] H. J. Engell and K. Hauffe, *Z. Elektrochem.* **57**, 762 (1953).

The second of these possibilities will be discussed in more detail in Section 25d.

The dissociation of zinc oxide leads to an excess of zinc in the lattice. One obtains the following equations of reaction

$$ZnO \rightleftarrows Zn^{+} \text{ (as excess in lattice)} + e^{-} + \tfrac{1}{2}O_2 \text{ (gas)} \quad (24.1)$$

$$ZnO \rightleftarrows Zn^{++} \text{ (as excess in lattice)} + 2e^{-} + \tfrac{1}{2}O_2 \text{ (gas)} \quad (24.2)$$

according to whether thermal excitation dissociates one or two electrons from the excess zinc. In equilibrium one obtains the following equations of mass action, respectively,

$$[Zn^{+}] \times [e^{-}] \times p^{\frac{1}{2}} = \text{const} \quad (24.3)$$

$$[Zn^{++}] \times [e^{-}]^2 \times p^{\frac{1}{2}} = \text{const.} \quad (24.4)$$

The chemical symbols in square bracket designate the concentrations. Here $[e^{-}]$ = electron concentration $\equiv n$. With the neutrality condition $n = [e^{-}] = [Zn^{+}]$, or $n = [e^{-}] = 2[Zn^{++}]$, it follows further from (24.3) that

$$n \sim p^{-\frac{1}{4}} \quad (24.5)$$

and from (24.4)

$$n \sim p^{-\frac{1}{6}}. \quad (24.6)$$

Actually the measured dependence of the conductivity upon the oxygen pressure p should be given by these relations, for the mobility is practically independent of the concentration of zinc. Lattice scattering dominates completely at the higher temperatures. Since the dependence of the conductivity upon pressure is weak, one cannot measure the exponent of p very accurately. Thus, one cannot distinguish between the alternatives (24.1) and (24.2). It is also possible that values between $\frac{1}{4}$ and $\frac{1}{6}$ are real. This would imply that the second electron evaporates from only a fraction of the excess zinc.

According to electron theory, there is a linear relation between the logarithm of the electron concentration and the thermoelectric power (18.1). The dependence of the thermoelectric power of zinc oxide upon the pressure of oxygen (Fig. 39) can be explained in terms of these considerations.

The activation energy ($\epsilon = 2.3$ ev in Fig. 46) determined from the temperature dependence of the conductivity is interrelated to the energy of the reactions (24.1) and (24.2). Thus, from start one should not anticipate a direct relationship with the separation of bands, as would be the case for true intrinsic conductivity.

It is not possible, on the basis of these considerations, to decide whether the excess zinc is situated at interstitial positions or in the form

of oxygen vacancies, for both assumptions give the same dependence upon pressure. With respect to recent investigations at Erlangen on the diffusion of zinc and oxygen it seems probable, that the excess zinc can exist in the form of oxygen vacancies as well as in interstitial positions.

In the case of zinc oxide containing trivalent donors (Section 18c), the influence of oxygen is only slight, for the electron concentration is given essentially by the concentration of additions. In a quantitative discussion it is necessary to take into account the cooperative action of the dissociation equilibrium (24.1) and (24.2), along with the equilibrium of the defects associated with the additions. Unintentional additions can reduce the influence of oxygen in a similar way. For this reason one can observe the conductivity that is characteristic of the dissociation equilibrium primarily at very high temperatures where the total conductivity is large compared to the conductivity determined by additions, even though equilibrium is established in convenient times at low temperatures.

(2) Zinc oxide in equilibrium with hydrogen at high temperatures. The equilibrium of a solution of hydrogen in zinc oxide can be described in terms of the reaction[33]

$$H_2 \text{ (gas)} \rightleftarrows 2H^+ \text{ (in lattice)} + 2e^-. \tag{24.7}$$

It follows from the neutrality condition $n = [e^-] = [H^+]$ and the law of mass action that $n \sim p^{+\frac{1}{2}}$, in which p is the pressure of hydrogen in the surrounding atmosphere. As a result, one has the proportionality found experimentally, namely, $\sigma \sim p^{+\frac{1}{2}}$ (Fig. 51), for the mobility is also independent of the concentration of imperfections in this case. Once again Eq. (24.7) does not require definite assumptions concerning the form in which hydrogen is bound into the lattice. The simplest possibility is that the protons are located at interstitial positions. However, an association of the protons with typical O^{--} ions of the lattice, whereby hydroxyl ions OH^- would be formed, would give the same dependence of the conductivity upon the pressure of hydrogen. From the temperature dependence of the electron concentration (Fig. 50, $n \sim \exp -\epsilon/kT$), one obtains an activation energy $\epsilon = 0.8$ ev. Once again, this energy is connected with the energy of the reaction (24.7) and, hence, is not to be interpreted as the ionization energy of the hydrogen donor or something similar.

If donors are present in zinc oxide in a concentration which is not altered during the establishment of the hydrogen equilibrium, the hydrogen will cause an increase $\Delta\sigma$ of the conductivity σ induced by the original donors.[32] If $\Delta\sigma \ll \sigma$, that is, if $\Delta n \ll n$, the quantity n appearing in the law of mass action is practically constant. It follows that $\Delta\sigma \sim \Delta n \sim p^{\frac{1}{2}}\sigma^{-1}$. This relationship, insofar as it depends upon pressure, is found experimentally (Section 19b). It does not appear to be known, however, whether the appropriate dependence on σ occurs.

It is not only true that hydrogen dissolves in the lattice of zinc oxide according to Eq. (24.7) at high temperatures, but it is also true that the surface of the crystal is reduced. During this process a large concentration of excess zinc can occur in a thin surface layer before the destruction becomes visible. It is possible that the relatively suitably surface conduction produced by heating in hydrogen (type *B*, in Section 19c) occurs in this way.

c Volume Conductivity and Thermoelectric Power at Low Temperatures

In this section low temperatures are taken to be those at which the concentration and distribution of the imperfections do not vary. Under these circumstances, the conductivity is determined entirely by the equilibrium between the free electrons and the imperfections. For example, it is possible to retain hydrogen in zinc oxide by freezing the equilibrium (24.7). One obtains specimens with similar properties by heating the crystals in Zn or Cd vapor or by incorporating trivalent metals such as indium during the growth of the crystals. All these procedures engender in zinc oxide an impurity-produced conductivity possessing properties similar to those obtained by doping silicon or germanium with elements of the fifth group. In view of these general principles, the information contained in Figs. 52, 53, 56, 57, 58, 59, and 60 requires no particular explanation.

Consider the case of the conduction produced by donors with a definite energy level. At sufficiently low temperatures, the concentration of electrons is

$$n = (N_C N_D)^{\frac{1}{2}} d^{-\frac{1}{2}} \exp(-\Delta E/2kT) \tag{24.8}$$

in which $N_C = 2(2\pi m_n kT/h^2)^{\frac{3}{2}}$, as long as only a fraction of all donors are ionized. One can attempt to determine the effective mass m_n from these relationships. The quantities n, T, and ΔE (24.8) can be determined directly from the measurements. The concentration of donors N_D is equal to the electron concentration in the saturation range at high temperatures where all donors are ionized. The concentration of electrons is then independent of temperature. The quantity d is the degeneracy factor of the donors. It can have the value 2 or $\frac{1}{2}$. If the saturation range is not observed, it is still possible to estimate N_D with fairly good accuracy in many cases. N_D must be larger than the largest measured value of the electron concentration; however, it must be smaller than the value of n obtained by extrapolation to infinitely high temperature, that is, when $1/T = 0$. One can see from Fig. 52 that the uncertainty of this method of estimation is not large. For example, one finds[85] that the effective masses lie between the values $m_n = 0.14m_0$ and $m_n = 0.58m_0$ from hydrogen-doped crystals if one assumes the degeneracy factor $d = 2$. Hutson[119]

has found the value $m_n = 0.5m_0$ from the temperature dependence of the Hall effect on specimens doped weakly with hydrogen or zinc. With the help of the hydrogenic model for the donor, he has estimated an effective mass for the electron bound to the donor and has obtained the value $m^{(H)} = 0.27m_0$ from the largest measured activation energy (0.051 ev). In this work he employed the value of the dielectric constant determined recently, namely, $\epsilon = 8.5$.[4]

The validity of (24.8) is based on the assumption that there is only *one* fixed energy level of the donor. The activation energy determined from the Hall effect is, however, smaller the larger the electron concentration, for fixed temperature. For this reason it is not feasible to determine the effective mass accurately from the temperature dependence of the Hall effect. Two possible causes for this variation of the activation energy will be mentioned here briefly. It can happen that there is a large number of traps having a wide continuous energy spectrum, in addition to the donors. Depending upon the number of donors, these traps will be filled to a definite level and this level determines the measured activation energy. These energies, calculated from $n \sim \exp[-\epsilon/kT]$, lie between 0.02 and 0.04 ev for the cases shown in Fig. 52 (H_2 doping). The energy is about 0.03 ev in Fig. 54 (H_2 and Zn doping), whereas the values are 0.03 and 0.035 ev for the two lower curves in Fig. 56 (Zn doping), which are practically straight lines.

The decrease of the activation energy with increasing density of donors can also be related to an increase in the overlapping of the wave functions of the bound electrons. The impurity band formed in this way becomes broader with increasing density of donors. The ionization energy of the donors vanishes when the impurity band reaches the lower edge of the conduction band.[121,123] Assuming $\epsilon = 8.5$ and $m^{(H)} = 0.27\ m_0$, one obtains $N_D = 6 \times 10^{18}$ cm^{-3} for the critical donor concentration in ZnO.[119] In this treatment a regular arrangement of donors rather than a statistical one was assumed. The results shown in Figs. 52, 56, and 59 do not contradict this estimate.

The conductivity of zinc oxide is lowered by the incorporation of monovalent copper on substitutional sites (Fig. 61), in contrast to the effect of substitutional additions of trivalent indium. In other words, copper behaves as an acceptor as one might expect. In n-conducting ZnO this implies the introduction of deep-lying traps for free electrons. The activation energy ϵ for the two curves shown in Fig. 62 is about 0.22 ev. In other words, it is almost a full order of magnitude larger than in Figs. 52, 54, and 56, although it is definitely smaller than half the width of the forbidden band. This does not mean, however, that the cop-

[123] H. Brooks, *Advances in Electronics and Electron Phys.* **7**, 85 (1955).

per level must be only 0.2 ev below the conduction band. As in ZnS it could well lie in the lower part of the forbidden band. In this case another imperfection with a level at 0.2 ev must be present. This appears only when nearly all electrons from higher donor levels have been trapped by the copper centers because of a high copper concentration.

Sintered samples behave similarly in many respects at low temperatures. The activation energy for the temperature dependence of the electron concentration is of the same order of magnitude as for crystals, namely, 0.029 ev, as shown in Fig. 41. The influence of foreign metal atoms upon the conductivity shown in Fig. 44 corresponds qualitatively

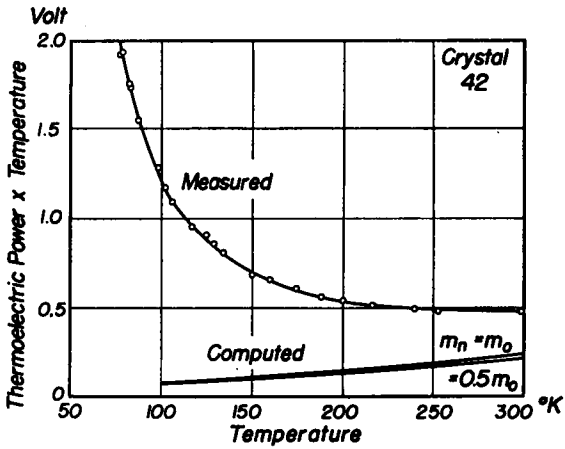

FIG. 94. Crystal. Comparison of the measured thermoelectric power (No. 42, Fig. 47) with that computed from the theory without phonon drag, using two different values of effective mass. Plotted is the product of thermoelectric power and absolute temperature. After Hutson.[100]

to the action of In and Cu on single crystals, particularly at small concentrations of the additions. Li^+ ions substituting for Zn^{++} ions behave like acceptors because of the large ionization energy of the helium-like Li^+ ion. The ultimate rise of the conductivity with increasing Li_2O concentration, shown in Fig. 44, is striking and could be regarded as a trend toward *p*-type conductivity. This question has not been investigated further in an experimental way, so that the assumption that an inversion of type could be produced is somewhat doubtful. It is quite possible that the ultimate rise of conductivity has another explanation. For example, it is possible that the solubility limit for substitutional Li is exceeded and that Li donors enter interstitial positions or produce complicated effects on the grain boundaries of the polycrystalline sample.

The thermoelectric power of the crystals found at low temperatures (Fig. 47) cannot be explained in terms of the older theory. It is clear from Fig. 94 that at low temperatures the measured thermoelectric power is considerably larger than that calculated by Eq. (18.1). An explanation is provided by the transfer of momentum of acoustical phonons to the conduction electrons[100] (phonon drag effect).[124] The influence of the concentration of carriers can be viewed in terms of the same general picture. There is no contradiction between these measurements on single crystals at low temperatures and the observations with sintered specimens at high temperatures (Fig. 39). The phonon drag effect decreases with increasing temperature as is shown in Fig. 94. In both cases the thermoelectric power decreases with increasing carrier density.

25. Surface Effects

a. Influence of Boundary Layers upon the Conductance

The concentration of electrons at the surface of zinc oxide can be changed in various ways: by the adsorption of gases as a result of electron exchange with ZnO, by the field effect, and by irradiation with light lying in the fundamental band. Such surface effects play a role in the following Sections: 7a, 10, 13 to 15, 17, 18, 19c, 20 to 23. They will be discussed together here. For a discussion of the chemisorption and heterogeneous catalysis on semiconductors see the work of K. Hauffe.[81,82]

Surface charges can have an influence only to a definite depth, for they will be neutralized by a space-charge layer which screens the interior. The thickness l of this layer lies in the range from 10^{-7} to 10^{-5} cm, as in other semiconductors. If l is larger than the thickness l' of the conducting layer which determines the resistivity, the influence of the surface will extend over the entire cross section of the current path. Examples of such cases are provided by single crystals having a large surface conductivity (accumulation layer, Fig. 95a), thin layers, and fine-grained powders. Even when l is less than l', however, the conductance of the specimen can be influenced by surface effects in a definite way, such as when poorly conducting depletion layers lie across the path of the current (Fig. 95b). Coarsely crystalline specimens provide an example of this.

(*1*) *Action of traps.*[104] The study of the volume properties of zinc oxide crystals provides an indication that electron traps as well as donors are present (Section 24c). This assumption is necessary if one hopes to explain the observed surface effects. The traps are always in equilibrium with the conduction band so that the distribution of the electrons can

[124] C. Herring, *Phys. Rev.* **96,** 1163 (1954).

be described in terms of a quasi Fermi level ζ. The action of the traps will be discussed for the case in which the influence of surface effects extends uniformly over the entire cross section of the current path, $l > l'$.

A variation in the total electron concentration Δn induced by influences on the surface can be divided between a component in the conduction band (Δn_C) and in traps (Δn_t):

$$\Delta n = \Delta n_C + \Delta n_t. \tag{25.1}$$

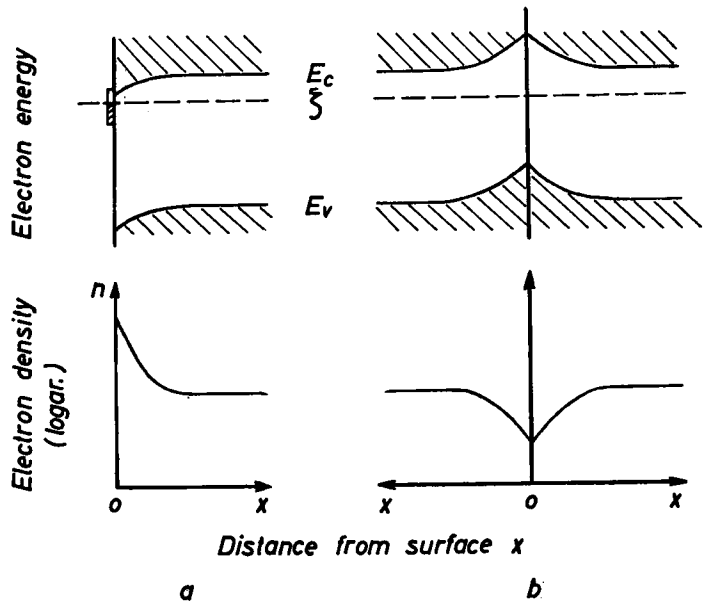

FIG. 95. Schematic representation of the behavior of the electron energy and electron density on the surface. Band separation about 3 ev. In the interior of the crystal $E_c - \zeta < 0.2$ ev. a: Accumulation layer and surface traps. The current flows perpendicularly to the plane of the paper. b: Exhaustion layer on the region of contact between two crystallites. The current flows parallel to the x direction.

The variation can be described in terms of a displacement of the Fermi level. One has the relation

$$n_C \sim \exp\left[-(E_C - \zeta)/kT\right] \tag{25.2}$$

in which the conduction band is not degenerate. It is possible to deal with the differentials for small variations:

$$dn_C = n_C d\zeta/kT. \tag{25.3}$$

If one assumes that the traps have a quasi-continuous energy spectrum,

and that the concentration per unit energy $N_E(E)$ varies only slightly over an interval kT, one has

$$\Delta n_t = \left(\frac{dN_t(E)}{dE}\right)_t \Delta\zeta = N_E(\zeta)\Delta\zeta \tag{25.4}$$

that is, for $\Delta n_C \ll n_C$

$$\Delta n_C = \Delta n \Big/ \left(1 + \frac{N_E(\zeta)kT}{n_C}\right). \tag{25.5}$$

For the most part, the overwhelming number of electrons are in the traps, so that $\Delta n_C \ll \Delta n$. Thus,

$$\Delta n_C = n_C \frac{1}{N_E(\zeta)kT} \times \Delta n. \tag{25.6}$$

In other words, the division of the variation Δn in the total electron concentration, produced by influences on the surface, between the conduction band and traps depends upon the position of the Fermi level, which determines n_C, and upon the density of traps. The higher the Fermi level and the lower the density of traps, the higher will be the quantity

$$\frac{\Delta n_C}{\Delta n} = \frac{n_C}{N_E(\zeta)kT} \tag{25.6a}$$

which we may call the "efficiency" of the variation Δn of the total electron concentration in producing a change in the concentration Δn_C of the conduction electrons. This quantity is proportional to n_C. For large variations, when the relation $\Delta n_C \ll n_C$ is no longer valid, Eq. (25.6) must be integrated. The increase of Δn_C with Δn is then exponential[104] in the case in which the density of traps is constant.

(2) Accumulation layers. All specimens of zinc oxide studied to date are n-type. Therefore, in an accumulation layer a positive surface charge of ionized surface donors is bordered by a negative space charge of electrons. The contribution of the donors in the volume can be neglected generally when the surface conductivity is measurable. In order to describe the phenomena of the field effect, it is necessary to assume the presence of a density of traps which either lie on the surface, and extend continuously for an energy range of the order of 0.2 ev below the conduction band, or are distributed as a continuous or discrete density of levels below the conduction band which penetrates the entire space-charge layer. Since the calculations are simpler, we shall discuss only the case of the continuum on the surface (Fig. 95a). The distribution will be characterized in terms of the surface density of traps per unit energy interval $S_E(E)$. In this case the traps effect only the surface density Σ of the surface charge.

Only a thin layer of the region of space charge is significant for the conductance along the surface, namely, the layer in which the potential varies by an amount of the order kT/e from the surface. In this case the space-charge density ρ will be given approximately by the concentration n_{CR} of the conduction electrons at the surface, namely, $\rho = -en_{CR}$. With the neutrality condition $\Sigma = \nu_C \approx n_{CR} \cdot l$ and Poisson's equation, one obtains

$$\frac{kT}{e} = \frac{en_{CR}l^2}{2\epsilon\epsilon_0} = \frac{e}{2\epsilon\epsilon_0} \cdot \frac{\nu_C^2}{n_{CR}}, \qquad n_{CR} = \frac{e^2}{2\epsilon\epsilon_0 kT} \cdot \nu_C^2 \tag{25.7}$$

and

$$l = \nu_C/n_{CR} \sim 1/\nu_C. \tag{25.8}$$

In the case in which there is no degeneracy, this approximation for (25.7) and (25.8) leads to the same result as the solution of the differential equation.[125] For the degenerate case see the same reference. With increasing surface density ν_C the thickness l of the accumulation layer decreases in contrast to the depletion layer.

From Eq. (25.6) we obtain

$$\Delta\nu_C = \nu_C \frac{\Delta\nu}{2S_E(\zeta)kT} \tag{25.9}$$

as a result of integration over the thickness of the layer with the use of (25.7). The proportionality of $\Delta\nu_C$ and ν_C and of Δn_C and n_C in (25.6) is noteworthy.

(3) *Depletion layers.* In the case of the exhaustion layer a negative surface charge of adsorbed acceptors is neutralized by a positive space charge of ionized volume donors.[122,126] As a result, the space-charge density ρ is given by the concentration of the donors N_D, that is, $\rho = eN_D$. In terms of the density of the surface charge Σe, the neutrality condition has the form $\Sigma = N_D l$. Using Poisson's equation one obtains the following expression for the potential difference V across the boundary layer:

$$V = \frac{\rho}{2\epsilon\epsilon_0} \times l^2 = \frac{e}{2\epsilon\epsilon_0} \times \frac{\Sigma^2}{N_D}, \text{ compare (25.7)} \tag{25.10}$$

as well as

$$V/l = \Sigma e/2\epsilon\epsilon_0. \tag{25.11}$$

Since the concentration of free electrons at the surface n_{CR} depends exponentially on V, we have

$$\Delta n_{CR} = -n_{CR} \frac{e}{kT} \times \Delta V = -n_{CR} \frac{2eV}{kT} \times \frac{d\Sigma}{\Sigma}. \tag{25.12}$$

[125] G. Heiland, *Z. Physik* **148**, 28 (1957).
[126] W. Schottky, *Z. Physik* **113**, 367 (1939).

As in the case of the trap model, one also has $\Delta n_{CR} \sim n_{CR}$ in this case. The cause is the same in the two cases, namely, the differential of an exponential function derived from Boltzmann's statistics is used. As was already mentioned above, the poorly conducting depletion layers affect the conductance of a "thick" specimen ($l \ll l'$) when they cross the path of the current. In this case one obtains a conductance which is proportional to n_{CR}.[127] Depletion layers do not obey Ohm's law. Nevertheless, Ohm's law can be expected in the polycrystalline material discussed here, so that one can expect to give a definite value for the conductance. The reason for this is that many boundary layers are joined in series in this case; only a small fraction of the applied voltage is distributed across a single member. In this event one can approximate the characteristic curve of the boundary layer with a straight line (zero resistance).

b. Surface Conduction on Single Crystals

(*1*) *Effect of hydrogen and zinc vapor.* As was indicated in Section 19c, one can produce good conducting layers on the surface of the crystals by the action of hydrogen or zinc vapor. Donors which cannot diffuse into the interior of the crystal at the temperatures employed are formed in this way. Moreover, the electrons provided by the donors are hindered from going to the interior of the crystal because of the diffusion potential which is generated. In other words, one forms an accumulation layer on the *n*-type crystal (Fig. 95a). A more detailed discussion follows in Sections (*3*) and (*4*).

(*2*) *Effect of oxygen.* Oxygen is chemisorbed on the surface of the crystals even at low temperatures and forms surface acceptors. These acceptors capture conduction electrons from the surface region. A depletion layer whose thickness depends upon the concentration of the donors N_D arises. The negative surface charge of the adsorbed oxygen corresponds to the positive space charge of the ionized donors. The rectification of crystals charged with oxygen can be understood in these terms (Fig. 63). If one has a good conducting surface layer, the surface conductivity can be decreased by orders of magnitude as a result of adsorption of oxygen. In the language of the band model, this behavior has the following meaning: the treatment with hydrogen or zinc vapor bends the band edges at the surface downward, whereas oxygen affects it in the opposite direction (Fig. 95).

(*3*) *Surface conduction of type B (after heating in hydrogen).*[87] Two different types of surface conductivity produced by exposure to hydrogen can be distinguished. Type *B* is observed after heating the crystals in hydrogen (800°K, 15 min, 6 atmos) and is very stable (Fig. 64). One can

[127] F. Stöckmann, *Z. Physik* **146**, 407 (1956).

then adsorb oxygen and lower the conductivity. After driving off the adsorbed oxygen with heat in a vacuum, the large surface conductivity returns almost unchanged. Essentially higher temperatures are required in order to remove the surface donors.

What can be said regarding the nature of these donors? According to Section 8, donors diffuse into the interior of the crystal when it is heated in hydrogen. The penetration depth of these donors by diffusion during the hydrogen treatment, type *B*, is much larger than the thickness of the depletion layer produced by adsorbed oxygen. Therefore the conductance caused by these hydrogen donors could not be affected by the adsorption of oxygen. On the other hand, the volume conductivity obtained in equilibrium with hydrogen is orders of magnitude too small to be the origin of the surface conductance of type *B*. Possibly the surface is reduced by the hydrogen treatment with the production of an excess of zinc. However the type of donors diffusing into the crystal during heating in zinc vapor (Section 7c) can be excluded by means of the arguments used in discussion of the hydrogen donors. However, one cannot exclude the possibility that an excess of zinc is present at the surface in the form of vacancies in the oxygen lattice which are occupied by electrons and have a very low diffusion coefficient at 500°C.

Figure 64 can be explained in the following manner. After the crystal has been heated to incandescence, the volume conductance is predominant and the contribution from surface donors is negligible (curve 8). Under these circumstances, the influence of oxygen is not significant. The thickness of the depletion layer is small compared to the diameter of the crystal. After heating to 900°K in 50 atmospheres of hydrogen, the conductivity in the volume becomes so large, as a result of penetration of the hydrogen donors by diffusion, that the surface conductance can no longer be observed (curve 1). In the case of curve 2, the volume conductance produced by hydrogen (800°K, 25 atmos) is, indeed, comparable with the surface conductance. However, the influence of oxygen is already noticeable. In the cases associated with curves 4 and 6, on the other hand, the conductance at low temperatures is determined only by the surface donors (oxygen vacancies). If one takes the value of the electron mobility on the surface to be 100 cm^2/volt sec, one obtains a value of the density of conduction electrons per unit area of the surface of about 2×10^{13} cm^{-2} from curve 3, using the decrease of the conductance at 90°K under the action of oxygen. Corresponding values obtained from curves 5 and 7 are about 5×10^{12} cm^{-2}.

In other words, the amount of oxygen adsorbed attains values corresponding to a surface density of 10^{13} cm^{-2}. This value is about two orders of magnitude lower than the density of molecules in a monomolecular

layer. Some possible causes for the limitation of the adsorption of oxygen may be mentioned here. The potential of the surface becomes continually more negative relative to the interior of the crystal with increasing surface charge [Eq. (25.10), Fig. 95b]. The level of the adsorbed oxygen is below the Fermi level initially; however, it attains the Fermi level with increasing bending of the bands. This produces a limitation on the transfer of electrons from the crystal to the adsorbed oxygen. Actually this equilibrium will not be attained under certain circumstances. The concentration of the conduction electrons on the surface decreases exponentially as the potential difference across the boundary layer increases. The reaction velocity is proportional to the concentration of electrons and can be so small that the adsorption process practically comes to a standstill. Finally, it should be mentioned that the electric field at the surface attains the value

$$E_R = \Sigma e/\epsilon\epsilon_0 \approx 2 \times 10^6 \text{ volt/cm} \tag{25.13}$$

for a charge density of 10^{13} electrons/cm^2 on the surface. This is of the order of magnitude of the breakdown potential.

(*4*) *Surface conduction of type A* (*after the action of atomic hydrogen*). Surface layers which conduct well and possess low stability can be produced by the action of atomic hydrogen even at low temperatures[97] (86°K). This contribution to the conductance vanishes when oxygen is adsorbed. The surface conductance does not reappear when the specimen is heated in such a manner as to drive off the oxygen. The layers can also be destroyed, without prior adsorption of oxygen, by heating the crystals in a vacuum to 600°K.

The situation clearly is one in which adsorbed donors or acceptors are produced on the surface by a surface reaction and remain there. The layers can also be produced at low temperatures where all diffusion is frozen. One expects the chemisorbed hydrogen atoms to contribute electrons to the crystal. These electrons become divided between the traps and the conduction band. The protons probably remain attached to the crystal surface near O^{--} ions and form OH^- ions.[35] It is possible that the reaction proceeds further until excess zinc atoms are produced and Zn^+ ions appear on the surface. Whereas, the surface conductivity of type *B* corresponds to a situation in which the donors have migrated into the outermost layers of the crystal, one may assume that the donors are only loosely bound upon the surface in the case of type *A*.

The increase of surface conductance resulting from the effect of atomic hydrogen as a function of time (Fig. 65) occurs in a way similar to the increase of the amount of chemisorbed hydrogen in an atmosphere of molecular hydrogen (Fig. 30). Molecular hydrogen, however, does not

induce a measurable surface conductivity even after exposure for hours in the temperature range shown in Fig. 30. The reason for this remains an open question at the present time.

If one assumes that the electron mobility in the accumulation layer is 100 cm^2/volt sec, one obtains a surface density of conduction electrons of 6×10^{12} cm^{-2} from the saturation value of the surface conductivity, namely about 10^{-4} ohm^{-1} (Fig. 65). According to the condition of neutrality, the surface density of donors must have the same value, although it can be even greater in the case in which electrons are bound at traps. Thus, the surface density lies in the same range as in the case in which oxygen is adsorbed (Section 25b(*3*)). It follows that the field at the surface is of the same order of magnitude [see Eq. (25.13)]. The application of the equation in this section requires that the donors be on the crystal surface. If they actually are distributed in the outer lattice planes of the crystal and are surrounded by conduction electrons, the field at the surface will be smaller.

In the case of the surface conduction induced by zinc vapor there is insufficient information available to make certain it is either of the more stable type *B* or the type *A*. The broad independence of the saturation conductivity upon zinc vapor pressure and crystal temperature during the treatment with zinc can be explained in terms of a limitation on the amount of zinc which can be adsorbed as a result of the increase in the electric field at the surface, in accordance with Eq. (25.13).

Figure 66 shows clearly that the volume conductivity has no influence upon the surface conductivity. As a result, the donors in the volume can be neglected in considering the space charge of the accumulation layer. With these assumptions, the differential equation of the accumulation layer may be integrated.[125] Two cases can be treated in this procedure, namely, those associated with the nondegenerate and the completely degenerate electron gas at the surface. Thus, from the saturation value of the surface conductivity one estimates an electron concentration at the surface n_{CR} lying in the range from 10^{19} to 10^{20} cm^{-3}. This corresponds to the case of complete degeneracy. The electron concentration falls to a value of about $\frac{1}{64}$ of the surface value at a depth of about 10^{-6} cm. In addition, it is necessary to take into account the possibility that there is a direct interaction between the individual donors. The average distance beween two surface donors is about as close as the distance between volume donors at a concentration of about 1.5×10^{19} cm^{-3} when the surface density is as high as 6×10^{12} cm^{-2}. As was mentioned in Section 24c, one not only has an impurity band at a donor concentration above 6×10^{18} cm^{-3}, but, in fact, the activation energy of the donors (or traps) disappears as a result of the overlapping of the wave functions.

For complete degeneracy not only the density but also the mobility of the conduction electrons is expected to show no temperature dependence if determined by impurity scattering, for the energy of these electrons is quite independent of temperature. In this connection, we may refer once again to the very weak temperature dependence of the maximum surface conductivity (type *B*, Fig. 64, curves 4, 5, and 6; type *A*, Fig. 66, curves *b*).

c. Field Effect on Single Crystals

According to Fig. 68, the drift mobility increases with the surface conductivity. The basis for an explanation of this relationship lies in the principle that only a fraction of the electrons which are influenced by the field or are released by the absorption of light are freely mobile. The majority are bound in traps. The observed relationship between the mobility and the surface conductivity cannot be described in terms of a model which assumes one single discrete trapping level at the surface of the crystal. If the discrete high-lying level of the trap runs across the entire space-charge layer, an explanation of the observation does, indeed, appear to be possible. Assuming the simplest situation, the relationship between the drift mobility and the surface conductivity can be explained on the assumption that there is a continuum $S_E(E)$ of trap energies upon the crystal surface. The continuum must at least extend over the entire range of energy through which the Fermi level at the surface varies when the surface conductivity extends over the range from 10^{-9} to 10^{-4} ohm^{-1}. The consequences of this simple model will be developed briefly in the following and will be compared with the measurements.[104]

Since the field effect is observed in single crystals only when an accumulation layer is present, Eq. (25.9) can be used to describe the experiments. In place of the quantity $\Delta\nu$, the surface density $\Delta\nu_{Fd}$ of the influenced electrons appears. The field effect mobility was defined in terms of the relation

$$\mu_{Fd} = \Delta G_{Fd}/e\Delta\nu_{Fd} \qquad (20.1) = (25.14)$$

in Section 20. The surface conductivity is

$$G = e\mu_C\nu_C. \qquad (19.1) = (25.15)$$

Here ν_C is the surface density of the conduction electrons in the accumulation layer, ν_S is the surface density of the electrons in traps, and μ_C is the mobility of the conduction electrons at the surface. The quantity μ_{Fd} behaves in the manner of the drift mobility of the totality of the electrons in the conduction band and in traps:

$$\begin{aligned} \Delta G_{Fd} &= e\mu_{Fd}\Delta\nu_{Fd} = e\mu_{Fd}(\Delta\nu_C + \Delta\nu_S) = e\mu_C\Delta\nu_C \qquad (25.16) \\ \mu_{Fd} &= \mu_C\Delta\nu_C/(\Delta\nu_C + \Delta\nu_S). \end{aligned}$$

Using (25.9), it then follows that

$$\mu_{Fd} = \mu_C \nu_C / 2S_E(\zeta)kT = G/2eS_E(\zeta)kT. \tag{25.17}$$

For constant trap density S_E, one readily obtains $\mu_{Fd} \sim G$ which was observed for small values of the conductivity (Fig. 68). If the mobility grows more slowly with the conductivity, it follows that the density of traps must be rising toward the conduction band. According to (25.17), the quantity $S_E kT$ grows from 3×10^{11} cm^{-2} at small values of the conductivity to 3×10^{12} cm^{-2} at large values. In other words, S_E extends over the range from 4×10^{13} to 4×10^{14} cm^{-2} ev^{-1}. The relationship $\mu_{Fd} \ll \mu_C$, that is, $\Delta\nu_C \ll \Delta\nu_{Fd}$, is valid over the greatest range of Fig. 68. This justifies the use of (25.6) instead of (25.5).

Moreover, the exponential behavior of the dependence of the field effect upon potential between field probe and crystal (Fig. 67) is now understandable. In (25.3), only the differential of the exponential function appearing in Boltzmann statistics need be applied; that is, the calculation is valid only for small relative variations of the conductivity. This limitation also corresponds to the procedure used in the measurement of the field effect mobility. If on the other hand, $\Delta G_{Fd} > G$, one expects an exponential rise of ΔG_{Fd} with the charge which is influenced, that is, with the potential between the field electrode and the crystal. The spectrum of traps influences this rise.

At the smallest surface conductivities investigated, the Fermi level on the surface does not lie more than 0.2 ev below the conduction band and should approach the latter with increasing conductivity. The traps for electrons also lie in this domain.

d. Influence of Oxygen on the Conductivity of Thin Layers and Sintered Specimens

The conductivities of thin layers possess a similar, often astonishing, sensitivity toward oxygen (Sections 17 and 21), much as the surface conduction of single crystals (Sections 19c and 25b). All diffusion processes are frozen-in over the temperature range investigated. Thus, the oxygen is effective only because it is adsorbed and forms surface acceptors which bind conduction electrons. The equilibrium between gaseous and adsorbed oxygen is established slowly below about 600°K because the process of adsorption is hindered more and more as a result of the development of a potential across the exhaustion layer. The process practically comes to a standstill before equilibrium is attained under certain circumstances. Desorption behaves in the same way. For example, it is extraordinarily slow in a vacuum at these temperatures. As a result, the conductance depends upon the amount of oxygen adsorbed as a result of the

previous treatment. All treatments in which the quantity of adsorbed oxygen is varied have an irreversible effect upon the conductance. An example is given in Fig. 69. If the layer which has been treated with oxygen is brought into a vacuum, there is no irreversible variation of the conductivity at first, even when the specimen is warmed to about 400°K; that is, the adsorbed oxygen is held tightly even in a vacuum. The equilibrium between gaseous and adsorbed oxygen takes place too slowly. An irreversible increase in the conductivity only occurs at higher temperatures. This increase can be related to the desorption of oxygen. The conductivity decreases again to the initial value after the introduction of air at room temperature. The process can be repeated arbitrarily often. In contrast, the conductance decreases irreversibly when the specimen is warmed in oxygen or air, even when the donor concentration in the interior of the crystallites cannot vary because the temperature is too low.

The thickness of the depletion layer is generally larger than the thickness of the crystallites if the donor density is not very high. Under these conditions, the principles developed in Section 25a can be applied in considering the experiment involving the adsorption of oxygen which was described in Section 21. The conductivity of the layer, or the current flowing at constant voltage, is proportional to the concentration n_C of the conduction electrons. The adsorption decreases the oxygen pressure by Δp_{O_2} and the total concentration of electrons in traps and in the conduction band by $\Delta n \sim \Delta p_{O_2}$. In other words, Eq. (25.6) describes the experiment exactly at constant density of traps. The increase in the "efficiency" for the adsorption of oxygen, which occurs along with the increase in conductivity, can be related to the screening action of the traps in the same way as the "efficiency" for the field effect.

A qualitative explanation of Fig. 35 is also possible with use of Eq. (25.6). The curves in the figure are distinguished by the amount of oxygen adsorbed. The larger the slope, the lower the Fermi level lies, that is, the larger the number of the traps which have been emptied. Equation (25.12) will lead to a relationship similar to (25.6) if boundary layers perpendicular to the current play a role at large densities of donors.

A representation of the increase of the different curves in Fig. 35 is given in Fig. 96 as a function of the conductivity for three different temperatures. The slope E_s is given by the relation

$$E_s = -k \frac{d \ln (\sigma/\sigma_0)}{d\, 1/T}. \tag{25.18}$$

It follows from Fig. 96 that

$$E_s = -0.4kT \ln (\sigma/\sigma_0) \text{ with } \sigma_0 \approx 1 \text{ ohm}^{-1} \text{ cm}^{-1}. \tag{25.19}$$

Measurements of the influence of oxygen upon the conductivity have been made on sintered specimens in the range of temperature extending from 500 to 1000°C (see Section 18a, Fig. 38, and the discussion in Section 24b). It is questionable whether one is dealing with volume or surface effects in this work. In considering the conductivity observed on single crystals at high temperatures (above 1400°C, Fig. 46), it is assumed that ZnO decomposes on the surface in a way which is influenced by the pressure of the oxygen (Section 24b). The conductivity in the interior of the crystal then can be altered by the diffusion of an excess of zinc.

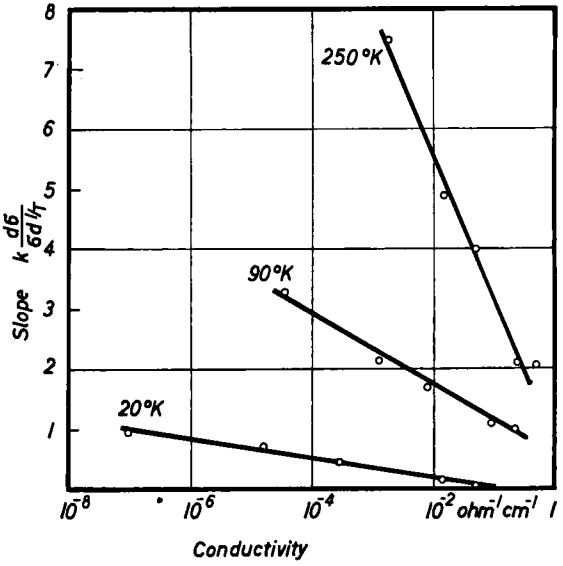

FIG. 96. Thin layer. Slope of the curves given in Fig. 35 at different temperatures as a function of conductivity.

In contrast, one must consider surface effects in the case of sintered specimens (Figs. 37, 38, 43). Moreover, it is not certain that the excess zinc can diffuse sufficiently rapidly in the temperature range investigated. One has the relation

$$4(e^-)_{\text{crystal}} + (O_2)_{\text{gas}} \rightleftharpoons 2(O^{--})_{\text{adsorbed}} \tag{25.20}$$

when the system is in equilibrium with an atmosphere of oxygen.[92,122] The law of mass action then leads to

$$n_{CR}^4 \times p_{O_2} \sim [O^{--}]^2 = \Sigma^2. \tag{25.21}$$

It follows from Eq. (25.10) that

$$n_{CR} \sim p_{O_2}^{-\frac{1}{4}} \times (VN_D)^{\frac{1}{4}}. \tag{25.22}$$

The conductance is proportional to the boundary concentration of electrons n_{CR} in the case of perpendicular depletion layers (Fig. 95b). If the adsorbed oxygen possesses a double charge, one obtains the same dependence of the conductivity upon oxygen pressure as if one assumes that the ZnO decomposes and simple ionized donors penetrate by diffusion. It is clear that one must assume a dissociation equilibrium in considering the case of the crystals. In this case it is not sensible to suppose that exhaustion layers extend transverse to the current path or that sufficient amounts of oxygen can be adsorbed at such high temperatures. In contrast, it is probable that one has equilibrium of adsorption in thin layers and sintered specimens. The following points can be regarded to favor this model: (1) the different activation energies, which are 2.3 ev for crystals and 1 ev for thin layers and sintered specimens; (2) the difficulties of extrapolation to higher temperatures when one attempts to join the measurements on thin layers and sintered specimens to those of single crystals; (3) the large deviations between specimens of different origin, which can be explained by differences in donor concentration (Fig. 43).

e. Irradiation with Light and Electrons. Slow Processes

A distinction between fast and slow processes was made in the discussion of the photoelectric processes in zinc oxide in Sections 22 and 23. As will be pointed out in detail in Section 25f, the fast processes correspond to purely electronic phenomena. In contrast, ionic migration plays a role in the slow process, particularly in the desorption and readsorption of chemisorbed oxygen. A sequence of arguments support this. (1) Gas is given off[128] during the irradiation of zinc oxide. Since the material acts as a photocatalyst for oxidation processes during irradiation, it is probable that the gas is oxygen, although this has not been proved by direct analysis up to the present time. (2) The stationary value of the photoconductivity depends upon the partial pressure of oxygen in the environment in the case of the slow process. (3) The increase in conductivity is irreversible in a vacuum; however, it reverses when oxygen is introduced. In contrast, other gases such as nitrogen or argon have no effect.

One can describe the slow process in a qualitative way on the basis of these observations. Chemisorbed oxygen is emitted from the surface during the irradiation, either as a result of the capture of holes or by direct ionization. The oxygen is desorbed as a consequence and, indeed, in an active form. This provides an explanation of the photocatalyzed oxidations observed when zinc oxide is irradiated. At the same time, the concentration of free electrons and, hence, the electrical conductivity

[128] D. Medved, University of Pennsylvania, Tech. Rept. 4, February 21, 1955.

increases in zinc oxide. The opposite reaction is the readsorption of oxygen which leads to the binding of electrons. The velocity of adsorption depends upon the pressure of oxygen. Hence, both the stationary value of the photoconductivity and the decrease which follows when the radiation ceases are functions of this pressure. To obtain a quantitative interpretation of the observed relations, one would need assurance concerning the detailed assumptions regarding the mechanism of the individual processes, which, although plausible, have not been justified completely by experiment. As a result, the following considerations should not be regarded as providing a rigorously valid model of the slow processes. Rather, they are to be looked upon primarily as furnishing examples of the way in which such problems can be considered.

In the case of the slow processes observed on thin layers, the increase of the conductivity observed during irradiation with light depends upon the lowest value of the dark conductivity σ_T which is achieved after standing for a long time in air, according to (22.1) and (22.2). Thus it will be assumed, in agreement with the discussion of Section 25d, that the value obtained in air corresponds to the adsorption equilibrium given by (25.21), namely,

$$n_{CR} \sim [O^{--}]^{\frac{1}{2}} \times p_{O_2}^{-\frac{1}{4}}. \tag{25.23}$$

In the case of thin layers, which in the main have been used for the investigations, the diameter of the crystallite l' is small compared to the thickness l of the completely developed exhaustion layer. Thus one is dealing with the situation developed in Section 25a(1) corresponding to no space-charge layers. Hence, we have

$$\sigma \sim n_C = n_{CR}. \tag{25.24}$$

The neutrality condition is

$$n_C l' = \nu_C = N_D \times l' - 2[O^{--}] - \nu_S. \tag{25.25}$$

In the case of the lowest conductivity σ_T, one can neglect the surface density ν_S of the filled traps in comparison with the density of adsorbed oxygen. Moreover, the concentration of conduction electrons n_C is generally small compared to the density of donors N_D (the case of exhaustion). It follows then, as a consequence of (25.23), that the lowest value of the conductivity attainable by adsorption of oxygen is

$$\sigma_T \sim n_{CT} \sim [O^{--}]^{\frac{1}{2}} \times p_{O_2}^{-\frac{1}{4}} \sim (N_D l')^{\frac{1}{2}} \times p_{O_2}^{-\frac{1}{4}} \tag{25.26}$$

σ_T is always measured after the layers have stood in air for a long time. According to (25.26), it provides a measure for the greatest coverage with oxygen that can be attained under these conditions. The oxygen coverage is determined by the density of donors and the grain size. If the conduc-

tivity is increased by desorption, it is found experimentally (Section 21), and on the basis with the trap model, that the number of electrons freed (25.6) is many times smaller than the number of oxygen molecules desorbed. In spite of this, the relative variation of the coverage with oxygen can be very small even when the conductivity changes by orders of magnitude. The origin of this fact clearly resides in the neutrality conditions (25.25), for the surface density ν_C of the conduction electron enters as the small difference of quantities which are many orders of magnitude larger than it. The situation differs from this only when the conductivity is very large.

Equation (22.1) can be given a plausible explanation on this basis: the increase in the conductivity is given by the rate of desorption which, in turn, is proportional to the coverage of oxygen and the intensity of irradiation. The coverage with oxygen remains approximately constant for a long period of time during the increase and is coupled to the lowest conductivity σ_T in accordance with (25.26). The circumstance that the slope $(d\sigma/dt)_I$ is independent of oxygen pressure and is proportional to σ_T follows as a consequence. Once a value of σ_T has been established in air, one does not need to be concerned with the change which is produced as a result of the variation in oxygen pressure, in accordance with (25.26), because the time in which a measurement is made is short.

The stationary value σ_{max} of the conductivity of a thin layer which is attained in an atmosphere of oxygen during irradiation with light, in accordance with (22.2), decreases with increasing oxygen pressure and depends upon the intensity of radiation through a fractional exponent. Both observations appear plausible if one assumes that a reverse reaction eventually occurs with increasing conductivity. This reaction arises from an adsorption process which depends upon the pressure of oxygen. With appropriate reservations, we should mention here that the experimental results expressed by Eq. (22.2) can be completely explained if one assumes that the law of mass action can be used also in this case: One inserts two light quanta in the right-hand side of the reaction Eq. (25.20) for the dark conduction

$$(O^{--})_{absorbed} + h\nu \rightleftharpoons \tfrac{1}{2}(O_2)_{gas} + 2(e^-)_{crystal} \qquad (25.20a)$$

and applies the law of mass action, in which the amount of adsorbed oxygen is proportional to σ_T^2 according to Eq. (25.26).

Many purely qualitative effects must be taken into account in an accurate treatment. The assumption that the layer is free of space charge is only an approximation.

The situation represented in Fig. 80, namely, that the conductivity of a crystal can be *decreased* slowly and irreversibly by irradiation with

electrons, can be explained very simply. The electron beam frees gas molecules or atoms from the crystals or from surfaces near the crystal. These molecules are adsorbed on the crystal surface and bind conduction electrons. This interpretation is confirmed by the observation that the conductance of the crystal can be decreased by orders of magnitude even when only one side is irradiated. The observation of "negative" photoconductivity in zinc oxide, quoted in the literature, may well be given a good explanation in terms of gas adsorption on this basis.

f. Irradiation with Light and Electrons. Fast Processes

The fast processes described in Section 23 do not exhibit influences of the type described in Section 25e, which led us to conclude that the slow processes depend upon chemisorption. In particular, the fast processes are completely reversible even in a high vacuum. As a result, it is safe to assume that they originate in purely electronic phenomenon. Nevertheless, the fast processes constitute a surface effect. They are stimulated only by light in the spectral range of the fundamental band (Figs. 20, 88, and 92) or by electrons, that is, by radiation which does not penetrate deeply. Moreover, the dark conductivity, which is an important parameter, is established by the amount of oxygen or hydrogen which is chemisorbed on the surface. Still further, one does not observe the fast processes in crystals which have a large volume conductivity or in coarsely crystalline preparations. They are observed only with crystals which possess a surface conduction or with thin layers in which the factors which affect the surface can have an influence on the entire current. If space-charge effects are neglected in such cases, in accordance with the discussion of Section 25a, the fast processes occur in a thin surface layer, much like the homogeneous volume effects. This explains the similarity of the spectral distribution of the fast process to the absorption spectrum of zinc oxide.

In the first quantitative model which was developed, it was assumed that the only imperfections which could occur in zinc oxide consist of interstitial zinc atoms which originate in an excess of zinc and that an ionized donor Zn^+ canl ose a second electron either by direct ionisation[129] or by the capture of holes generated in the interior of the crystal as a result of irradiation with light in the fundamental band.[130] This model can be used to explain the dependence of the photocurrent on both the dark current and the intensity of radiation. It can also be used to explain the time dependence. In fact, this development represents one of the first investigations in which an attempt was made to explain the photoelectric

[129] E. Mollwo and F. Stöckmann, *Ann. Physik* [6] **3**, 240 (1948).
[130] G. Heiland, *Z. Physik* **132**, 367 (1952).

processes in a quantitative way in terms of specific assumptions concerning the atomic structure of lattice defects. In another model[127] the zinc donors in the volume are replaced by chemisorbed oxygen atoms on the surface. This development, which requires the inclusion of space-charge effects, also provides an account of the relationships observed experimentally. The two models possess in common the property that the essential imperfection can occur in three states. These states are Zn, Zn^+, and Zn^{++} in the first case, and O^{--}, O^-, and O in the second. The proportionality between i_p and $I^{\frac{1}{3}}$ described in Section 23 follows from this fact in these models. The same is true for the proportionality between i_p and $i_0^{\frac{2}{3}}$ or $G_0^{\frac{2}{3}}$. It seems questionable at the present time whether the

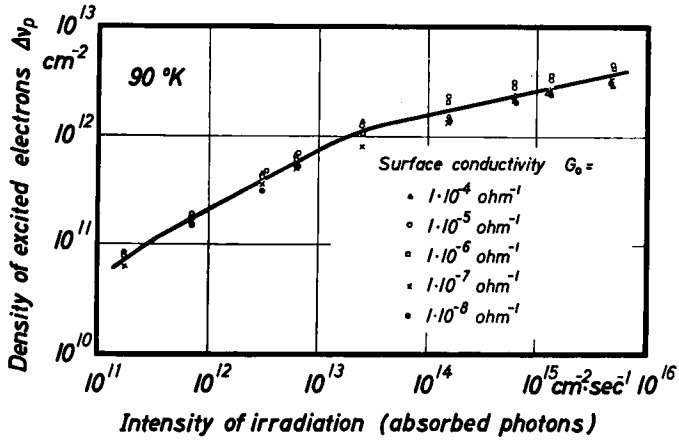

FIG. 97. Crystal 12. Surface density of electrons in excited states $\Delta\nu_p$ as a function of the intensity of radiation, calculated from Figs. 91 and 68. After Heiland.[104]

explanation of these power laws actually requires such specialized assumptions. There is evidence that the relationships actually occur under circumstances in which the models are not appropriate. It is quite possible that the observed power laws provide an approximate representation of what is basically a complicated relationship.

Other models which provide an interpretation of the known observations concerning the field effect in crystals can be developed. In these developments, the rise and fall of the photoconductivity is determined essentially by the filling and emptying of surface traps. In considering these we shall first make the following evaluation of the measurements.

If the drift mobility of the electrons is known, one can determine a surface density of excited electrons from the photo-surface-conductivity. One obtains in this way not the increase in the conduction electrons, but

the sum of the electrons in traps and in the conduction band which are excited by absorption of light (compare 25.16). The surface density of excited electrons must be equal to the total density of holes in imperfections and in the valence band. In the case of crystal number 12, the surface density of excited electrons was calculated from the relation

$$\Delta\nu_p = \Delta G_p / e\mu_p \tag{25.27}$$

by using the stationary photoconductivity ΔG_p derived from Fig. 91 and the drift mobility μ_p obtained from Fig. 68. Figure 97 shows the result. In accordance with what we might expect from the parallel course of the

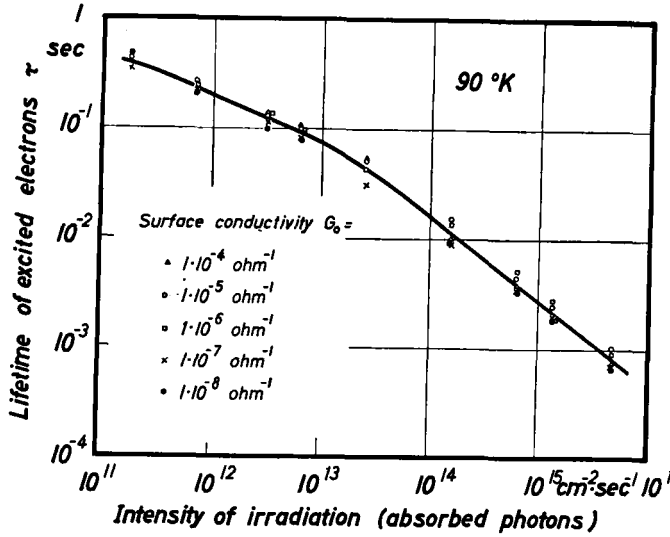

FIG. 98. Crystal 12. Lifetime τ of electrons in excited states as a function of the intensity of irradiation, calculated from Fig. 97. After Heiland.[104]

curves in Figs. 68 and 90, the influence of the surface conductivity G_0 drops out, in spite of the fact that it varies over four orders of magnitude. In brief, the five curves shown in Fig. 91 can be brought practically to coincidence by expressing them in terms of the drift mobility. A value of the lifetime of the excited electrons (or holes) can be determined from the data of Fig. 97 by using the relation

$$\tau = \Delta\nu_p / I. \tag{25.28}$$

Here I is the number of photons absorbed per second and cm^2. Figure 98 shows that the lifetime drops from 0.5 sec to 7×10^{-4} sec with increasing intensity of radiation, even though it is completely independent of the

surface conductivity. It should be emphasized again that we are not dealing with the lifetime of free carriers but with the lifetime of excited states which is increased by the trap effect.

These observations can be explained with the help of the trap model.[104] The model and its consequences can be described only briefly within the confines of this article. The principal relations are as follows.

As long as the drift mobility (either μ_{Fd} or μ_p) is small compared to the microscopic mobility μ_c [Eq. (25.16)], the greater fraction of the electrons excited by light are in traps (Section 25c). The surface density of excited electrons is $\Delta\nu_p$. Former experiments indicate that electrons actually carry the overwhelming part of the photocurrent.[91] Thus the largest part of the holes must be bound in traps. The traps which play a role in this case must be distributed in a small range of energy above the valence band. Moreover, the holes which occupy them are protected from recombination. As the intensity of irradiation increases, the quasi-Fermi level for the holes moves toward the valence band and an increasing fraction of all holes takes part in recombination. Figures 97 and 98 can be explained quantitatively with a density of traps for holes which increases from 10^{13} to 10^{14} cm^{-2} ev^{-1} towards the valence band.

We are led to the following conclusions. Whereas the influence of the dark conductivity on the photoconductivity [Figs. 89 and 90, Eq. (23.5)] can be interpreted with the use of a continuum of electron traps lying just below the conduction band and an accompanying drift mobility, the influence of the intensity of radiation [see Fig. 91, Eq. (23.6)] can be described in terms of a system of traps for holes which lie just above the valence band and a process of monomolecular recombination which is independent of the density of electrons. The traps for holes provide the basis for explaining the large lifetimes of the excited states.

The corresponding relations which are found for thin layers probably are only approximately power laws either and can be understood in a similar way. For example, Figs. 84 and 86 and Eqs. (23.3) and (23.4) can be interpreted in terms of Eq. (25.6) if one makes the transition from Δn_c to dn_c/dt and from Δn to dn/dt. The following quantities are then proportional to one another: $dn_c/dt \sim (di/dt)_s$; $n_c \sim i_0$; $dn/dt \sim I$. It should be emphasized again that Eq. (25.12) corresponds closely to Eq. (25.6). Hence, the regularities governing the initial rise $(di/dt)_s$ of the fast photoelectric processes can be interpreted in a similar way in terms of the assumption that exhaustion layers cross the current path.

The slow and the fast processes have approximately the same magnitude in many cases. They cannot be separated clearly under these circumstances. The overlapping of the two can cause the current to behave in a complicated way. It is possible that curve 1 in Fig. 77 corresponds to a

situation in which the fast process is present alone for all practical purposes. In contrast, it is possible that both are present in the case of curve 2 and that the fast process has decayed so that only the slow one is effective in the case of curve 3 when all three curves come together.

Sensitized photoconduction provides another example in which the relative importance of the fast or the slow processes is not clear. This was mentioned briefly in Section 23c in connection with the Electrofax system. Explicit investigations concerning it are not available. Organic dyes can be adsorbed on zinc oxide, as in the case of sensitized photographic emulsions. Light which is adsorbed by the sensitizers can then excite photoconduction in zinc oxide even in regions of the spectrum in which zinc oxide actually does not absorb and in which the material normally would be photoelectrically inactive. The excitation spectrum for this sensitized photoconduction agrees with the absorption spectrum of the sensitizer. In other words, the primary photoelectric process presumably is associated with direct ionization of the sensitizer. Subsequent processes, about which nothing is known, determine whether the sensitized photoconduction depends upon the slow or the fast processes.